Developing Budding Yeast as a Cell Factory for Production of the Antioxidant Ergothioneine

A thesis submitted to the

National University of Ireland Maynooth

For the degree of

Research Masters

By

Daragh Cuskelly B.Sc.

Supervisor
Prof. Gary Jones
Dept. of Biology
Maynooth University
County Kildare

Co-Supervisor
Prof. Sean Doyle
Dept. of Biology
Maynooth University
County Kildare

Head of Department
Prof. Paul Moynagh
Dept. of Biology
Maynooth University
County Kildare

February 2016

Table of Contents

List of Figures

List of Tables

Declaration of Authorship

This thesis has not been previously submitted in whole or part to this or any other University for any other degree. This thesis is the sole work of the author.

Daragh Cuskelly B.Sc.

Acknowledgments

I would like to sincerely thank Prof. Gary Jones and Prof Sean Doyle for giving me the opportunity to work on such an interesting project. It was their mentorship and guidance throughout the project that helped me see the project through to its successful completion.

I would also like to thank everyone in Maynooth Biology Department especially my fellow lab members Elizabeth and Linan for all their yeast wisdom as well as the constant supply of cake and Chinese food! I want thank Grainne and Rebecca for always taking a moment to answer a question or two no matter how silly it may be. Thanks to Lara, Nicola, Rose, Kevin, Stephen D and Stephen B in the Biotech lab for all the tea breaks and craic through the years.

I want to thank my parents and my sister Becky who never really quite knew what I was doing but supported me anyway, that's dedication for you! Mam and Dah I truly appreciate all you have done for me. Helen thank you for listening to many a rant from your scientist boyfriend and being there for me while writing my thesis. I promise to make it up to you.

Presentations

Oral Presentation

''Expression of recombinant EgtA in *S. cerevisiae* causes production of the Antioxidant Ergothioneine'' Biology Departmental Talk, Maynooth University, Kildare, August 2015

''The use of Budding Yeast as a Cell Factory for Production of the Antioxidant Ergothioneine'' Biology Research Day, Maynooth University, Kildare, September 2014

''A novel biosynthetic approach to producing the antioxidant Ergothioneine'' Biology Departmental Talk, Maynooth University, Kildare, July 2014

Poster Presentations

''Developing Budding Yeast as a Cell Factory for Production of the Antioxidant Ergothioneine'' International Congress on Stress and Health, Huangshan, China, September 2015

''Developing Budding Yeast as a Cell Factory for Production of the Antioxidant Ergothioneine'' Irish Fungal Society Meeting, Maynooth University, Kildare, June 2015

''The use of Budding Yeast as a Cell Factory for Production of the Antioxidant Ergothioneine'' Biology Research Day, Maynooth University, Kildare, May 2015

Abbreviations

5'IAF	5'-Iodoacetamidofluorescein
aa	Amino acid
ATCC	American Type Cell Culture
bp	base pairs
BSA	Bovine Serum Albumin
cDNA	Complementary deoxyribose nucleic acid
cds	Coding Sequence
DMSO	Dimethyl sulfoxide
DNA	Deoxyribose nucleic acid
ECL	Enhanced chemiluminescent
EDTA	Ethylenediaminetetraacetic acid
EGT	Ergothioneine
gDNA	Genomic Deoxyribose nucleic acid
GSH	Glutathione
GSSG	Glutathione disulphide
H_2O_2	Hydrogen Peroxide
LC-MS	Liquid Chromatography Mass Spectrometry
NP	Natural Product
RP-HPLC	Reverse Phase High Power Liquid Chromatography
SN	Supernatant

Abstract

Ergothioneine (EGT) is a naturally occurring sulphur-containing modified amino acid which has been shown to exhibit anti-oxidant properties. EGT is produced by selected fungi and prokaryotes, however *Saccharomyces cerevisiae* does not naturally produce EGT. Up to 5 genes are involved in bacterial EGT biosynthesis while in fungi, two genes have been identified to be involved in EGT biosynthesis, and one such gene is *egtA* from *Aspergillus fumigatus*. Here, it is shown that expression of EgtA alone in the GRAS organism *Saccharomyces cerevisiae* facilities the production of EGT. The novel production of EGT in *S. cerevisiae* was confirmed by both HPLC and LC-MS analysis, and quantification of resultant EGT revealed a significantly ($P < 0.0001$) larger quantity of EGT present extracellularly in culture supernatants and accumulated therein until the time point of 96 h was reached. To complete the EGT biosynthetic process, a cysteine desulfurase is required, and two candidates were identified in *A. fumigatus*, namely AFUA_2G13295 and AFUA_3G14240, termed *egt2a* and *egt2b* in this study. Co-expression of *egtA* and *egt2a* in *S. cerevisiae* using high expression 2μ vectors was expected to increase EGT production, however EGT levels were seen to be significantly decreased ($P < 0.05$). As expression of *egtA* alone in *S. cerevisiae* been shown to effect EGT biosynthesis this raised the question of the ability of *S. cerevisiae* to complete the EGT biosynthetic process. A putative endogenous cysteine desulfurase Nfs1 was identified in *S. cerevisiae*. Interestingly decreasing the expression of Nfs1 was shown to increase levels of EGT. Moreover, manipulation of the conserved residue Thr^{213} in EgtA indicates indiscriminate phosphorylation by threonine kinases could be negatively regulating EGT production in *S. cerevisiae*. This study demonstrates quite remarkably that *S. cerevisiae* can produce EGT with the expression of just one additional protein. Hence, production of EGT using a synthetic biology approach now opens the possibility to economically viable means of producing EGT.

Chapter 1

Introduction

1.1 The *Aspergilli*

The *Aspergilli* are a diverse genus of over 250 different species of filamentous fungi known for the production of a wide array of natural products (NPs). NPs also referred to as secondary metabolites as their role is believed not to be crucial to the biochemical mechanisms that underpin the survival or the organism. Some members of *Aspergillus* have long held commercial applications such as *A. oryzae* used in the production of East Asian food products such as sake. Others like *A. flavus* are known for their economic and human cost infecting crops such as corn and peanuts which then go on to infect grain fed livestock (Payne *et al*., 1993). Because of this Aspergilli are thought of as both friends and foes through their role in producing high value food products and important NPs as well there economic and human cost through food spoilage and being an opportunistic pathogen. A key example of this is *A. terreus* an opportunistic human pathogen but is also the main source of the anticholesterol drug lovastatin with worldwide sales topping $10 billion annually (Kennedy *et al.,* 1999). The potential discovery of NPs from fungi such as the aspergilli for anti-cancer drugs, nutraceuticals and antibiotics now has the possibility of growing with the genome sequencing of several key species such as *A. fumigatus, A. oryzae, A. niger* and *A. nidulans (Nierman et al*., 2005; Galagan *et al*., 2005; Machida *et al*., 2005; Pel *et al*., 2007). As well as this over 266 gene clusters have been identified producing known and unknown NPs from *A. nidulans, A. oryzae, A. niger* and *A. fumigatus* alone (Inglis *et al*., 2013).

1.2. *Aspergillus fumigatus*

Aspergillus fumigatus is a saprophytic fungus that is ubiquitous in the environment, playing an essential role in the carbon and nitrogen cycle colonising decaying organic matter and soil environments. *A. fumigatus* is one of 20 species in the genus *Aspergillus* known most for its pathogenicity constituting 90% of all invasive aspergillosis infections (Geiser *et al*., 2007). *A. fumigatus* grows as a mass of septate fungal hyphae which produce asexual spores known as conidia which are commonly found in indoor and outdoor air at a concentration of 1 to 100 per cubic metre (Sullivan *et al.,* 2011). Conidia (only 2-3μm in diameter) are routinely inhaled by humans and penetrate deep into the lungs where they are typically destroyed by alveolar macrophages (Latgé, 2001). In immunocompromised patients or those with an underlying lung condition conidia are not killed by the host's immune system which

can then cause a variety of respiratory infections. The three most common being allergic broncho-pulmonary aspergillosis, aspergilloma and invasive aspergillosis (Daly, 2001; Thompson & Patterson, 2008; Agarwal, 2009).

Allergic broncho-pulmonary aspergillosis is an immunologic pulmonary disorder caused by hypersensitivity to *A. fumigatus* which manifests in non-immune compromised individuals with either severe asthma or cystic fibrosis (Agarwal, 2009; Greenberger, 2002; Tillie-Leblond & Tonnel, 2005). Aspergilloma is another infection caused by *A. fumigatus* which is the formation of a fungal ball in the upper respiratory tract and a sign of chronic cavity pulmonary aspergillosis. Infected individuals have a damaged respiratory tract usually from tuberculosis or sarcoidosis, which results in significant morbidity with severe cases requiring surgical intervention. The infection will develop over an extended period lasting months to even years (Tillie-Leblond & Tonnel, 2005; Pendleton & Denning, 2012; Howard *et al*., 2013). Invasive aspergillosis is the most common form of infection by *A. fumigatus* with a 40-90% mortality rate in high risk patient groups traditionally infecting neutropenic individuals such as HIV patients (Sullivan *et al.,* 2011; Keeffe & Doyle, 2011). It has also been seen to infect individuals post organ transplant and haematopoietic stem cell recipients who recieve immunosuppressive drugs as well as those with an underlying condition such as leukaemia (Patterson *et al*., 2000; Marr *et al*., 2002). One feature which increases the virulence of *A. fumigatus* is its production of NPs which will be discussed in the next Section.

1.3 *A. fumigatus* genome a reservoir of natural Products

The genome of the *A. fumigatus* strain AF293 was first sequenced in 2005 and predicted to possess a total of 9,926 genes in 8 chromosomes totalling 29.4 Mb *(*Nierman *et al*., 2005). This has led to the identification of 323 *A. fumigatus* genes involved in thermotolerance as well as more than 500 putative *A. fumigatus* specific genes with no identified homologues in *A. nidulans* or *A. oryzae* (Nierman *et al.,* 2005). With the sequencing of the *A. fumigatus* strain AF293 genome mining for NP genes now uses many bioinformatics based tools to identify genes by their repetitive genomic patterns and unique domains (Ziemert *et al*., 2012). The Secondary Metabolite Unknown Region Finder (SMURF; www.jcvi.org/smurf), is a web based tool for the identification of NPs based on their genomic context and domain content (Khaldi *et al*., 2010). Another web based tool the antibiotics and Secondary Metabolite Analysis Shell (antiSMASH), locates novel NP genes using

biosynthetic loci from all of the known secondary metabolite classes (Medema *et al.*, 2011). Use of such bioinformatic tools has led to the identification of many NP genes, which unlike those encoding for the transformation or biosynthesis of primary fungal metabolites tend to be located in clusters making them easier to locate (Khaldi *et al.*, 2010). However many genes that encode NPs may not express under laboratory conditions leaving many gene products unknown (Brakhage & Schroeckh, 2011).

A. fumigatus when in the wild grows in highly competitive conditions, competing for space and nutrients. This has conferred selective pressures for the production of a wide array of NPs for better defence against other microorganisms, to increase the availability of nutrients and space for growth (Knox & Keller, 2015). NPs produced by *A. fumigatus* have a diverse range of beneficial applications such as anti-cancer, antimicrobial and others which aid in understanding the virulence of this organism (Wu *et al.*, 2007; Sanchez *et al.*, 2012).

NPs such as siderophores are produced in iron limiting conditions and sequester iron from the surrounding environment. *A. fumigatus* produces a number of different siderophores of the hydroxamate type named by the three hydroxamate bidentate ligand system that chelates the Fe^{3+} ion (Hofte, 1993; Saha *et al.*, 2013). Hydroxamate siderophores produced by *A. fumigatus* include fusarinine C an extracellular siderophore secreted by *A. fumigatus* which scavenges for iron in the environment and ferricrocin an intracellular siderophore used for iron storage (Barton & Hemming, 1993; Saha *et al.*, 2013). *A. fumigatus* has been shown to have several mechanisms for regulating siderophores depending on the availability of iron and siderophores have been shown to be key to virulence in mouse models of invasive aspergillosis (Haas *et al.*, 2008; Qin *et al.*, 2009; Schrettl *et al.*, 2007).

A significant contributing factor to the virulence of *A. fumigatus* is its production of harmful NPs such as helvolvic acid, fumigillin and the well characterised gliotoxin (Figure 1.1). These toxins have been shown to damage human respiratory epithelium and slow the ciliary beat frequency (a key airways defence mechanism) in vivo (Delmotte & Sanderson 2006; Amitani *et al.*, 1995). However the diversity of NPs produced by *A. fumigatus* has shown to have a range of beneficial properties. Helvolvic acid, long identified as having antimicrobial properties has been shown to enhance the killing of multi-drug resistant *Staphylococcus aureus* (MRSA) when combined with antibiotics such as erythromycin (Qin *et al.*, 2009). Fumagillin is an antimicrobial agent and is an effective treatment of microsporidial infection in patients with HIV (Zbidah *et al.*, 2013). Fumagillin has also been

shown to inhibit tumour induced angiogenesis *in vivo* and primary effusion lymphoma cell lines as well as lead to the development of fumagillin analogues with enhanced anti-tumour properties with less side effects (Zbidah *et al.*, 2013; Kanno *et al* 2015; Ingber *et al*. 1990).
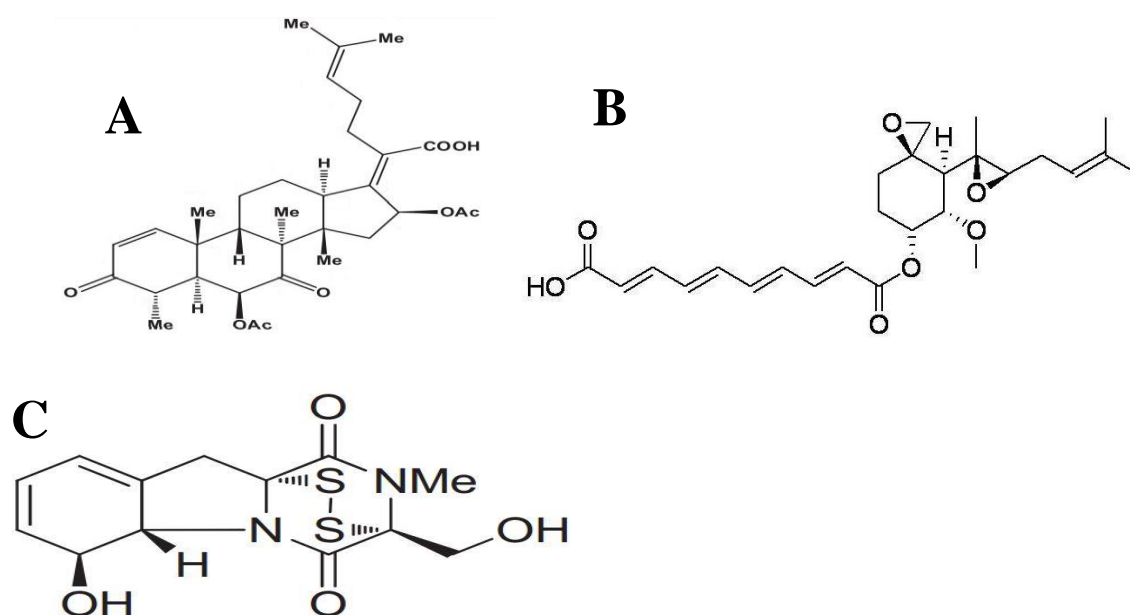
Figure 1.1 Natural products produced by *Aspergillus fumigatus*. The structures of helvolvic acid (A), fumagillin (B) and gliotoxin (C). Adapted from (Lee *et al.*, 2008; Zhang *et al.*, 2006; Davis *et al.*, 2011)

The fumitremorgins are a large group of prenylated indole alkaloid NPs produced by *A. fumigatus* containing either indole or indoline and isoprenoid moieties as well as their derivatives (Li, 2011). Derived from brevianamide F which consists of L-tryptophan and L-proline they have a diverse range of biochemical activities. Fumitremorgins A, B as well as verruculogen were identified as tremorgenic mycotoxins. However, others such as tryprostatin and fumitremorgin C have been seen to reverse the resistance of some tumour cell lines against antitumor agents (González-Lobato *et al.*, 2010; Wu *et al.*, 2007). Tryprostatin and fumitremorgin C were noted to be specific inhibitors of the breast cancer resistance protein ABCG2, an ATP-binding cassette transporter which efflux's

chemotherapeutic compounds out of tumour cells (Li, 2011; Rabindran *et al*., 2000; Staud & Pavek, 2005). Naturally occurring thiol NPs are required by microbes and *Mammalia* alike to detoxify harmful molecules and will be discussed in the following Section.

1.4 Production of thiol natural products by Microbes

Thiols are present in living systems and carry out essential cellular roles such as maintenance of cellular redox homeostasis, protein thiol disulphide ratios and protection from reactive oxygen species (ROS) (Hand & Honek, 2005). Glutathione (GSH) (Figure 1.2), is a well-known antioxidant produced by bacteria, fungi and *Mammalia* alike. In *Mammalia* it has been identified to be involved in the regulation of cell proliferation, apoptosis, immune function, and fibrogenesis (Lu, 2013). GSH is a γ-glutamyl-cysteinyl-glycine tripeptide it acts as a radical scavenger of ROS and xenobiotics which cause oxidative damage to proteins and macromolecules (Schafer & Buettner, 2001). GSH has also been shown to reduce unwanted protein disulphide formations created by the presence of ROS (Berndt *et al*., 2008). GSH exists in the thiol reduced form at physiological pH when it is most reactive until becoming oxidised to its disulphide form (GSSG) (Kaplowitz *et al*., 1985). The antioxidant function of GSH is largely accomplished by GSH peroxidase which catalyses the reduction of ROS such as hydrogen peroxide and lipid peroxide while GSH is oxidised. Disulphide GSH is then reduced back to GSH by GSH reductase (Lu, 2013).
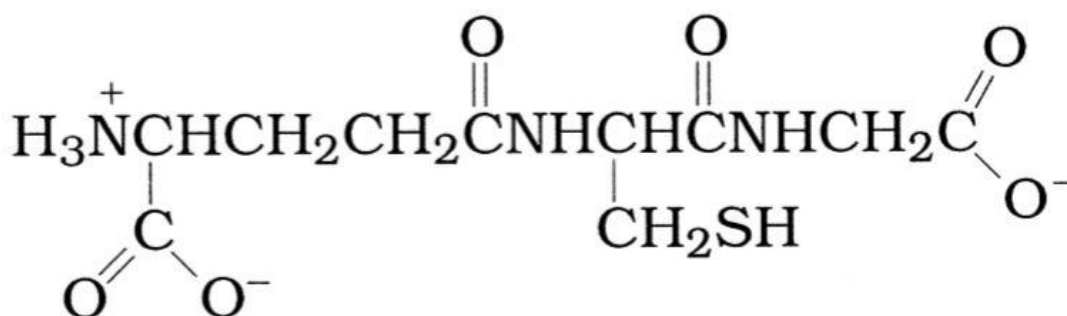
Figure 1.2 The structure of Glutathione. In its thiol form GSH is highly unstable and is easily oxidised to its disulphide form. Adapted from Schafer & Buettner, 2001.

Protozoa such as the *Trypanosoma* produce a unique thiol to deal with ROS. *Trypanosoma* such as *Trypanosoma brucei* which cause over 66,000 deaths annually produce trypanothione as well as GSH to dissipate ROS (Fairlamb *et al*., 1985). Certain bacteria do not utilize GSH for redox homeostasis and use other thiols instead such as mycothiol (MSH) (Figure 1.3), used by *Mycobacteria* and *Streptomyces* species (Hand & Honek, 2005). MSH has a wide range of roles as well as deactivating free radicals it also mediates antibiotic resistance as demonstrated in *Mycobacterium smegmatis* (Rawat *et al*., 2002). MSH is also required in the synthesis of the antibiotic lincomycin in *Streptomyces lincolnensis* (Zhao *et al*., 2015). However *Mycobacteria* such as *Mycobacterium smegmatis* produce other NPs to help eliminate ROS. This indicates that GSH alone may not be enough for an organism to maintain their redox homeostasis and requires a variety thiol NPs to manage their redox homeostasis. One such NP is ergothioneine (EGT) which will be discussed more in the following Sections.
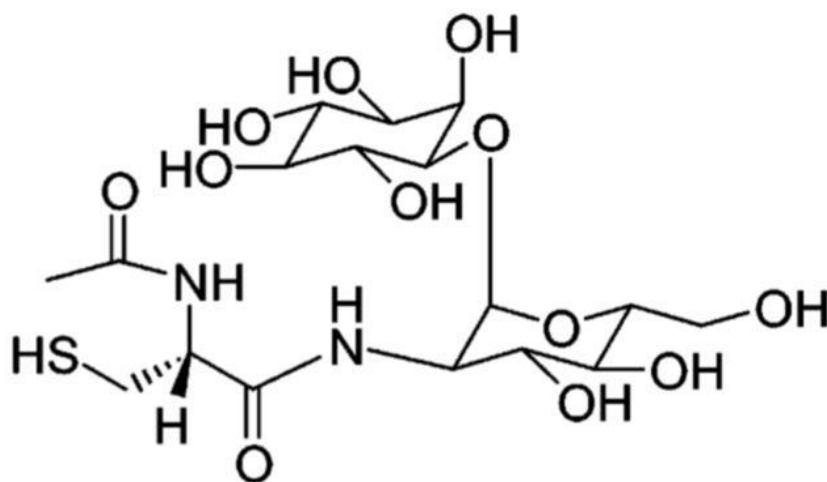
Figure 1.3 The structure of mycothiol. Detoxification of ROS is mediated through its reactive thiol group. Adapted from (Fahey, 2001).

1.5 Ergothioneine

EGT is a low molecular mass thiol metabolite produced by various bacteria and non-yeast fungi and has been observed to have antioxidant properties. First identified by Tanret in 1909 in the ergot fungus *Claviceps purpurea* EGT has now been identified to be produced across the bacterial and fungal kingdoms in model organism such as *A. fumigatus* and *M. smegmatis* (Tanret, 1909). Plants and animals do not synthesize EGT but acquire it through dietary means. Plants acquire EGT through their roots or via microbial symbionts (Park *et al*., 2010). Animals acquire EGT from food including mushrooms, oats, beans and red meat which are all rich sources of EGT (Ey *et al*., 2007).

EGT is a betaine derivative of the proteinogenic amino acid histidine with a thiol group located on the C_2 atom of the imidazole ring (Halliwell & Gutteridge, 2007). EGT is tautomeric (Figure 1.4) and has a higher redox potential of -0.06 V compared to other naturally occurring thiols which have a typical range between -0.2 V and -0.32 V. This confers greater stability to EGT under physiological conditions preventing EGT from undergoing auto oxidation as rapidly as other thiols such as GSH which predominately exists as a thiol (Cheah & Halliwell, 2012).
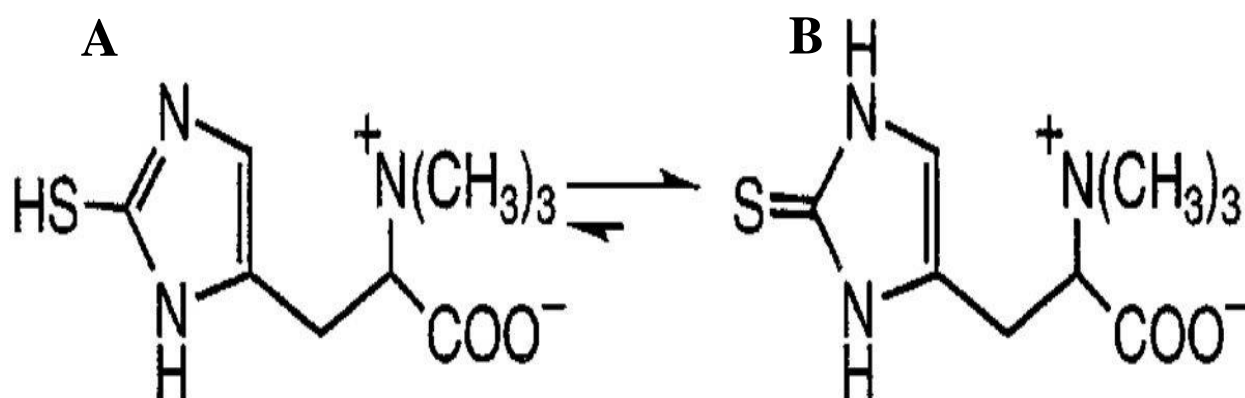
Figure 1.4 Ergothioneine in its thiol and thione form. (A) Ergothioneine in its thiol form attached to the imidazole ring by a single bond. (B) Ergothioneine in its thione form attached to the imidazole ring by a double bond. Adapted from Fahey, (2001).

EGT, because it is predominately in its thione form at physiological pH is highly stable (Hand *et al.*, 2005). One study demonstrated how rats fasted for 1 week showed no drop in the level of EGT in blood or liver (Mayumi *et al.*, 1978). In humans EGT accumulates in cells at a concentration between 100 µM and 2 mM and is most abundant in bone marrow, kidney, seminal fluid and the lens and cornea of the eyes (Shires *et al.*, 1997). The putative transporter protein formally known as organic cation transporter 1 (OCTN1) encoded by the gene SLC22A4 has been identified as having high affinity for EGT (Nikodemus *et al.*, 2011). OCTN1 now identified as an EGT transporter (ETT) actively retains EGT inside the cell (Nikodemus *et al.*, 2011). EGT exhibits antioxidant activity and has been identified as a cytoprotectant inside mammalian cells potentially representing a new vitamin (Paul & Snyder, 2009).

1.6 Biosynthetic pathways of ergothioneine

EGT has a molecular mass of 229.3 and a high solubility in aqueous solutions of 0.9 M at 25 °C (Halliwell & Gutteridge, 2007). Naturally occurring EGT is in the L-configuration, synthesized from L-Histidine always and followed by either γ-glu-cys or L-cysteine depending on what biosynthetic pathway is used (Seebeck, 2010; Bello *et al.*, 2012). A variation in the biosynthetic pathway occurs in bacteria and fungi through instances of a gene fusion event causing a change of substrates used in the pathway (Figure 1.5).
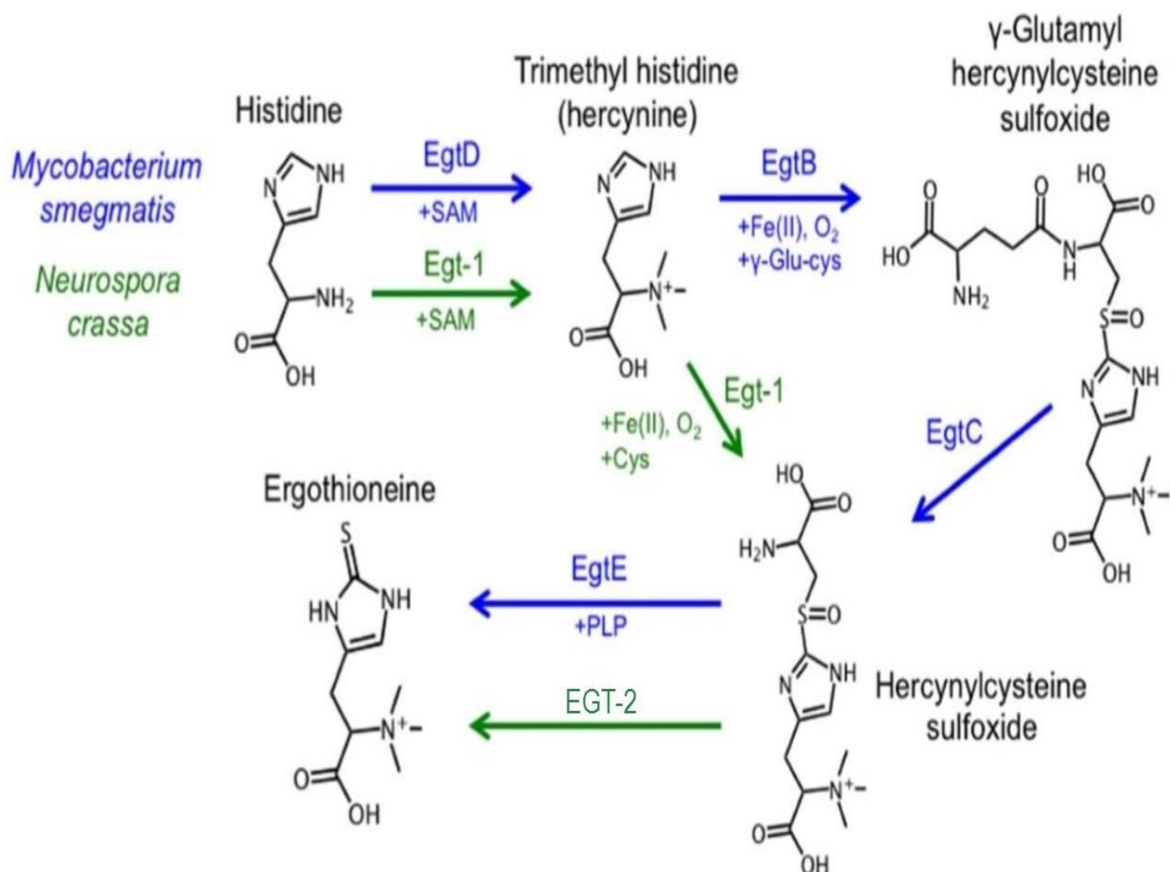
Figure 1.5 The ergothioneine biosynthetic pathways in *M. smegmatis* and *N. crassa*. Note how only 2 enzymes are required by *N. crassa* to synthesize EGT unlike *M. smegmatis* which requires 5 including EGTA to produce the substrate γ-glu-cys. EGT-1 like EGTD acts as a methyl transferase using the universal methyl donor SAM. However, when catalysing the C-S bond EGT-1 uses cysteine instead of γ-glu-cys as a substrate producing one less intermediate γ-glutamyl hercynyl sulfoxide. Both EGT-2 and EGTE carry out the same function as a desulfurase cleaving the C-S bond leaving the sulphur attached to C2 on the imidazole ring. Adapted from Pluskal *et al*., 2014.

In mycobacteria such as *Mycobacterium smegmatis* and *Mycobacterium tuberculosis* a 5 gene cluster (*egtA, egtB, egtC, egtD* and *egtE*) is responsible for the biosynthesis of EGT (Seebeck, 2010; Emani *et al*., 2013; Saini *et al*., 2015). EgtD identified by Seebeck (2010), as a methyltransferase transfers 3 methyl groups onto L-histidine using S-adenosyl methionine (SAM) as a cofactor forming hercynine the first step in EGT biosynthesis (Seebeck, 2010; Vit *et al*., 2014). EgtA was identified as a γ-glutamylcysteine ligase suggesting γ-glu-cys was the sulphur donor rather than cysteine. EgtB a sulfoxide synthase catalyses the formation of a C-S bond in an O_2 dependant manner using hercynine and γ-glu-cys as ligands in an octahedral iron binding site (Goncharenko *et al*., 2015). Fe(II) is required as a cofactor to initiate the catalytic mechanism for C-S bond formation by an iron(III)-complexed thiyl (Goncharenko *et al*., 2015; Seebeck, 2010). $FeSO_4$ acts as the iron cofactor for the iron(III)-complexed thiyl radical which attacks the imidazole ring of hercynine catalysed by EgtB using hercynyl and γ-glu-cys as substrates to produce S-hercynyl-γ-glutamylcysteine (Goncharenko *et al*., 2015). EgtC a glutamine amidohydrolase removes the γ-glutamyl tail generating hercynylcysteine sulfoxide (Vit *et al*., 2015). The final step is carried out by EgtE a pyridoxal-5-phosphate-dependent ß-lyase which cleaves the cysteine residue causing a net transfer of the sulphur atom from cysteine to histidine forming EGT (Seebeck, 2010; Song *et al*., 2015).

The *Neurospora crassa egt-1 (Ncegt-1)* was the first fungal EGT biosynthetic gene identified by Bello *et al* in *Neurospora crassa. Ncegt-1* was identified as a fusion protein of EgtD and EgtB containing a SAM dependant methyltransferase domain as well as a sulfoxide synthase domain (Bello *et al*., 2012). This fusion event is not restricted to fungal species, Jones *et al* observed 2 independent instances with 5 species of the α-protobacteria order having a fusion protein of *egtB* and *egtD* (Jones *et al*., 2014). The Egt-1 fusion protein is still more common in fungi with 73 Egt-1 orthologues identified based on NcEgt-1 however all Saccharomycotina species are missing Egt-1 (Bello *et al*., 2012; Jones *et al*., 2014). It is interesting that many species that produce ergothioneine do not have orthologues to the genes *egtA, egtC* or *egtE* suggesting they are not as crucial as *EgtB* and *EgtD* (Jones *et al*., 2014; Pfeiffer *et al*., 2011). Further evidence from *M. tuberculosis* has shown how *egtB* and *egtD* are expressed in tandem unlike *EgtA, EgtC* or *EgtE* suggesting other enzymes may play a role in completing the biosynthesis of EGT (Jones *et al*., 2014).

1.7 Ergothioneine redox activity and potential uses

In vitro EGT is known to be a powerful scavenger of hydroxyl radicals (OH), hypochlorous acid (HOCL), and peroxynitrite (ONOO⁻) (Whiteman & Halliwell 1997), (Franzoni *et al*., 2006). EGT was also shown to deactivate singlet oxygen at a higher rate than other simple thiols including GSH (Rougee *et al*., 1988). *In vitro* EGT has been demonstrated to chelate divalent metal ions and to form complexes with Cu^{2+}, Hg^{2+}, Zn^{2+}, Cd^{2+}, $Co2^+$, Fe^{2+}, and Ni^{2+} (Hanlon, 1971; Motohashi *et al*., 1974). A molar ratio of 2:1 is formed with metal ions the most stable being Cu^{2+} (Motohashi *et al*., 1974). This was taken one step further by Zhu *et al* who identified EGT as protecting DNA and protein against damage induced by Cu^{2+}, hydrogen peroxide and ascorbate by forming a redox inactive EGT-Cu complex *in vitro* (Zhu *et al*., 2011). This is unlike GSH which has been shown to generate superoxide anions when in a Cu(I)-GSH complex (Speisky *et al*., 2008). However *in vivo* studies have shown EGT not to be involved in sequestering Cu^{2+} (Bello *et al*., 2012).

EGT is noted to be highly stable especially at physiological pH, a contributing factor of this is its unique oxidation. Servillo *et al.,* (2015) demonstrated that EGT in the presence of either hypochlorite, peroxynitrite or hydrogen peroxide were shown to produce the products EGT disulphide, EGT sulfonic acid and hercynine *in vitro* (Figure 1.6). Further analysis showed that EGT disulphide decomposed into EGT sulfenic acid and EGT with ESOH as well breaking down into EGT and ESO_2H (Figure 1.7), (Servillo *et al*., 2015). This perhaps helps explain how even a low EGT diet causes its accumulation in tissues and to remain there for a considerable length of time compared to other thiols such as GSH (Halliwell *et al*., 2016).
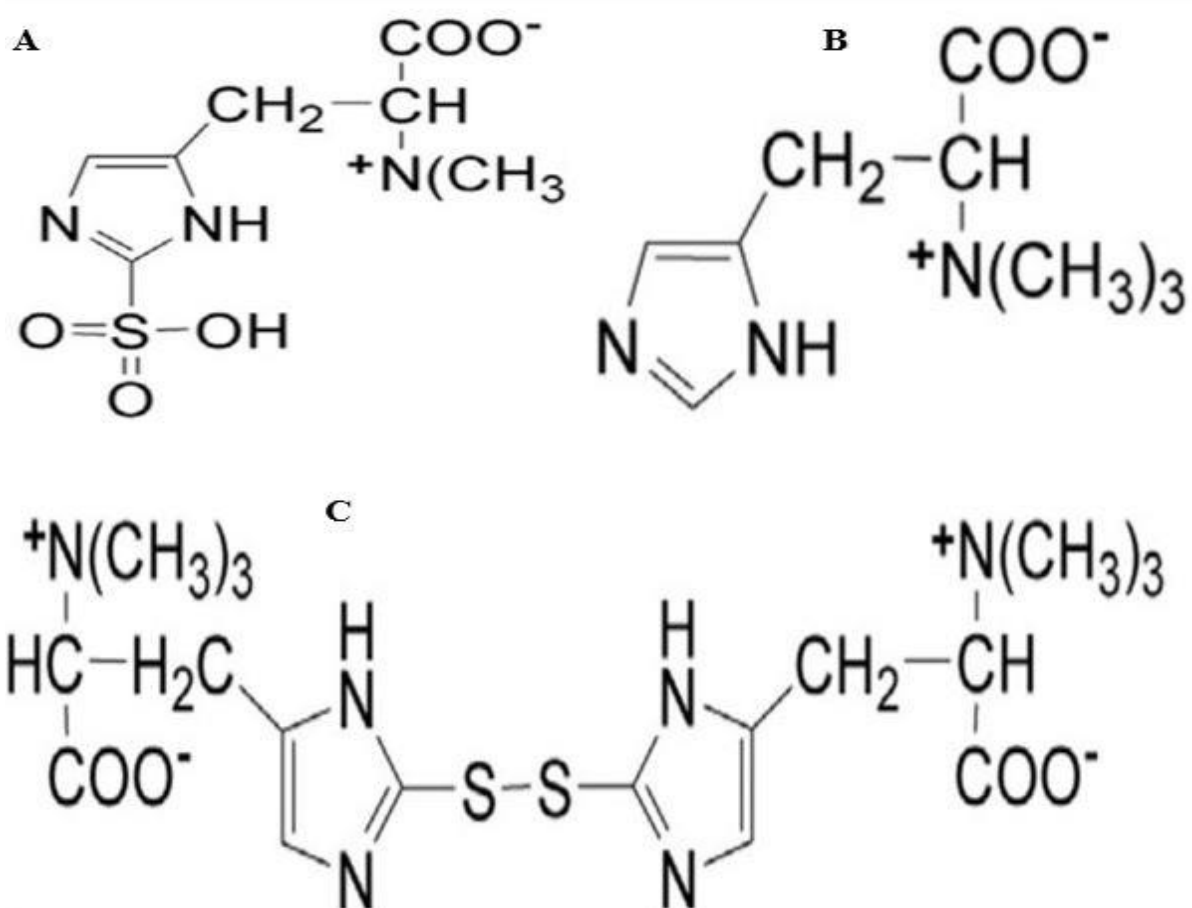
Figure 1.6 A-C Novel products of the oxidation of ergothioneine by the ROS hypochlorite, peroxynitrite and hydrogen peroxide. (A) Ergothioneine sulfonic acid (ESOH), (B) hercynine (EH) and (C) ergothioneine disulphide (ESSE). Adapted from (Servillo *et al.*, 2015).

$$ESH + ROS \rightleftharpoons ESSE$$

$$2\ ESSE + H_2O \rightleftharpoons 2\ ESOH + 2\ ESH$$

$$2\ ESOH \rightleftharpoons ESO_2H + ESH$$

$$ESO_2H + ESH \rightleftharpoons EH + H_2SO_2$$
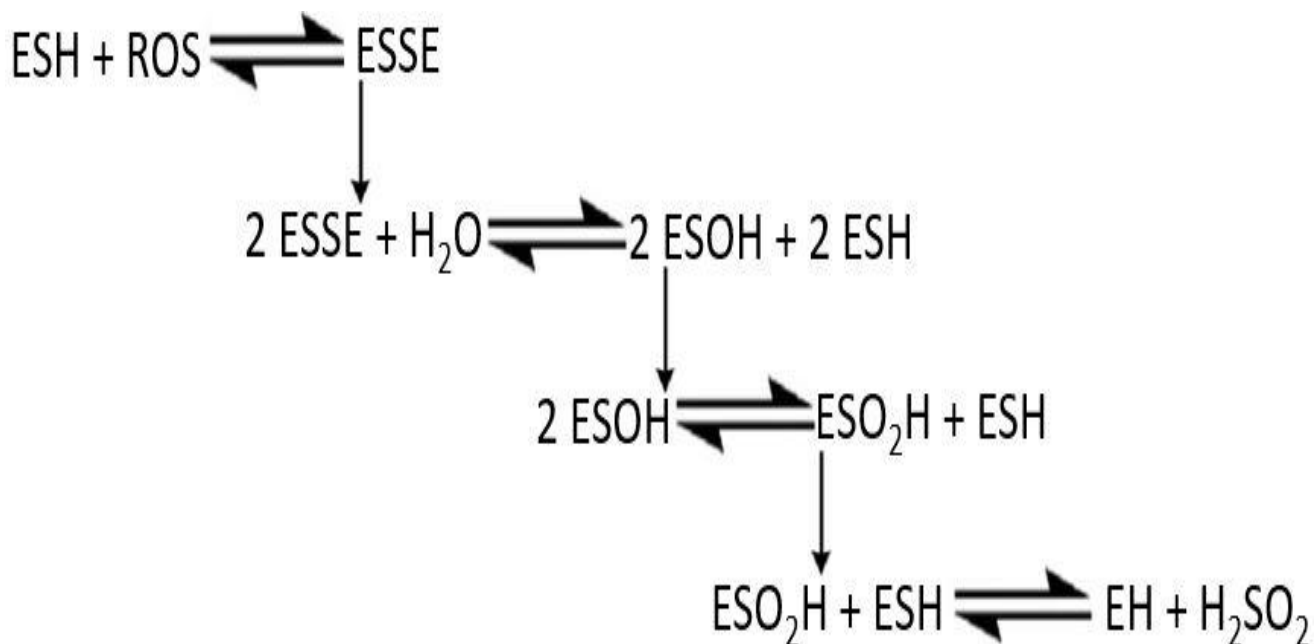
Figure 1.7 A-D Proposed decomposition of EGT. EGT reacts with ROS undergoing oxidation into ESSE which undergoes hydrolysis. Each 2 mol of ESSE disproportionates into 2 mol of highly reactive ESOH and 2 mol of EGT. 2mol of ESOH disproportionates into 1 mol of ESO_2H and 1 mol of EGT. ESO_2H then decomposes irreversibly into EH and H_2SO_2 (Servillo *et al*., 2015).

No functional role of EGT has been conclusively determined yet for EGT in mammalian tissue. EGT has demonstrated as having considerable antioxidant activity *in vitro* however its role *in vivo* is still unclear. One possible role may be as a cytoprotectant from ultraviolet (UV) light which damages skin by inducing ROS (Norins, 1962). Studies have shown EGT to protect against UV damage and absorb light in the UV range (Cheah & Halliwell, 2012). The cytoprotective effect of EGT against UV damage of cells is well documented (Botta *et al*., 2008; Pinnell *et al*., 2009). EGT has been shown to be of use in the food industry acting as a preservative to prevent discolouration of red meat and fish as well as inhibiting lipid peroxidation and melanin blackspot formation from phenoloxidase activity (Bao *et al*., 2010; Fedorova *et al*., 2008).

1.8 The ergothioneine transporter

OCTN1 the EGT transporter (ETT) is a Na^+ dependant membrane protein of the SLC22A4 transport protein family identified by Gründemann (2012). ETT has a highly conserved amino acid sequence between orthologues such as rat with 85.5 % similarity (Gründemann, 2012). Its 3D structure has not yet been elucidated but from hydropathy plot analysis it has a large extracellular loop with multiple potential N-glycosylation sites between its transmembrane regions 1 and 2 with multiple potential phosphorylation sites (Gründemann, 2012). ETT has a very high specificity for EGT compared to other similar compounds such as hercynine and carnitine with a 25 and 100 fold lower transport rate respectively (Cheah & Halliwell, 2012 ;Gründemann *et al*., 2005). High expression of ETT is directly linked to the accumulation of high quantities of EGT intracellularly as EGT is prevented from crossing the cell membrane due to it being a hydrophilic zwitterion(Gruber *et al*., 2013). Because of this expression of ETT gives insight into EGT activity due to the selectivity of ETT for EGT. Cells such as developing red blood cells, seminal vesicles all express ETT highly and have been shown to contain EGT at high levels (Nikodemus *et al*., 2011; Paul & Snyder, 2009).

ETTs main site of localisation is the plasma membrane and reportedly at the mitochondria but this is not yet clear. Lamhonwah & Tein (2006) identified the majority of ETT in the membrane of mitochondria using a GFP fusion protein of human ETT at the N-terminus. However it was argued by Gründemann (2012), that this study was invalid as the fusion construct lacked 34 original amino acids of the N-terminus including 13 out of the 21 amino acids in the transmembrane segment 1 and had an additional 36 non-natural amino acids. This was supported by Bacher *et al*., (2009) who showed that GFP attached to the C terminus of human ETT with the original amino acid structure was located in the plasma membrane only. Contrary to this Kawano *et al*., (1982) in a study demonstrated that radiolabelled EGT fed to rats accumulated most in the mitochondria. Paul & Snyder (2009) in a comprehensive *in vivo* study silenced ETT expression in HeLa cells using RNAi knockdown. They demonstrated how HeLa cells no longer expressing ETT had a higher degree of mitochondrial DNA (mtDNA) damage than cells which still had ETT after cells were supplemented with EGT and stressed with hydrogen peroxide. From such studies evidence suggests ETT is expressed on the mitochondrial membrane as well as the plasma membrane of cells and may have an antioxidant role in the mitochondria protecting mtDNA

however more *in vivo* studies need to be undertaken (Kawano *et al*., 1982; Lamhonwah & Tein, 2006; Paul & Snyder, 2009).

1.9 Conditions associated with ergothioneine

1.9.1 The role of ergothioneine in inflammatory diseases

The transcription factor NF-κß which regulates inflammatory genes has binding sites in the promoter of human ETT and actively regulates its expression (Maeda *et al*., 2007). ETT expression has also seen to be upregulated by inflammatory cytokines (Tokuhiro et al. 2003; Peltekova *et al*., 2004; Taubert *et al*., 2009; Rahman *et al*., 2003; Maeda *et al*., 2007). This accounts for a higher level of EGT in erythrocytes of rheumatoid arthritis sufferers as inflammatory cytokines are also upregulated (Taubert *et al*., 2006). With this in mind EGT could perhaps act as a biomarker in certain inflammatory diseases (Gründemann, 2012). ETT is also seen to be selectively expressed when needed during different developmental stages such as being highly expressed in foetal liver and during liver regeneration but not in adult liver (Nakamura *et al*., 2007; Gründemann, 2012).

ETT upregulation has been associated with auto-inflammatory diseases such as rheumatoid arthritis, ulcerative colitis, Crohns disease and neurodegenerative diseases such as Parkinson's and Alzheimer's disease (Maeda *et al*., 2007; Kato *et al*., 2010; Santiago *et a*l., 2006; Taubert *et al*., 2006). The ETT gene is in close proximity to genes involved in inflammatory responses such as the caspase recruitment domain family and CARD 15 (Bene *et al*., 2006). ETT is also highly expressed in $CD14^+$ macrophages and monocytes both with a key inflammatory role (Paul & Snyder, 2009). Silencing of ETT in HeLa cells has shown cells pre-treated with 1 mM EGT have been significantly more resistant to hydrogen peroxide than HeLa cells deficient of ETT with a distinct correlation between ETT depletion and apoptosis (Paul & Snyder, 2009). EGT has also been shown to inhibit the release of the pro-inflammatory cytokine IL-8 by inhibiting there release from TNF-α in alveolar macrophages (Rahman *et al*., 2003). Patients with rheumatoid arthritis have high levels of EGT in there synoviocytes (Nakamura *et al*., 2007).

1.9.2 The role of ergothioneine in Crohns Disease

Polymorphisms in the ETT gene SLC22A4 have been attributed to several diseases and the information is as of yet inconclusive. European patients with Crohns disease CD have been identified as having significantly lower blood levels of EGT in their blood as well as a high risk haplotype identified by single nucleotide polymorphisms present at the IBD5 locus in SLC22A4 (Kato *et al*., 2010) . These mutations are L503F and G207C, with L503F being of great interest due to it increasing the ETT intrinsic transport efficiency by 50% compared with the non-risk variant 503L (Taubert *et al*., 2009). However a study by Fisher *et al*., (2006) concluded the frequencies of individuals who did not carry the general IBD5 risk haplotype was not significantly different in cases and controls. A study of Japanese CD sufferers also came to the conclusion the mutations L503F and G-207C attributed with disease pathology in Caucasian CD patients were not present at all in any of the patients tested (Kato *et al*., 2010). This indicates these mutations may not be involved in disease etiology and could perhaps be used as a genetic marker for CD in European patients. Patients with CD have been identified as having significantly lower levels in their blood indicating that perhaps EGT is undergoing oxidation (Kato *et al*., 2010).

1.9.3 Ergothioneine protects against Neurodegeneration

EGT has been identified in mammalian cells at a concentration between 1 and 2 mM and is able to permeate the blood brain barrier (Yang *et al*., 2012). EGT is detected in sheep, rat, guinea pig, rabbit, cat and mouse brains between 0.3 and 1 mg per 100 g of brain tissue (Briggs, 1972; Crossland *et al*., 1966; Kaneko *et al*., 1980). EGT exhibits a protective role against neurodegeneration *in vitro* and *in vivo*. Rat pheochromocytoma cells (PC12) are a common model for neurobiological studies possessing neuron like features such as neurite formation and terminal differentiation in response to growth factors as well as expressing ETT. Cisplatin is an anti-tumour agent that has nephrotoxic and neurotoxic side effects when administered during chemotherapy. When cisplatin is incubated with PC12 cells a marked decrease in PC12 proliferation as well as strong inhibition of axon and dendrite growth was observed. When PC12 cells were incubated with EGT prior to incubation with cisplatin the effects of cisplatin were significantly inhibited (Song *et al*., 2010). An *in vivo* study also demonstrated how mice injected with cisplatin had increased learning and memory deficits

compared to mice injected with cisplatin and fed a high EGT diet which significantly restored learning and memory deficits (Song *et al*., 2010).

EGT has been shown *in vivo* to protect against the ß-amyloid peptides which are neurotoxic and contribute to Alzheimer's disease (Pike *et al*., 1991). Mice given a dose of ß-amyloid directly into the hippocampus showed increased brain lipid peroxidation and acetylcholinesterase activity, significant decreases in GSH as well as significant decreases in superoxide dismutase activity of brain tissue (Yang *et al*., 2012). Groups fed a dose a low as 0.5 EGT/ kg daily over two separate intervals before and after injection of ß-amyloid showed a significant decrease in brain lipid peroxidation and acetylcholinesterase activity, a significant decrease in the decline of GSH as well as significantly increasing the level of superoxide dismutase activity in brain tissue (Yang *et al*., 2012).

1.9.4 The role of ergothioneine in Parkinsons disease

As noted ETT is present on the membrane of mitochondria with high levels of EGT shown to accumulate there (Lamhonwah & Tein, 2006). MtDNA is uniquely susceptible to oxidative damage as unlike nuclear DNA mtDNA is not protected by histones and lacks efficient DNA repair mechanisms (Godley *et al*., 2005). Evidence suggests that mitochondria contribute to aging and cognitive decline by production of ROS which are produced as part of the electron transport chain of mitochondria (Gruber *et al*., 2013). ROS damages mtDNA causing point mutations which increase as the individual ages (Lin & Beal, 2006 ;Trifunovic *et al*., 2005). With the brain being a high energy organ ROS damage to mtDNA has been identified as being involved in neurodegenerative diseases such as Parkinson's disease (PD) and Alzheimer's disease (Lin & Beal, 2006). Clinical studies of patients with PD contain significantly lower levels of EGT as well as the antioxidant bilirubin in blood indicating elevated levels of oxidative stress (Hatano *et al*., 2015). The reduced level of EGT correlated with disease severity and may have potential to use EGT as a biomarker in PD as well as a supplement to help maintain redox balance lost during PD. It has been argued that EGT now meets the requirement to be designated a vitamin as its deficiency has been shown to have several cytotoxic consequences in cell lines both *in vivo* and *in vitro* (Cheah & Halliwell, 2012; Paul & Snyder, 2009; Rahman *et al*., 2003). EGT has been suggested as a dietary supplement to treat chronic obstructive pulmonary disease (Biswas *et al*., 2013). However as

of yet EGT deficiency on its own has not been shown to cause disease (Cheah & Halliwell, 2012; Kawano *et al*., 1982; Kato *et al*., 2010).

1.10 Ergothioneine in Bacteria and Fungi

1.10.1 The role of ergothioneine in redox homeostasis, virulence and NP production in Bacteria

Mycobacteria do not produce GSH the well-established antioxidant known for its efficient scavenging and detoxifying of ROS such as hydrogen peroxide (Lu, 2013) . Instead Mycobacteria produce low molecular mass thiols MSH and EGT (Van Laer *et al*., 2013). In *M. tuberculosis* MSH deficient mutants have been shown to have increased sensitivity to oxidative stress, alkylating agents as well as a range of antibiotics such as erythromycin, vancomycin and streptomycin (Saini *et al*., 2015). EGT has also been shown to play a role in redox balance which is essential for energy metabolism, such as glycolysis, the tricarboxylic cycle and oxidative phosphorylation (Saini *et al*., 2015). In *M. tuberculosis* EGT was identified to be regulated by the oxidative stress sensor and regulator of bioenergetics homeostasis WHIB3 (Saini *et al*., 2015). MSH and EGT have both been shown to be critical for bioenergetic redox homeostasis with a lack of either altering cellular respiration (Saini *et al*., 2015).

Upregulation of EGT biosynthesis in *Mycobacterium* has also been identified in nutrient starved conditions by a decrease in phosphorylation of the methyltransferase EGTD on T-213. (Richard-Greenblatt *et al*., 2015). EGT has been identified as playing a role in the virulence of *M. tuberculosis* with EGT biosynthesis upregulated during the infection of mice and macrophages as well as required for long term infection (Saini *et al*., 2015; Richard-Greenblatt *et al*., 2015). Additionally EGT in *M. tuberculosis* mediates resistance to antibiotics such as rifampicin and isoniazid (Saini *et al*., 2016). However studies using *M. smegmatis* which secretes EGT and have shown it to protect against peroxides but not increase susceptibility to antibiotics such as isoniazid, ethambutol and kanamycin in *egtD* deletion mutants (Emani *et al*., 2013)

For first time EGT has shown to be involved in enzymatic reactions involving the biosynthesis of the antibiotic lincomycin in *Streptomyces lincolnensis*. EGT was shown to be involved in a unique S-glycosylation step acting as a carrier of the lincomycin precursor

lincosamide and is removed by a unique thiol exchange with mycothiol which allows the recycling of EGT (Zhao *et al*., 2015). Cyanobacteria have also been seen to produce large quantities of EGT, and also produce GSH (Pfeiffer *et al*., 2011). Interestingly deletion of *gshB* in *Cyanobacterium synechocystis* which codes for a GSH synthase protein caused abolition of intracellular EGT production causing accumulation of the precursor hercynine (Narainsamy *et al*., 2015). This indicates a different EGT biosynthetic pathway dependant on GSH.

1.10.2 The role of ergothioneine in redox homeostasis in Fungi

In *N. crassa in vivo* EGT was shown to be one third the antioxidant capacity in conidia, protecting conidia against peroxide damage, but played no significant role in antioxidant stress in the mycelia (Bello *et al*., 2012; Bello *et al*., 2014). EGT involvement in protection of DNA was investigated with EGT having no effect on the rate of DNA mutation caused by UV light (Bello *et al*., 2014). In *A. fumigatus* deletion of the *gliK* gene involved in gliotoxin biosynthesis and mediation of oxidative stress caused a significant increase in the level of intracellular EGT indicating an attempt by the fungus to mediate resistance to increased oxidative stress (Gallagher *et al*., 2012). In the fission yeast *Schizosaccharomyces pombe* EGT production has been identified as well as the genes responsible *egt-1* and *egt-2*. In overexpression or deletion mutants of *egt-1* no increase in resistance or increased sensitivity to ROS was observed when mutants were exposed to hydrogen peroxide and tert-butyl hydroperoxide (Pluskal *et al*., 2014). Interestingly it was also shown that supplementation of media with sodium selenate allowed the synthesis of the selenium analogue to EGT selenoneine (Pluskal *et al*., 2014). Selenoneine has been shown be present in fish such as mackerel and tuna and to have antioxidant properties *in vitro* (Yamashita *et al*., 2013)This shows the flexibility of EGT-1 to bind to other substrates most likely selenocysteine as an alternative substrate to cysteine as hercynyl selenocysteine was also identified using metabolomic analysis (Pluskal *et al*., 2014).

1.11 The use of yeast in biotechnology

Yeast are single celled eukaryotic organisms often used for producing recombinant proteins that are not well produced in bacteria such as *E. coli* because of problems with folding or glycosylation. They are easier and less expensive to work with than mammalian cells such as Chinese hamster ovary (CHO) cells (Demain & Vaishnav, 2009). Yeast is used to produce vaccines against tumour antigens such as vaccines generated against RAS antigens on RAS oncoproteins (Ardiani *et al*., 2010). It can also secrete protein into the supernatant with the proper signals and produce high levels of heterologous recombinant protein such as producing 9 g/L of the enzyme glucose oxidase (Demain & Vaishnav, 2009).

1.11.1 *S. cerevisiae* as a cell factory

Saccharomyces cerevisiae was the first eukaryotic cell engineered to express heterologous proteins due to it possessing many favourable features such as rapid growth by cell division, having its own autonomously replicating plasmid, its formation of discrete colonies and ability to carry out post translational modifications of expressed proteins (Curran and Bugeja, 2011). *S. cerevisiae* has GRAS status having a long history of safe use in the commercial fermentation process and unlike *Escherichia coli* does not produce pyrogens and endotoxins (Rosales-Mendoza *et al*., 2015). *S. cerevisiae* is excellent at producing recombinant proteins from other eukaryotic organisms and is used successfully to produce insulin and hepatitis B vaccine (Demain & Vaishnav, 2009). However *S. cerevisiae* mediated over glycosylation of N linked sites can cause reduced activity and immunological problems in the production of mammalian recombinant proteins (Demain & Vaishnav, 2009). Better engineering of strains and the development of protease-deficient strains will allow increased production of mammalian proteins such as interferon ß (Tomimoto *et al*., 2013; Zhang *et al*., 2012) . This makes *S. cerevisiae* an ideal for the expression of recombinant proteins.

1.12 Aims of Study

Characterisation and elucidation of the small molecule EGT has shown it may play a role as an antioxidant and cytoprotective *in vivo*. These interesting cellular roles make EGT a potential nutraceutical and perhaps capable of being utilized as a food additive. However no economically viable means of producing EGT has yet been established.

To achieve this:

1)   The primary objective of this study is to biosynthetically produce the natural product EGT in the yeast *S. cerevisiae* by expression of recombinant EgtA from *A. fumigatus*, or with the co-expression of other foreign genes if required.

2)   Quantify how much EGT is being produced by the expression of recombinant proteins in *S. cerevisiae* and determine if EGT is inside the cell or in the culture supernatant.

3)   Investigate whether production of EGT by *S. cerevisiae* has any benefit to the organism such as alleviation of oxidative stress.

4)   Identify ways to increase the amount of EGT produced by *S. cerevisiae* through further genetic manipulation of EgtA and *S. cerevisiae* and in doing so gain a better understanding of how EGT is produced in *S. cerevisiae*

Chapter 2
Materials and Methods

2.1 Materials

2.1.1 Strains in this study

Table 2.1 *S. cerevisiae* and bacterial strains used

Strain	Genotype	Source
BY4741	MATa *his3*Δ 1; *leu2*Δ; *met15*Δ 0; *ura3*Δ 0	Euroscarf
R1158	MATa *his3*Δ 1; *leu2*Δ; *met15*Δ; pNFS1::kanR-tet07-TATA; *ura3*::CMV-tTA	Dharmacon
R1158	MATa *his3*Δ 1; *leu2*Δ; *met15*Δ; pSAH1::kanR-tet07-TATA; *ura3*::CMV-tTA	Dharmacon
Y258	MATa pep4-3; his4-580; ura3-52; leu2-3	Dharmacon
Top 10	*E. coli*	This study
Xli-blue	*E. coli*	This study

2.1.2 Plasmids used in this study

Table 2.2 Plasmid vectors used in this study

Plasmid name	Description	Source
PUC57	*E. coli* expression vector	Genscript
pRS316	Centromeric *Saccharomyces cerevisiae* shuttle vector- *URA3* marker	Sikorski and Hieter, 1989
pC210	*SSA1* under control of *SSA2* promoter- *LEU2* marker	Schwimmer and Masison, 2002
p413-ADH	Low copy centromeric plasmid with an *ADH* promoter based on the pRS vector series- *HIS3* marker	Mumberg, *et al* 1995

p413-GPD	Low copy centromeric plasmid with a *GPD* promoter based on the pRS vector series- *HIS3* marker	Mumberg, *et al* 1995
p416-ADH	Low copy centromeric plasmid with an *ADH* promoter based on the pRS vector series- *URA3* marker	Mumberg, *et al* 1995
p416-GPD	Low copy centromeric plasmid with a *GPD* promoter based on the pRS vector series- *URA3* marker	Mumberg, *et al* 1995
p423-ADH	High copy 2μ plasmid with an *ADH* promoter based on the pRS vector series- *HIS3* marker	Mumberg, *et al* 1995
p423-GPD	High copy 2μ plasmid with a *GPD* promoter based on the pRS vector series- *HIS3* marker	Mumberg, *et al* 1995
p426-ADH	High copy 2μ plasmid with an *ADH* promoter based on the pRS vector series- *URA3* marker	Mumberg, *et al* 1995
p426-GPD	High copy 2μ plasmid with a *GPD* promoter based on the pRS vector series- *URA3* marker	Mumberg, *et al* 1995
p426-GPD-egtA	*Aspergillus fumigatus egtA* under control of *GDP* promoter- *URA3* marker	This study
P423-ADH-egta	*Aspergillus fumigatus egt2a* under control of *ADH* promoter- *HIS3* marker	This study
P423-ADH-egt2b	*Aspergillus fumigatus egt2b* under control of *ADH* promoter- *HIS3* marker	This study

2.1.3 Primers used in this study

Table 2.3 Primer sequences used in this study

Primer name	Sequence (5'-3')
EgtA F	AAATTTACTAGTATGTCCCCGTTGCCG
EgtA R	AATTCCCTCGAGCTACTGGCTGCGCACG
EgtA Internal F	AGAACCTACAGCGTCCCACTG
EgtA Internal R	CTTGACCTCCTCATAAGTGGG
Egt-2a F	AGATGCACTAGTATGTCCGCTCCCACA
Egt-2a R	AAGTCAGAATTCTCACAACTTTGGCTC
Egt-2b F	GGGCCCACTAGTATGTCTAGCGTTACGCCATCT
Egt-2b R	GGGCCCGAATTCCTAATGCTGACTCCATTGGAT
EgtA N-terminal His tag	AGAACTAGTATGCATCATCACCACCACCATGTCCCCGTTGCCGTGTCC
Egt-2a N-terminal His tag	GGGCCCACTAGTATGCATCATCACCACCACCATATGTCCGCTCCCACA
Egt-2b N-terminal His tag	GGGCCCACTAGTATGCATCATCACCACCACCATATGTCTAGCGTTACGCCATC
Egt-2b C-terminal His tag	GAGGAATTCCTAATGGTGGTGGTGATGATGATGCTGACTCCATTGGAT

Pc210 F	CAACCAACCCTTTTACGGTCTC
Pc210 R	AATTAGTACGGGCGTGTGGTCT
ADH F	GTTTCCTCGTCATTGTTCTCG
GPD F	CGGTAGGTATTGATTGTAATTCTG
CYC R	GTTGTCTAACTCCTTCCTTTTCG
T213A F	GGCTAGATGCTTGTGCAGACCCGGACAAGG
T213A R	CCTTGTCCGGGTCTGCACAAGCATCTAGCC

2.1.4 Reagents used in this study

All chemicals and reagents were ordered from Sigma-Aldrich ltd, unless otherwise stated.

2.1.4.1 Hydrogen Peroxide

A 30% (w/w) stock of H_2O_2, 9.8 M was ordered and kept at 4 °C This was diluted in in molten agar (50 - 60 °C) to the desired molarity.

2.1.4.2 Ampicillin

Ampicillin salt was added to 100 ml dH_2O to create a 50 mg/ml stock, which was filter sterilised and stored at -20 °C until required.

2.1.4.3 100 % Trichloroacetic acid solution

Trichloroacetic acid (20 g) was added to 9.1 ml of dH_2O and let dissolve to create a 100 % TCA solution.

2.1.5 Microbiological reagents used in this study

2.1.5.1 Yeast Peptone Dextrose (YPD)

Bacto-yeast extract (10 g, BD & Co.), bacto-peptone (20g, BD & Co.) and D-glucose

2.1.5.2 YPD Agar

Bacto-Agar (20 g, BD & Co.) was added to liquid YPD prior to being made up to 1 L with dH$_2$O. This was then autoclaved, allowed to cool and poured into sterile petri dishes under sterile conditions till it had solidified. Subsequent agar plates were stored at 4 °C until required.

2.1.5.3 Dropout Mix

The following amino acids (2 g) were added to a sterile pestle and mortar (Table 2.4) where they were ground and mixed and stored at RT:

Table 2.4 Amino acids required for dropout mix

Amino Acid
Alanine, Arginine, Aspartic acid, Cysteine, Glutamic acid, Glutamine, Isoleucine, Phenylalanine, Proline, Serine, Threonine, Tyrosine, Valine, Inositol, para-aminobenzoic, lysine

2.1.5.4 Amino Acid Supplemental Stocks

Strains used in this study are auxotrophic for particular amino acids depending on their genotypes background (Table 2.1). Working stocks of amino acid supplemental stocks were made as described (Table 2.5).

Table 2.5 Amino acid stock concentrations and final concentration when added to SC media

Amino acid	Working Stock Conc.	Volume added to 1 L SC media	Final Amino acid Conc. (µg/ml)
L-Leucine	1 g/100 ml	10 ml	100
L-Histidine	1 g/100 ml	2 ml	20
L-Uracil	0.2 g/100 ml	10 ml	20
L-Methionine	1 g/100 ml	2 ml	20
L-Lysine	0.2 g/100 ml	10 ml	20

2.1.5.5 Synthetic Complete (SC) media

Yeast nitrogen base (YNB) without amino acids (6.7 g, BD & Co.), D-glucose (20 g) and dropout mix (1.5 g) were added to 800 ml dH_2O and dissolved. This was supplemented as required with the necessary amino acids using stocks as described in Section 2.1.5.4. This was topped up to 1 L using dH_2O, autoclaved and stored at room temperature.

2.1.5.6 SC agar

Bacto-Agar (20 g) was added to liquid SC prior to being topped up to 1 L using dH_2O. This was autoclaved and then allowed to cool. SC agar plates were stored at 4 °C.

2.1.5.7 Phosphate Buffered Saline (PBS)

PBS (1 X tablet; Oxoid Ltd., Basingstoke, Hampshire, England) was added to 200 ml of dH_2O and autoclaved. PBS was stored at room temperature until required.

2.1.5.8 Phosphate Buffered Saline-Tween-20 (PBST)

Tween-20 (0.1 ml) was added to 200 ml PBS (Section 2.1.3.7). This was filter sterilised through a 45 µm filter to create 50 ml aliquots which were stored at room temperature.

2.1.5.9 Luria-Bertani (LB) Broth

LB broth (25 g, Difco, Maryland, USA) was added to 1 L dH_2O and dissolved with the aid of a magnetic stirring rod. LB solution was autoclaved and stored at 4 °C.

2.1.5.10 LB Agar

LB agar (40 g Difco, Maryland, USA) was added to 1 L dH_2O and dissolved with the aid of a magnetic stirring rod. LB agar was autoclaved and once cool, was poured (25 ml) under sterile conditions into petri dishes. Solidified agar plates were stored at 4 °C until required.

2.1.5.11 LB Broth + Ampicillin

LB broth was made up as previously described in Section 2.1.5.9. Before inoculation, using a 50 mg/ml ampicillin stock, ampicillin (0.1 mg/ml) was added and LB-agar-ampicillin was poured (25 ml) under sterile conditions into petri dishes.

2.1.5.12 LB Agar + Ampicillin

LB agar was made up as previously described in Section 2.1.5.10. Before inoculation, using a 50 mg/ml ampicillin stock, ampicillin (0.1 mg/ml) was added to 5 ml LB broth.

2.1.5.13 Sabouraud-Dextrose (SB) media

Sabouraud-Dextrose media (30.12 g ; Oxoid Ltd, Basingstoke, Hampshire, England) was added to 800 ml dH$_2$O and dissolved. Solution was made up to 1 L and autoclaved. SB media was stored at 4 °C until required.

2.1.6 Agarose Gel Electrophoresis Reagents

2.1.6.1 50 X Tris-Acetate (TAE)

Trizma base (342 g) was added to 57.1 ml of glacial acetic acid and 100 ml of EDTA (0.5 M). This was pH adjusted to pH 8.0 and made up to 1 L with dH$_2$O and stored at room temperature.

2.1.6.2 1 X TAE

50 X TAE (20 ml) (Section 2.1.4.1) was added to 980 ml dH$_2$O. 1 X TAE was mixed and subsequently stored at room temperature until required.

2.1.6.3 0.8 % (w/v) Agarose Gel

Agarose (0.4 g) was dissolved in 50 ml 1 X TAE (Section 2.1.4.1). This was brought to boil until all the agarose had been dissolved then allowed to cool until 'hand hot'. Ethidium bromide was added by taking 4 µl of a 10 mg/ml stock which was mixed into the molten agar by pouring the molten agar into a gel casting tray allowing for visualisation of DNA under U.V. lamp.

2.1.7 Yeast Transformation Buffers

2.1.7.1 50 % (w/v) Polyethylene Glycerol (PEG)

PEG (50 g) was dissolved in 100 ml dH$_2$O, autoclaved and stored at room temperature.

2.1.7.2 1 M Lithium Acetate

Lithium acetate (6.59 g) was dissolved in 100 ml of dH$_2$O, autoclaved and stored at room temperature.

2.1.7.3 100 mM Lithium Acetate

1 M Lithium acetate (1 ml) (Section 2.1.5.2) was added to 100 ml of dH_2O that was sterile filtered with a 45 µm filter.

2.1.8 *E. coli* Transformation Buffer

2.1.8.1 Transformation Storage Buffer (TSB)

PEG (1 g), Dimethyl sulfoxide (50 µl), Glycerol (2 ml), 20.4 mg of Magnesium chloride ($MgCl_2$6 H_2O) and 24.6 mg of Magnesium sulphate ($MgSO_4$7 H_2O) was made up to 10 ml using LB broth.

2.1.8.2 5 X KCM

0.5 M Potassium chloride (KCl), 0.15 M Calcium chloride ($CaCl_2$2H_2O) and 0.25 M Magnesium chloride ($MgCl_2$6 H_2O).

2.1.9 Sodium Dodecyl Sulphate-Poly Acrylamide Gel Electrophoresis (SDS-PAGE) Reagents

2.1.9.1 12.5 % SDS-PAGE gel

The materials for both running gel and stacking gel as in table 2.6 and table 2.7 were prepared as follows: 4 X running buffer was prepared by adding 34.75 g of Tris base and 4g SDS was dissolved in 500 ml of dH_2O, pH adjusted to 8. 10 % Ammonium persulfate (APS) 40 mg was added to 400 ul of dH_2O and vortexed into solution. 2 X Stacking buffer was prepared by adding 15 g of Tris base and 0.2 g SDS was dissolved in 500 ml of dH_2O, pH adjusted to 8.

Table 2.6 Running gel

Reagents	Volume
4X Running Buffer	2.5 ml
dH$_2$O	3.3 ml
Protogel	4.15 ml
10 % ammonium persulphate	100 µl
TEMED	10 µl

Table 2.7 Stacking gel

Reagents	Volume
2X Stacking Buffer	1.25 ml
dH$_2$O	0.825 ml
Protogel	400 µl
10 % ammonium persulphate	25 µl
TEMED	2.5 µl

2.1.9.2 1 X Running Buffer

Diluted 4 X running buffer (250 ml) by adding 750 ml of dH$_2$O.

2.1.9.3 6 X Protein Sample Buffer

Made up to 50 ml in milliQ H$_2$O.

Table 2.8 Preparation of 6X protein sample buffer

Reagents	Quantity
2X Stacking Buffer	21 ml
SDS	2.7 g
DTT	385 mg
Bromophenol Blue	3.6 mg
Glycerol	21 ml

2.1.9.4 Coomassie Brilliant blue stain solution

Methanol 30 % (v/v), Acetic Acid 10 % (v/v), and Coomassie brilliant blue G-250 0.1 % (w/v) was made up to a volume of 500 ml with dH_2O.

2.1.9.5 Detaining solution

Ethanol (100 ml) and acetic acid (100 ml) was added to 800 ml of dH_2O.

2.1.10 Western Blot Reagents

2.1.10.1 Towbin Electrotransfer Buffer

Tris (3.03 g), glycine (14.4 g) and methanol (200 ml) was adjusted to 1 L with dH_2O.

2.1.10.2 Blocking buffer

Marvel 5 % (w/v) solution was made by adding marvel (1 g) and Bovine serum albumin 1 % (w/v) was made by adding BSA (200 mg) to 20 ml of PBST (Section 2.1.3.8).

2.1.10.3 Antibody Buffer

Marvel 1 % (w/v) was made by adding marvel (100 mg) and Bovine serum albumin 1 % (w/v) was made by adding BSA (100 mg) to 10 ml of PBST (Section 2.1.3.8).

2.1.10.4 Primary Antibody

Anti-His from mouse (Biolegend Cat no: 652502) was used at a dilution of 1/3000 in antibody buffer (Section 2.1.8.3).

2.1.10.5 Secondary Antibody

Horse radish peroxidase (HRP) anti-mouse IgG from Goat (Biolegend Cat no: 405306) was used at a dilution of 1/3000 in antibody buffer (Section 2.1.8.3).

2.1.11 High Power Liquid Chromatography (HPLC)

2.1.11.1 HPLC System

RP-HPLC analysis was conducted using a Shimadzu prominence HPLC system using a SPD-M20A diode array detector.

2.1.11.2 Mobile Phase Buffer A

Trifluoroacetic (1 ml) acid (TFA) added to 1 L of mH_2O.

2.1.11.3 Mobile Phase Buffer B

Acetonitrile (1 L) had 1 ml of TFA added to it. See 2.1.12.1.

2.1.11.4 Stationary phase

An Agilent Eclipse XDA-C18 column was used for all RP-HPLC work.

2.1.12 Mass Spectrometry Reagents

2.1.12.1 Destaining Buffer

Ammonium bicarbonate (0.79 g) was dissolved in 100 ml deionised H_2O and diluted 1:1 HPLC grade acetonitrile. This was made fresh on the day.

2.1.12.2 Trypsin Reconstitution Buffer

Ammonium bicarbonate (10 mM and 10 % (v/v) HPLC grade acetonitrile was brought to a final volume of 10 ml using deionised H_2O. This was made fresh on the day.

2.1.12.3 Trypsin Digestion Buffer

Trypsin (20 µg) was diluted in a 1.5 ml reconstitution buffer giving 13 ng/µl working stock. Surplus trypsin digestion buffer was stored at -20 °C.

2.1.12.4 50 mM Ammonium Bicarbonate

Ammonium bicarbonate (200 mg)was dissolved in 50 ml deionised H_2O, on the day.

2.1.12.5 Extraction Buffer

A 5 % (v/v) formic acid and HPLC grade acetonitrile were mixed 1:2 (v/v). This was made fresh on the day.

2.1.12.6 0.1 % Formic Acid

A 0.1 % (v/v) formic acid solution was prepared by adding 10 µl of formic acid to 10 ml of deionised H_2O on the day.

2.1.13 Zip Tip buffers

2.1.13.1 Resuspension Buffer

TFA (5 µl) was placed in 995 µl of milliQ H_2O in a 1.5 ml microfuge tube.

2.1.13.2 Equilibration and Wash Buffer

TFA (1 µl) was placed in 999 µl of milliQ H_2O in a 1.5 ml microfuge tube.

2.1.13.3 Wetting Buffer

Acetonitrile (800 µl) was placed in 199 µl of milliQ H_2O with 1 µl of TFA in a 1.5 ml microfuge tube.

2.1.13.4 Elution Buffer

Acetonitrile (600 µl) was placed in 399 µl of milliQ H_2O with 1 µl of TFA in a 1.5 ml microfuge tube.

2.1.13.5 Buffer A

Acetic acid (5 µl) was placed in 975 µl of milliQ H_2O with 20 µl of acetonitrile in a 1.5 ml microfuge tube.

2.2 Methods

2.2.1 Microbiological Methods

2.2.1.1 *S. cerevisiae* growth, maintenance and storage

S. cerevisiae strains were grown on YPD agar plates (Section 2.1.3.2) at 30 °C in a static incubator for 48 h in the dark. For liquid cultures, *S. cerevisiae* strains were inoculated in liquid YPD (Section 2.1.3.1) at 200 rpm (Innova 4000 orbital shaker, New Brunswick Scientific, UK) at 30 °C. Growth and maintenance of those strains which contained plasmids was carried out using SC media (Section 2.1.3.5) or SC agar (Section 2.13.6) lacking an appropriate amino acid to maintain selection for that particular plasmid. Working stocks of strains were kept at 4 °C for short term use and were re-inoculated every few weeks. Long term stocks were generated using 500 µl of freshly grown cells, mixed with 40 % (v/v) glycerol in a 1.5 ml tube. This was then flash frozen using liquid N_2 and stored at -70 °C until required.

2.2.1.2 *E.coli* growth maintenance and storage

E. coli cells were grown on LB-ampicillin plates (Section 2.1.3) and grown at 37 °C, or in LB-amp broth (Section 2.1.3.23) at 37 °C shaking. Working stocks were kept at 4 °C for short term use. Long term stocks were generated using 500 µl of freshly grown cells and mixed with 40 % glycerol (Section 2.1.3.) This was then 'flash frozen' in liquid Nitrogen and stored at -70 °C before use.

2.2.1.3 Measuring *S. cerevisiae* cell density

Overnight cultures were diluted 1/50 by adding 100 µl of culture to 4.9 ml fresh media. The $OD_{600\,nm}$ = was then measured using a spectrophotometer (Eppendorf). Depending on the $OD_{600\,nm}$ required, more culture would be added to increase the OD or removed and more media added in its place to lower the OD until at a desired concentration. This was carried out under sterile conditions.

2.2.1.4 Dot Assay/Comparative growth analysis

Overnight cultures (5 ml) were diluted the next morning to an $OD_{600\,nm}$ = 0.2 in 5 ml of fresh media. Diluted cultures were incubated at 30 °C at 200 rpm until at a concentration of 3 x 10^6 cells/ml. Cultures were pelleted by centrifugation at 1677 g for 5 min and re-suspended to a concentration of 5 x 10^6 cells/ml. Using a 96 well plate (Starstedt), 200 µl neat culture was added to wells in column '1'. In the wells of column 2-6 inclusive, 160 µl of fresh media was added. Using a multi-channel pipette, a 1/5 serial dilution was carried out by removing and adding 40 µl from well A1 through to well A6. With a sterilised 96 well replicator (Sigma), cells where transferred under sterile conditions. Cells were allowed to dry before being incubated at 30 °C static for 48 h.

2.2.2 Molecular Biological Methods

2.2.2.1 Polymerase Chain Reaction

PCR was employed to amplify fragments of DNA for cloning into plasmids and confirmation of cloning. For amplification of DNA fragment for cloning into plasmids a high proof read *Taq* polymerase was used NEB Q5 *Taq* polymerase. All other PCR reactions used Bioline My *Taq* polymerase.

PCR using NEB Q5 *Taq* polymerase

5X Q5 Reaction Buffer	**5 µl**
10 mM dNTP's	**0.5 µl**
10 µM Forward Primer	**1.25 µl**
10 µM Reverse Primer	**1.25 µl**
Template DNA	**50 – 500 ng**
Q5 High Fidelity DNA polymerase	**0.2 µl**
Nuclease free water	**to total volume of 25 µl**

PCR using Bioline My *Taq* polymerase

5X My *Taq* Reaction Buffer (with dNTP's)	**5 µl**
20 µM Forward Primer	**0.5 µl**
20 µM Reverse Primer	**0.5 µl**
Template DNA	**50 – 500 ng**
My *Taq* DNA polymerase	**0.2 µl**
Nuclease free water	**to total volume of 25 µl**

PCR reaction cycle

A typical PCR reaction cycle using NEB Q5 *Taq* polymerase used unless otherwise stated: Step1: 95 °C (denaturing) 5 min; Step 2 95 °C (denaturing) 1 min; Step 3: 55 °C* (annealing) 1 min 30 sec; Step 4 72 °C ** (extension) 30 sec per kb of amplified DNA; repeat X30 cycles from step2; Step 5: 72 °C (extending) 10 min.

* Annealing temperatures were calculated by setting 4 °C below the lowest melting temperature (T_m) of the primers being used.

** Extension for My *Taq* DNA polymerase was chosen as 1 min/kb of target DNA. The extension time was also reduced to 68 as per suppliers °C as per supplier's recommendations.

2.2.2.2 Site-directed mutagenesis of plasmid DNA

Site directed mutagenesis (SDM) is an effective molecular biology technique that can be used to incorporate nucleotide changes in a fragment of the DNA molecule thus generating mutants of interest at specific amino acid residues. The technique was first described by Hutchison *et al*., (1978). Complementary primer pairs were designed to anneal to egtA causing a mismatch of base pairs. The primer pairs were designed to replace Thr^{213} with alanine which is unable to undergo phosphorylation. Plasmid DNA was prepared as described in Section 2.2.4.1 and PCR reactions were carried out using a PTC-200 Peltier Thermal Cycler (MJ Research) as described below using primers the primers T213A F and T213A R (Table 2.3). The PCR products were treated with 1 µl of *Dpn1* (New England Biolabs) and 2.5 µl of NEB buffer 4 (New England Biolabs) and incubated for 2 h at 37 °C to get rid of any methylated parental DNA. Approximately 8 µl of PCR product was transformed into the super competent *E. coli* strain *xl1-Blue* using the long transformation method as described in Section 2.2.4.5. Four colonies were picked randomly from each transformation and the plasmid DNA extracted as described in Section 2.2.4.1. The plasmid DNA was then quantified using a Nanodrop Spectrophotometer (Mason Technology) and sent for sequencing to LGC genomics as described in Section 2.2.2.3. Using the primers GDP promoter F and CYC promoter R (Table 2.3). After confirmation of the presence of the required mutation by DNA sequence analysis, the plasmid was then transformed into yeast for phenotypic characterisation. The plasmids were also fully sequenced to confirm that there is no other undesired mutations.

PCR Mixture (25 µl)	PCR Cycle (Time in min)
PFU Ultra Buffer (Stratagene) = 1 X	Step 1 = 95 °C 1:00
dNTP mix (Promega) = 0.2 mM each	Step 2 = 95 °C 0:30
Forward primer = 100 ng	Step 3 = 55 °C 1:00
Reverse primer = 100 ng	Step 4 = 68 °C 2:00 per kb
Template DNA = 50 ng	Step 5= Go to step 2, 12 times
HF PFU ULTRA (Stratagene) = 2.5 U	Step 6 = 68 °C 7:00
Molecular grade H_2O adjusted to 25 µl	Step 7 = 4 °C forever
	Step 8 - end

2.2.2.3 Sequencing of plasmid DNA

Plasmid DNA was prepared as in Section 2.2.4.1. Approximately 1 µg of DNA was mixed with 20 pmol of an appropriate primer and the final volume was adjusted to 15 µl with sterile dH_2O in a 1.5 ml microfuge tube. The microfuge tubes were then labelled with prepaid barcodes purchased from LGC Genomics and the samples were sent to Sanger sequencing (LGC genomics Germany). DNA was sequenced by dye-terminator sequencing and results were available for downloading after 3-5 days from LGC- Genomics website. Primers were designed to cover the complete sequence of egtA.

2.2.3 DNA Gel Electrophoresis

2.2.3.1 Preparation of a 0.8 % Agarose Gel

Gels were cast in a Biorad casting tray by adding 0.4 g electrophoresis agarose into 50 ml. (0.8 % w/v) 1X TAE buffer (Section 2.1.5.) and heated to boiling using a microwave set at maximum power for 1 min. This was allowed to cool till hand hot and was poured into the casting mould. 1 µl of a 10 mg/ml ethidium bromide was added and mixed into the agar solution by stirring gently. A well comb was then secured in place to create wells for the addition of samples, and allowed to set for 30 min.

2.2.3.2 Loading and Running of Samples

Before loading into a gel, DNA samples must first be mixed with 6X loading dye (NEB). To estimate sample size, a molecular weight marker was also added to one lane. A 1 kb DNA ladder (NEB), was used throughout this study. Samples were loaded and run at 90 V for 45 min depending on the size of the expected sample.

2.2.3.3 DNA Gel Extraction

Bands were excised using a sterile scalpel and transferred to a sterile, pre weighed, 2 ml microfuge tube. The weight of the gel slice was then weighed and treated using QIA quick gel extraction kit (Qiagen) with the reagents and columns provided as per manufacturers guidelines. DNA was eluted using 30 µl sterile dH_2O added directly to the centre of the spin column, leaving to stand for 1 min. This was centrifuged at 16099 g for 1 min and the eluted DNA was stored at -20 °C until required.

2.2.3.4 DNA Restriction Digest

DNA restriction digest was used for the release of target regions contained within a plasmid, linearizing a plasmid and to enable the subsequent ligation of genes of interest into plasmid vectors. Restriction enzymes and buffers (NEB) were used as per instructions e.g.: DNA 1-5 ug; enzyme 1. 1 µl, enzyme 2. 1 µl; 10 X buffer 1.5 µl; sterile dH_2O to total volume of 15 ul. Reactions were usually carried out at 37 °C for 3 hours.

2.2.3.5 DNA Ligation

Genes to be cloned into plasmid vectors were ligated with T4 DNA ligase (Promega). After the creation of compatible fragments by restriction digest (Section 2.2.3.4) digested DNA fragments were separated via gel electrophoresis (Section 2.2.3.1.). Correctly sized bands were excised from the gel (Section 2.2.3.3.). DNA fragments were ligated using T4 DNA ligase (Promega) as per manufacturer's guidelines. After double digestion both ends of double stranded DNA will have a single stranded overhang if they are cohesive ends. All digested DNA samples used in this study possessed cohesive ends. Ligation reactions were carried out using the formula

(ng of vector)(kb size of insert) X 3 = ng of insert

(kb size of vector)

2.2.4 Generation of Competent Cells

2.2.4.1 Competent *S. cerevisiae* cells

S. cerevisiae cells were inoculated in 5 ml YPD (Section 2.1.3.1) at 30 °C shaking. The next morning cultures were added to 50 ml of fresh media in a 250 ml conical flask at an $OD_{600\,nm}$ of 0.4. Incubated cells for approximately 3 h until a concentration of 1 x 10^7 cells/ml was reached. The culture was then split into two 25 ml fractions in two 50 ml falcon tubes. Cells were centrifuged at 1677 g for another 5 min and subsequently washed with 25 ml dH_2O then centrifuged again at 1677 g for another 5 min. Supernatants were removed from each respective tube, and the cell pellets were resuspended in 1 ml 100 mM lithium acetate (Section 2.1.6). Resuspended cells were transferred to microfuge tubes and centrifuged at 18894 g for 5 sec. Resulting pellets were resuspended in 500 µl 100 mM lithium acetate and stored at 4 °C for no longer than 5 days.

2.2.4.2 *S. cerevisiae* transformation of competent yeast

Competent yeast (50 µl) from Section 2.2.4.1 were centrifuged for 5 sec at 18894 g and any residual lithium acetate was aliquoted out. The following was added to the cell pellet in order: 240 µl 50 % (w/v) PEG (Section 2.1.6.); 36 µl 1 M lithium acetate (Section 2.1.6.); 25 µl single stranded carrier DNA (2 mg/ml stock) and 50 µl DNA/dH_2O. After all components were added yeast were vortexed into solution and incubated at 30 °C for 30 min. This was then treated to a 42 °C heat-shock (Accublock Digital Dry bath, Labnet International Inc) for 30 min. Mixtures were subsequently centrifuged at 18894 g for 15 sec and supernatants were removed. Resulting pellets were re-suspended in 200 µl dH_2O, plated onto selective agar plates incubated for 48 h at 30 °C static.

2.2.4.3 Competent *E.coli* cells

E. coli (Top ten) cells were inoculated in 5 ml LB broth (Section 2.1.3) and incubated at 37 °C, shaking overnight. Inoculated 500 µl to fresh 25 ml of LB media and incubated again at 37 °C at 200 rpm. This was left until an $OD_{600\,nm}$ of 0.6 is reached. Cells were centrifuged at 1677 g for 10 min at 4 °C. Supernatant was discarded and while on ice cell pellet was resuspended in 5 ml of TSB for 10 min (Section 2.1.8.1). Transferred to pre chilled micro centrifuge tubes, snap froze and stored at -70 °C.

2.2.4.4 Quick *E. coli* Transformation

LB-Amp-agar was pre heated to 37 °C for 1 hr prior to transformation. 1-5 µl of plasmid DNA was added to 50 µl of pre thawed *E.coli*. Incubated on ice for 10 min then plated onto pre-heated LB-amp-agar plates and incubated overnight at 37°C.

2.2.4.5 Long *E. coli* Transformation

DNA 1-3 µl (100 ng-1 µg) typically from a ligation reaction is added to 50 µl of competent *E. coli* and 10 µl of 5 X KCM (Section 2.1.8.2). Vortex mixture briefly and leave on ice for 20 min. Keep at room temperature for 10 min then, add 500 µl of LB media and incubate at 37 °C for 45- 60 min. Centrifuge 8050 g for 1 min and most of the supernatant leaving approximately 100-200 µl. Resuspended cells on LB-amp-agar plate and incubate overnight at 37°C.

2.2.5 Plasmid Isolation in *E. coli*

2.2.5.1 Plasmid Isolation and Purification from *E. coli*

A single colony from a transformed *E. coli* Amp-agar plate (Section 2.1.5.12) was inoculated overnight in 5 ml of LB broth + Ampicillin (Section 2.1.5.11) and incubated at 37 °C overnight. Cells were pelleted via centrifugation for 5 min at 1677 g. To elute the plasmid DNA 30 µl of dH$_2$O was added directly to the centre of the spin column and let stand for 1 min at room temperature. Plasmid DNA was collected by centrifugation at 18894 g for 1 min and stored at -20 °C until required.

2.2.6 RNA Analysis

All other materials used were double autoclaved and treated with RNase Zap™ (Invitrogen) prior to use to remove any unwanted RNases. All workplaces were thoroughly washed with 70 % (v/v) ethanol and RNase Zap for the same reason.

2.2.6.1 RNA extraction from *A. fumigatus*

RNA was extracted from *A. fumigatus* using the Qiagen RNeasy plant mini kit as per manufacturer's instructions. All buffers and filter columns were supplied with the kit as well as the constituents of the buffers used. SB media (50 ml) as in Section 2.1.5.13) was inoculated with 500 µl of conidial suspension and incubated overnight at 37 °C shaking. Mycelia were harvested through sterile Mira-cloth and excess medium was washed off using dH$_2$O. Mycelia were then dried using sterile tissue paper, wrapped in tin foil and snap froze in liquid nitrogen. Samples could be stored from this point at 70°C until required. Frozen mycelia were placed

in respective pestle and grinded till at a powdery consistency. Powdered tissue (100 mg) was added to a sterile 2 ml microfuge tube and kept in an ice bucket containing liquid N_2 until ready to proceed. Added 450 µl of buffer RLC (containing ß-mercaptoethanol added prior to first use) and vortex tube vigorously until homogenous.

RNA was eluted by adding 30 µl of RNase free water directly through the centre of the column and let it stand for 1 min. The column was then centrifuged at 11180 g for 1 min and the resulting eluent was aliquoted back up using a sterile tip and passed through the column again to increase RNA yield. RNA was then stored at -70 °C until required.

2.2.6.2 RNA extraction from *S. cerevisiae*

Yeast strains were inoculated overnight in 5 ml in SC media. The following day RNA was extracted using Qiagen RNAeasy kit. The overnight culture was harvested at 2500 rpm for 5 min at 4 °C. Pellets were then resuspended in 600 µl of buffer RLT and transferred to a 1.5 ml microfuge tube and left on ice. An equal volume of 0.5 mm soda lime glass beads were added to the 1.5 ml microfuge tubes and vortexed tubes for 30 s and left on ice for 30 s. This was repeated 5 times to ensure that the pellets were completely disrupted. The samples were then centrifuged at 4 °C for 3 min at 11180 g and the supernatants transferred to 1.5 ml microfuge tubes. One volume of 70 % molecular grade ethanol was added to the lysate, mixed and transferred to spin columns and centrifuged at 4 °C for 15 s at 11180 g. This was followed by addition of 700 µl of buffer RWI and samples were centrifuged again at 4 °C for 15 s at 11180 g. Then 500 µl of buffer RPE was added to the spin columns and centrifuged at 4 °C for 2 min at 11180 g. The RNA was then eluted in 40 µl RNase free H_2O by centrifugation at 11180 g for 2 min at 4 °C.

2.2.6.3 DNAse Treatment of RNA Samples

RNA samples extracted from *A. fumigatus* (Section 2.2.6.1) were DNase treated using a DNase kit purchased from Sigma Aldrich Ltd. 500 ng *A. fumigatus* was brought to a final volume of 8 µl using DEPC treated distilled water in a RNase free sterile 500 µl microfuge tube. To this, 1 µl 10 X reaction buffer and 1 µl DNase were added and were incubated at room temperature for 15 min. Afterwards, 1 µl stop solution (part of kit) was added and subsequently incubated at -70 °C for 10 min. Samples were placed on ice for at least 1 min and stored at -70 °C until required.

2.2.6.4 cDNA Synthesis

cDNA was synthesised using the qScript^{TM} cDNA supermix (Quanta Biosciences). All reagents and buffers contained a single reagent supplied in the kit. cDNA was synthesised as per manufacturer's instructions. 500 ng of RNA (Section 2.2.6.1) which had been DNase treated (Section 2.2.6.2) was added to DNase and RNase free 500 µl microfuge tubes. To this 4 µl of the qScriptTM cDNA Supermix 5 X was added and topped up to a final volume of 20 µl using diethyl-pyro carbonate (DEPC) treated dH$_2$O. Samples were vortexed briefly and centrifuged for a few seconds to collect all of the reaction mix. They were then incubated using a PCR cycler using the following incubation protocol: 5 min at 25 °C; 30 min at 42 °C 5 min at 85 °C; hold at 4 °C. Once completed the cDNA is now ready for use.

2.2.7 Proteomic Analysis

2.2.7.1 Protein extraction from *S. cerevisiae*

Yeast strains were cultured overnight in 5 ml YPD or selective media at 30 °C, shaking 200 rpm in triplicate. The following day cells were diluted in 25 ml of fresh media to an OD $_{600\ nm}$ of 0.2 as incubated before for a chosen time period. Cells were harvested by centrifugation at 4 °C; 5 min; 1677 g (5810R Eppendorf AG Hamburg). Pellets were resuspended in 1 ml of milliQ H$_2$O and pipetted into 2 ml tubes. Then centrifuged at 4 °C; 1 min; 18894 g (5415D Eppendorf AG Hamburg) and discarded supernatant. The wet weight of each culture was recorded and cells were then resuspended in 1 ml of milliQ H$_2$O. The following formula was used to work out what volume to take for 50 mg of cells and placed in fresh tube, centrifuged as above and supernatant removed.

$$\left(\frac{1000\ (\mu l) + \text{wet weight of cells (mg)}}{\text{wet weight of cells (mg)}} \times 50 = \quad \begin{array}{c} \text{Amount of liquid containing} \\ \text{50 mg of suspended cells} \end{array} \right)$$

Lysis buffer was prepared by adding 3 µl of protease cocktail inhibitor (P8215; for use with fungal and yeast extracts) per ml of Cell Lytic ^{TM} Yeast cell lysis reagent. DTT (10 mM) is also added to improve final protein yield, however DTT is not added if lysates are to be used in the ergothioneine alkylation assay as it interfered with 5'-Iodacetamidofluorescein labelling of ergothioneine. The prepared lysis buffer (900 µl) was then added to each tube containing 50 mg of cells. 0.5 mm soda lime glass beads (Biospec Cat No. 11079105) were then added to each tube until only a small amount of room remained. Tubes were bead beaten using a bead beater (Retsch mm 400) for 10 sec and then chilled on ice for 1 min, and was

repeated 10 times. Tubes were then centrifuged at 4 °C for 10 min at 18894 g and supernatants were transferred to pre chilled microfuge tubes and centrifuged again as above.

2.2.7.2 Bradford Protein Assay

Protein samples (Section 2.2.7.1) were quantified using the Bradford protein assay. Using a BSA stock (1 mg/ml) protein solutions of a known protein concentration were created to generate a protein standard curve in triplicate. Samples in triplicate were diluted 1:10, 2 µl of which was added to a 96 well plate (Starstedt). Biorad 1X protein assay (200 µl) was added to each sample/standard and following a 10 min incubation at room temperature, absorbance's were read using a spectrometer set at $A595_{nm}$ (Eppendorf Biophotometer). Protein concentration of samples was calculated using a plotted $A595_{nm}$ versus BSA concentration standard curve. All protein samples were analysed in triplicate.

2.2.7.3 Sodium Dodecyl Sulphate-Poly Acrylamide Gel Electrophoresis (SDS-PAGE)

12.5 % SDS-PAGE gels were prepared using one 1 mm Bio-Rad glass backplate and one front plate along with a 15 well combs having 44 µl sample capacity. The glass plates were cleaned thoroughly with 70 % ethanol and then rinsed with milliQ H_2O. The glass plates were then sealed in a Bio-Rad Gel Cassette and a casting frame which was then filled with milliQ H_2O to ensure the plates were sealed. The running gel was prepared first adding the materials in table 2.6 in order in a 50 ml falcon. Emptied plates of milliQ H_2O and gently pipetted the mixture in falcon tube between the glass plates to a capacity of approximately 70 % to allow room for stacking gel. MilliQ H_2O was then sprayed on top of the gel to the full capacity of the glass plates to ensure a smooth surface on the running gel once solidified. Once the gel had set millIQ H_2O was removed and the stacking gel was prepared as in Table 2.7 by adding the materials in the order listed in a 15 ml falcon. The stacking gel was then pipetted in between the plates to maximum capacity. A 15 well comb was cleaned with 70 % ethanol, rinsed with milliQ H_2O and placed between the plates. This was then left to set at room temperature for 20-30 min.

2.2.7.4 Sample preparation and SDS-PAGE

Using 6X protein sample buffer (Section 2.1.7.3) samples were prepared by adding 30 µl of cell lysate to 6 µl of protein sample buffer and boiled at 100 °C for 5 min in a digital dry bath. The prepared gels (Section 2.2.7.2) were removed from their casting tray and placed in the electrode assembly unit (Bio rad) with the thin front plates facing inwards. The electrode assembly was then placed in the electrophoresis tank (Bio rad). This was then filled with 1X

running buffer (Section 2.1.7.2) to the appropriate mark as denoted on tank. Protein samples were then loaded along with the protein ladder (Page ruler plus prestained protein ladder 10-250 kDa, Fermentas, Life Sciences). The gels were then resolved in 1X protein running buffer at 100 V per gel for 1.5 h with a Bio-Rad Powerpac Basics.

2.2.7.5 Western Blot

Proteins separated in the gels were then electrophoretically transferred to polyvinylidene difluoride (PVDF) membranes (Perkin Elmer) and processed for blotting as per recommendations for use with Bio-Rad gel transfer system. To prepare for the wet transfer Whatman filter paper was cut into six 8 cm X 5.5 cm pieces as well as one piece of PVDF membrane. PVDF was then soaked in 100 % methanol for 30 s. All six pieces of filter paper and PVDF membrane along with two fibre pads were then equilibrated in 1X transfer buffer (Section 2.1.8.1) for 15 min. After a good separation of proteins was achieved the stacking gel was removed and the gel was rinsed in milliQ H_2O. A gel membrane sandwich was assembled as follows cassette black side- fibre pad- 3 filter paper-gel- membrane- 3 filter paper- fibre pad- cassette white side. The gel- membrane sandwich was then rolled using a sterile pipette to remove any air bubbles. The cassette was then closed and placed in the transfer tank with the black side of the cassette going to the black side of the tank. The tank was filled with pre-chilled 1X transfer buffer and placed in an ice bucket. The cables were then connected to the power supply and an electric current was applied (100 V/ 350 A) for 1 h.

2.2.7.6 Immunoblotting

After the transfer of proteins to the PVDF membrane the membrane was blocked for 1 h at room temperature rocking by placing 20 ml of blocking solution on the membrane (Section 2.1.10.2). After blocking the membrane was incubated overnight at 4 °C with primary antibody and buffer (Section 2.1.10.3). The following day the membrane was washed 3 times in 25 ml of PBST (Section 2.1.3.8), 5 min per wash to remove excess antibody that might cause unspecific binding. This was followed by incubation with horse radish peroxidase labelled secondary antibody (Section 2.1.10.4) for 1 h. The membrane was then washed again 3 times with PBST as described earlier.

2.2.7.7 Chemiluminescence

Chemiluminescence used the substrate ECL (Bio-Rad Clarity™ Western ECL Blotting Substrate kit) and was exposed using the G: BOX F3 (SYNGENE) as per manufacturer's instructions. In brief the non-reflective panel was cleaned with 70 % ethanol and a fresh acetate sheet was then put down placing the PVDF membrane on top. The GENE SYS application is selected from the desktop, ECL is selected as the substrate along with 'visible marker' to co-visualise both the protein ladder and chemiluminescence. The cameras focus and zoom is then adjusted along with the preparation of the ECL substrate by adding 800 µl of peroxide solution to 800 µl of enhancer solution in 2 ml microfuge tube. The enhanced substrate is then evenly pipetted onto the membrane and the optimal exposure time is calculated by the G: BOX F3. Once exposure is complete the image is taken and exposure of the image can be adapted to best suit the sensitivity of antibody/substrate.

2.2.7.8 Coomassie staining of protein gels

SDS-PAGE gel was rinsed with dH$_2$O and transferred to coomassie brilliant blue stain, covering the gel (Section 2.1.9.4). Heated gel in microwave for 20 s (be careful not to melt gel) then transferred onto rocker at room temperature for 15 min. Removed coomassie and placed a clean piece of tissue paper in with gel (ensure gel is folded or stuck under tissue or will no stain or destain correctly) and added destain solution until covering gel (Section 2.1.9.5). Place in microwave for 20 s and leave for 1 h or overnight for cleaner background.

2.2.8 Mass Spectrometry (LC-MS)

2.2.8.1 Protein Spot Preparation-Shevchenko method (Shevchenko *et al* 2006)

SDS-Page bands were chosen based on the known size of the protein of interest EgtA from *A. fumigatus* (96.29 kDa). All reagents used were HPLC grade and 1.5 ml microfuge tubes were treated with acetonitrile before use. Each gel was washed once using sterile water before the chosen spots were cut out using a sterile scalpel and placed in a pre-washed 1.5 ml tube. Gel pieces were incubated in 100 µl de-staining buffer (Section 2.1.13.1), vortexed occasionally at room temperature for 30 min, or until all stain was removed. Acetonitrile (500 µl) was then added to each tube and left for 10 min at room temp causing the gel pieces to shrink and turn white indicating removal of the majority of the coomassie stain.

Samples were then trypsin digested with 50 µl (or enough to cover the gel piece) trypsin buffer (Section 2.1.13.3) and incubated on ice for 30 min. More trypsin buffer was added if necessary. Gel pieces were incubated on ice for 30 min. More trypsin buffer was

added if necessary. Gel pieces were incubated for a further 90 min to saturate gel pieces with trypsin. A 50 mM ammonium bicarbonate solution (20 µl) as in Section 2.1.13.4 was then added to prevent the gel piece becoming dehydrated during digestion. Gel pieces were then incubated at 37 °C static overnight to allow for complete trypsin digestion of sample peptides.

Digested peptide products were transferred to a new sterile 1.5 ml microfuge tube. 100 µl of extraction buffer (Section 2.1.13.5) was then added to each digested gel piece and incubated for 15 min at 37 °C shaking to help collect any residual peptide fragments. The supernatant from this was added to the trypsin digest and dried overnight in a vacuum centrifuge. Dried extracts could be stored at – 20 °C for several months if required.

2.2.8.2 Zip Tip of samples (for Q-Exactive MS analysis)

Resuspended sample with 20 µl of resuspension buffer (Section 2.1.14.1). Wet zip tip by aspirating and dispensing 10 µl of wetting solution into the tip. This was repeated 5 times. Equilibrated zip tip by aspirating and dispensing 10 µl of equilibration solution onto the tip 5 times. Bound sample to zip tip by aspirating and dispensing 10 µl of resuspended same 15 times. Washed sample by aspirating and dispensing 10 µl of washing solution from tip to waste. This was repeated 5 times. Eluted sample by aspirating and dispensing 10 µl of sample from the tip to a fresh 1.5 ml Eppendorf. Sample was then dried down in vacuum centrifuge and resuspended in 20 µl of buffer A (Section 2.1.14.5).

2.2.9 Detection and Quantification of Ergothioneine by RP-HPLC

2.2.9.1 Alkylation of Intracellular Ergothioneine

Cell lysates (30 µl) in Section 2.2.7.1 (made without the addition of DTT which is alkylated by the 5'-Iodoacetamidofluorecein (5'-IAF) label) was added to 90 µl of PBS and then vortexed. Samples were then centrifuged (18894 g, 5 min, at 4 °C). Each sample (50 µl) was placed in a fresh tinfoil covered tube and 10 µl of 3 mg/ml 5'-IAF was added (58.23 nmol) to alkylate each sample. Samples were left in the dark for 45 min then centrifuged (18894 g, 5 min, at 4 °C).

2.2.9.2 Alkylation of Extracellular Ergothioneine

Sample supernatant (500 µl) was dried down in a speedy vac. Dried samples were resuspended in 100 µl of 200 mM sodium phosphate buffer pH 7.6 by vigorously pipetting up and down. Centrifuged at 18894 g for 5 min, at 4 °C. Each sample (50 µl) was resuspended,

taken and placed in a fresh tinfoil covered tube and 10 µl of 5'-IAF 3 mg/ml was added (58.23 nmol) to alkylate each sample. Samples were left in the dark for 45 min then centrifuged (18894 g, 5 min, at 4 °C). A positive EGT control was prepared by adding 10 µl of 3 mg/ml 5'-IAF to 50 µl of 50 µg/ml ergothioneine in 200 mM sodium phosphate buffer pH 7.6. The following negative controls were prepared. A 5'-IAF solution (10 µl) of 3 mg/ml was added to 50 µl of 200 mM sodium phosphate buffer pH 7.6. Negative control SN was also prepared identically and alkylated.

2.2.9.3 Preparation Ergothioneine standard curve for Extracellular samples

EGT (20 µl) of 5 mg/ml (436.11 nmol) was added to 980 µl of negative control SN (SN from the yeast strain *BY4741* transformed with the empty vector pRS426-*GPD*) giving a concentration of 100 µg/ml of EGT. This was prepared in duplicate. SN containing 100 µg/ml of EGT was serially diluted by taking 500 µl and adding 500 µl of negative control SN giving a concentration of 50 µg/ml of EGT. This was repeated a further 5 times giving the EGT concentrations 100, 50, 25, 12.5, 6.25, 3.125 and 1.56 µg/ml (Figure 2.1). All seven tubes were then dried down in a speedy vac

Tube A: 100 µg/ml EGT in SN 1000 µl

(50 µg of EGT in Tube A)   500 ul from tube A to tube B

Tube B: 50 µg/ml EGT in SN 1000 µl

(25 µg of EGT in Tube B)   500 ul from tube B to tube C

Tube C: 25 µg/ml EGT in SN 1000 µl

(12.5 µg of EGT in Tube C)   500 ul from tube C to tube D

Tube D: 12.5 µg/ml EGT in SN 1000 µl

(6.25 µg of EGT in Tube D)   500 ul from tube D to tube E

Tube E: 6.25 µg/ml EGT in SN 1000 µl

(3.125 µg of EGT in Tube E)   500 ul from tube E to tube F

Tube F: 3.125 µg/ml EGT in SN 1000 µl SN

(1.56 µg of EGT in Tube F)   500 ul from tube F to tube G

Tube G: 1.56 µg/ml EGT in SN 1000 µl)

(0.78 µg of EGT in Tube G)   500 ul from tube G and discarded

Figure 2.1 Serial dilution for EGT standard curve.

Once dry, samples were resuspended by vigorously pipetting up and down in 100 µl of 200 mM sodium phosphate buffer pH 7.6. Samples were then centrifuged at 18894 g for 5 min, at 4 °C. Each resuspended sample 50 µl of was taken and placed in a fresh tinfoil covered tube and 10 µl of 5'-IAF 3 mg/ml was added (58.23 nmol) to alkylate each sample. Samples were left in the dark for 45 min then centrifuged (18894 g, 5 min, at 4 °C).
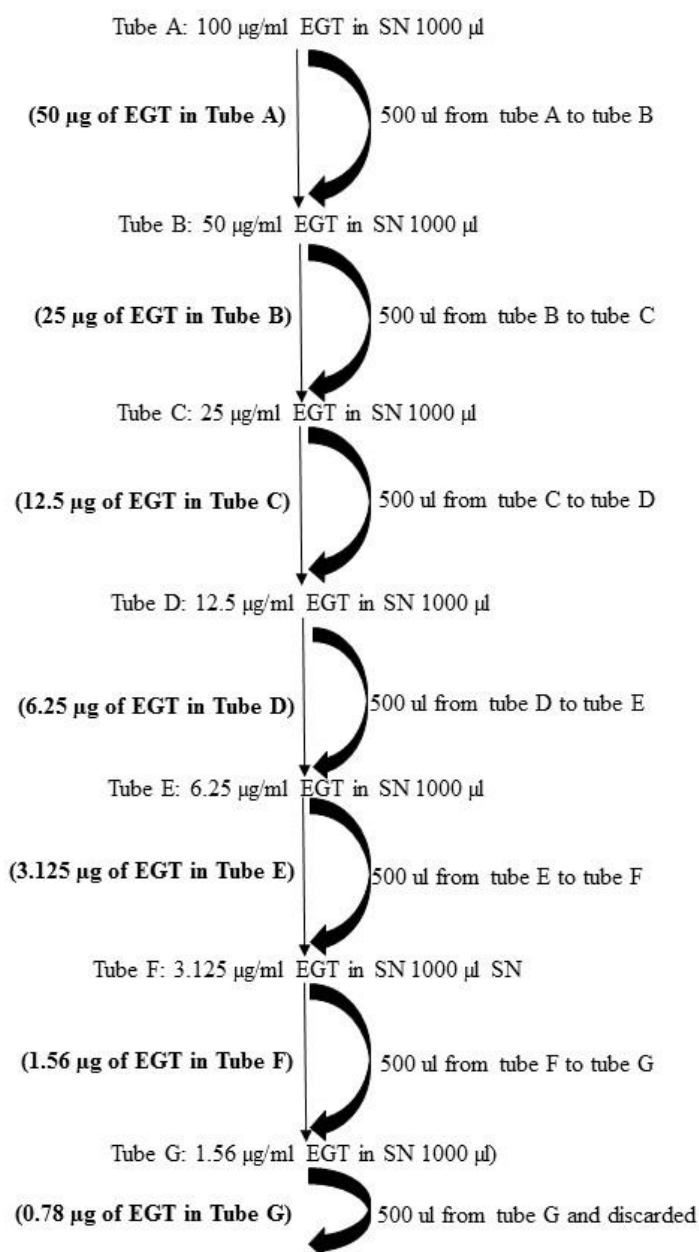
2.2.9.4 HPLC analysis of alkylated ergothioneine

Alkylated sample (50 µl) was placed in a HPLC vial and 30 µl was injected onto the column. The peak area was measured at the wavelength 442 nm. A 1 ml/min flow rate was used with each run which lasted a total of 40 min. Solvent B had a starting concentration of 5 % for the first 5 min minutes which was gradually risen to 100 % at 25 min. Solvent B was maintained at 100 % for 3 min to wash the column. At 29 min the concentration of solvent was dropped to 5 % to re-equilibration the column and 5 % was maintained until the end of the run at 40 min.

2.2.9.5 Calculation of extracellular EGT using the standard curve

The average peak area of each triplicate set of samples for each time point was obtained and input as the 'y' value into the equation of the line produced by the standard curve x=y/554456. The product from this was divided by a 104.2 as this is the amount in µl of supernatant loaded onto the column the product from this was then multiplied by 1000000 representing the culture size (µl). The final answer is then in terms mg/L.

2.2.9.6 Calculation of intracellular EGT using the standard curve

The average peak area of EGT at 13.8 min in 24 h BY4741$^{426\ GPD-EgtA}$ was taken away from the average peak area of the control culture peak 13.8 min peak. The product was multiplied by 4 representing the average wet weight cell mass of the 25 ml cultures used with 50 mg of cells used per cell lysate. The product was then input as the 'y' value into the equation of the line produced by the standard curve x= ((y-165765)/542544). The product was then multiplied by 40 bringing the final answer in terms of mg/L.

2.2.9.7 TCA precipitation of intracellular alkylated ergothioneine samples

A solution of 100 % TCA solution (15 µl) as in Section 2.1.4.3, was added to 85 µl of alkylated cell lysate from Section 2.2.9.1 and left at 4 °C for 3 h. Centrifuged (18894 g, 20 min, at 4 °C). The supernatant was then removed and placed in a fresh tube.

2.2.9.8 LC-MS analysis of alkylated ergothioneine

Samples from Sections 2.2.9.2 and 2.2.9.5 were diluted 1 in 100 in 0.1 % water formic acid (Section 2.1.13.6). 60 µl of sample was then placed in spin filter tubes and centrifuged (18894 g, 1 min, at RT). Samples (40 µl) were then placed in Q-Exactive LC-MS vials.

2.2.10 Statistical evaluation of experimental data

Statistical analysis was carried out using the software Graphpad Prism Version 6. The unpaired T test method was used for all significance tests. P values below $P < 0.05$ were considered significant.

Chapter 3

Recombinant EgtA expression in *S. cerevisiae* enables Ergothioneine biosynthesis

3.1 Introduction

The natural product ergothioneine (EGT) was first identified in *A. fumigatus* by Gallagher *et al*., (2012) in a *ΔgliK* mutant strain of *A. fumigatus* where a significantly higher level of ergothioneine was present in the *ΔGliK* strain compared to its wild type counterpart. Following this study, the first fungal EGT biosynthetic gene *egt-1* was identified in *Neurospora crassa* by Bello *et al*. (2012) by comparing homologues in *N. crassa* to EGT producing genes in Actinomycetes. A similar strategy was used to identify EGT producing genes in *A. fumigatus* by comparing *N. crassa egt-1* to homologues in *A. fumigatus*. From this the EGT producing gene AFU_2G15650 denoted *egtA* was identified (Figure 3.1), This gene has domains homologous to the SAM dependant methyl transferase domain in EgtB and the FGE sulfatase domain identified in EgtD in *M. smegmatis* (Seebeck, 2010). EGTA was confirmed to be involved in EGT biosynthesis by deletion of the *egtA* gene causing ablation of EGT production (Sheridan *et al*., personal communication).
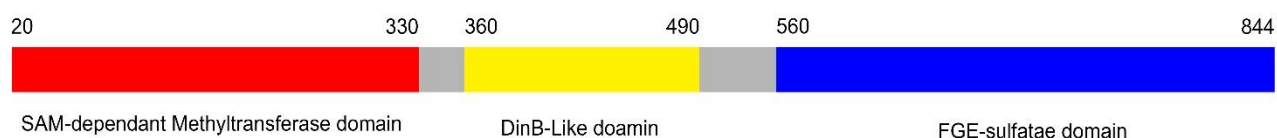
Figure 3.1 Conserved domains of EgtA. A SAM dependant methyltransferase domain can be seen along with an FGE Sulfatase domain.

As mentioned in Section 1 EGT shows significant potential for use as a food preservative and as a neutaceutical. This is through its ability to detoxify ROS such as HOCl, singlet O_2, $ONOO^-$ and $OH^{\cdot}$ as well as form stable complexes with iron and copper (Halliwell & Gutteridge, 2007). EGT has also been shown to extend the shelf life of fish such as tuna and slow the discolouration of meat (Bao *et al*., 2008). Another study demonstrated how ß-amyloid peptides which damage brain tissue by causing lipid peroxidation, were significantly reduced by a high EGT diet in another murine model (Yang *et al*., 2012).

Hampering the use of EGT as a preservative or nutraceutical is the cost of extracting EGT from sources with relatively low yields making EGT costly and unavailable for use as a nutraceutical. To make EGT viable for industrial use a source must be discovered that

produces high quantities of EGT in a reasonable time frame from which EGT can be easily extracted or purified. Fungal sources looked at include the king oyster mushroom *Pleurotus citrinopileatus* recorded to contain up to 113 mg/L or 14.67 mg/g (dry weight) of EGT in mycelium. These are highly optimised conditions of pH and nutrients with cultures incubated for 22 days before harvesting (Lin *et al*., 2015). An Egt-1 overexpression mutant of *Schizosaccharomyces pombe* was reported to have an intracellular EGT concentration of 266.3 mg/L produced over a 20 day period with the media changed every 6-7 days (Pluskal *et al*., 2014).

Bacteria could also be used as an EGT source with the Cyanobacteria species *Oscillatoria sp* CCAC M1944 identified to naturally produce high quantities of EGT of 0.8 mg/g dry weight in an unspecified time frame (Pfeiffer *et al*., 2011). Mycobacteria such as *M. smegmatis* were identified to secrete EGT as an extracellular metabolite as well as contain some intracellularly however levels were quite low for use as an industrial application with the largest extracellular quantity equivalent to 44 pg/10^5 cells (Emani *et al*., 2013). The chemical synthesis of EGT has been improved in recent years and uses histidine as the starting material which could prove to be reasonably cost effective (Khonde & Jardine, 2015).

Yeast are an ideal organism to produce EGT although they do not produce it themselves yeast such as *S. cerevisiae* can produce recombinant eukaryotic proteins such as granulocyte macrophage stimulating factor (Celik & Calık, 2012). It was seen how 20 % of all recombinant protein are produced in yeast with nearly all of these being produced by *S. cerevisiae* and is seen as the best choice for fungal enzymes (Mattanovich *et al*., 2012). *S. cerevisiae* can carry out post translational modifications like glycosylation as well as well as assisting with protein folding increasing the likelihood of producing a functional protein. (Gellissen *et al*., 1992). Unlike bacteria *S. cerevisiae* has a track record in the fermentation industry and has attained the status GRAS (generally regarded as safe) so is ideal for the production of a potential food additive like EGT. *S. cerevisiae* can rapidly grow in a chemically defined media offering a cost effective way of producing large amounts of recombinant protein coupled with the use of a high copy expression vector (Demain & Vaishnav, 2009). As well as this *S. cerevisiae* has been shown to be probiotic in the oral delivery of therapeutic proteins (Omara *et al*., 2010).

Eukaryotes utilize enzymatic and non-enzymatic means as part of their oxidative defence strategy to mediate harmful ROS that are a by-product of respiration (Nordberg &

Arnér, 2001; Lu, 2013). One such strategy employed to mediate oxidative stress is to produce the enzyme superoxide dismutase which dismutes O_2^- into molecular oxygen and hydrogen peroxide (Steinman, 1980). The tri peptide GSH a highly abundant intracellular thiol is also produced by *S. cerevisiae* and has been shown to be critical to mediating oxidation stress with mutants having impaired growth as well as increased sensitivity to oxidative stress (Grant *et al.*, 1996). Addition of EGT to the defence of *S. cerevisiae* against ROS may make the organism more resilient to oxidative stresses.

This project will recombinantly express the protein EgtA in *S. cerevisiae* and confirm expression of EgtA by protein mass spectrometry (Figure 3.2 A). Production of EGT in *S. cerevisiae* will be detected using the alkylating agent 5'-IAF and confirmed using mass spectrometry. Alkylated EGT will then be quantified using RP-HPLC analysis (Figure 3.2 B).
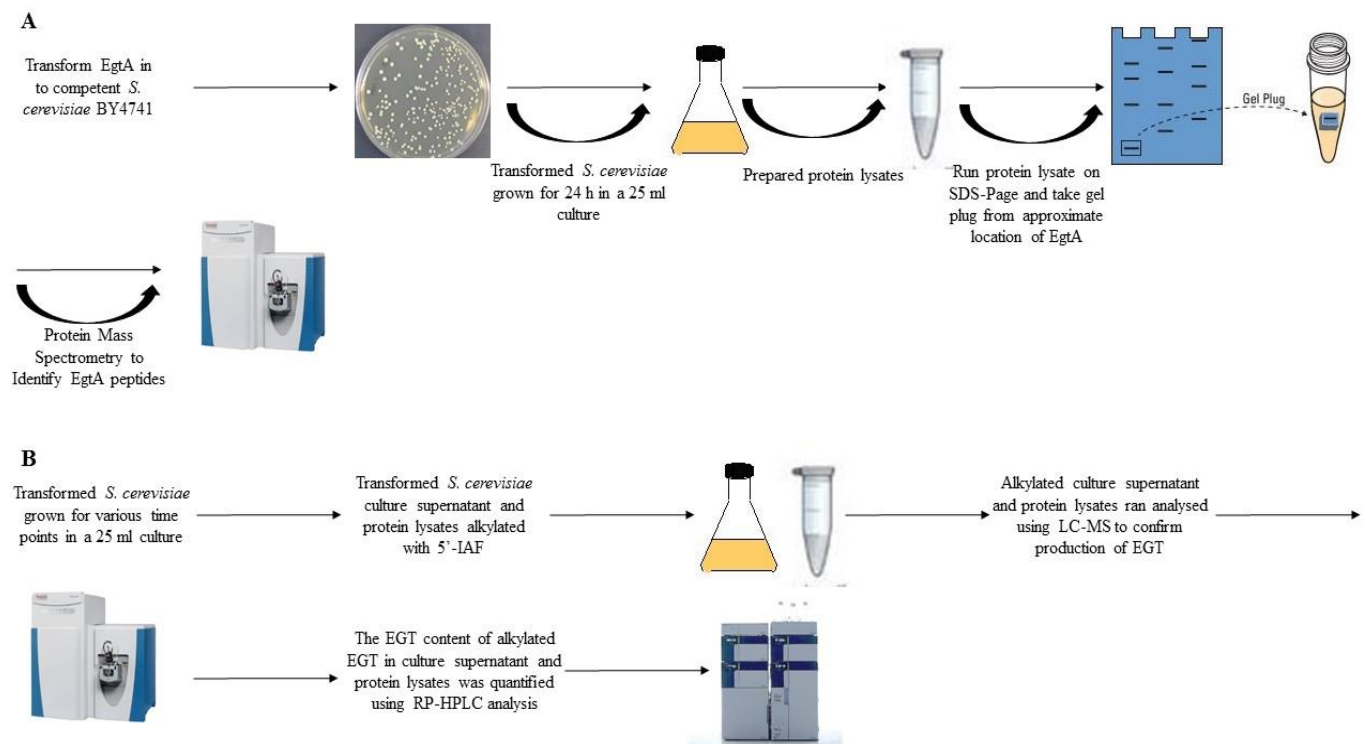
Figure 3.2 A-B Project work flow diagram showing how EgtA protein and metabolite EGT will be detected in *S. cerevisiae*.

3.2 Cloning of *egtA* into the budding yeast *S. cerevisiae* expression vectors

The yeast shuttle expression vector *p426-GPD* was chosen from a range of centromeric and episomal plasmids due to its established high expression of recombinant proteins (Mumberg *et al*., 1995) (Funk *et al*., 2002). In yeast, episomal plasmids such as *p426 -GPD* the level of heterologous mRNA in the cell is determined by the copy number of the expression vector which is in turn controlled by the replicon (Curran and Bugeja, 2011). *p426-GPD* (Figure 3.3), contains what is considered a high copy 2μ replicon derived from a natural yeast plasmid allowing 50+ copies per cell to propagate (Addgene, 2014). A strong promoter is required to drive transcription, in p*426-GPD* the endogenous promoter glyceraldehyde-3-phosphate dehydrogenase (GPD) is used which is the strongest constituent promoter available for *S. cerevisiae* and greatly increases the production of recombinant protein (Mumberg *et al*., 1995; Blazeck *et al*., 2012). Selection is maintained in *p426-GPD* by a *URA3* marker which is preferable to selection through a *HIS3* marker as this may become a limiting factor in the production of EGT as histidine is required for EGT biosynthesis.
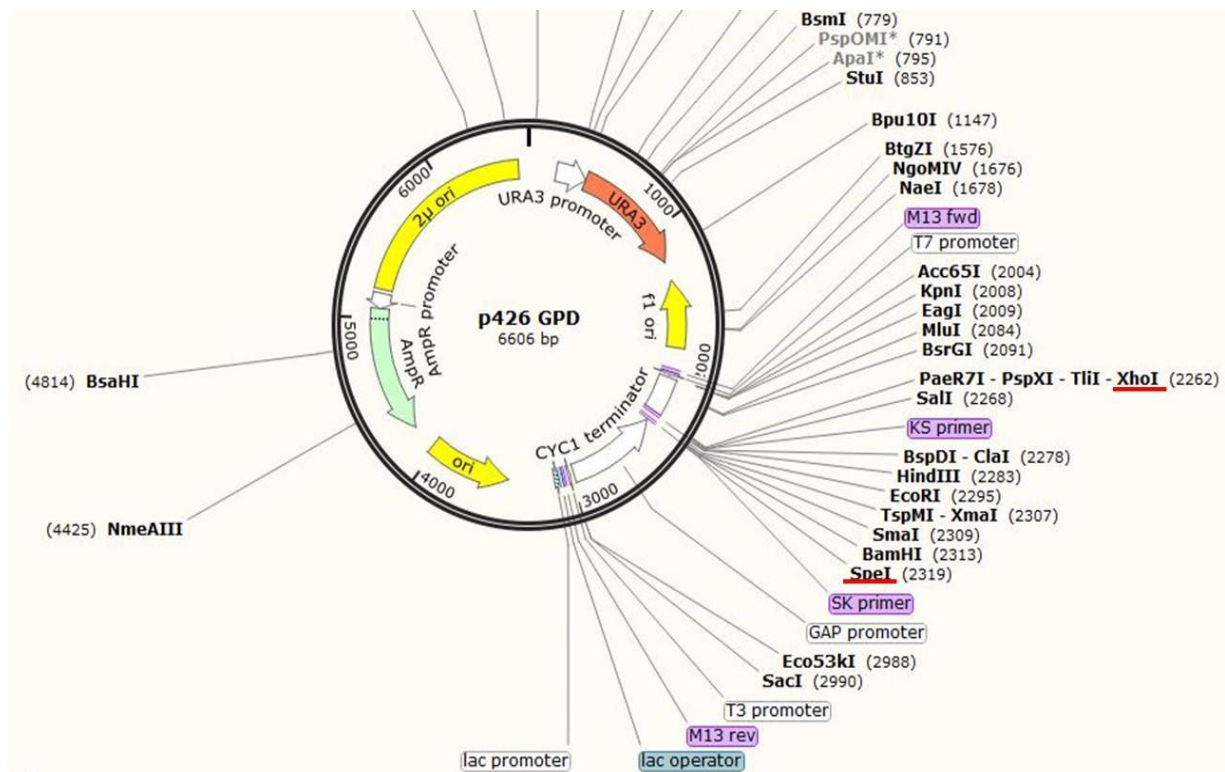
Figure 3.3 The 6.6 kb episomal *S. cerevisiae* shuttle vector *p426-GPD* used to express recombinant *egtA*. An *AmpR* gene for selection after cloning into *E. coli* is present along

with a *URA3* gene for selection after transformation of plasmid into *S. cerevisiae* and the restriction enzyme sites *Spe1* and *Xho1* used as part of the cloning strategy.

EgtA cDNA was synthesized by GenScript (860 Centennial Ave. Piscataway, NJ 08854 USA) and blunt end cloned into the vector *PUC57*. *EgtA* was amplified using high fidelity Taq polymerase with proof reading ability to ensure sequence integrity using the primers EgtA F and EgtA R (Table 2.3). A cloning strategy was employed using the restriction sites *Spe1* and *Xho1* at the 5' and 3' end respectively. PCR products were run on an agarose gel and separated via gel electrophoresis to check for a single band at the correct size of 2.5 kb (Figure 3.4).
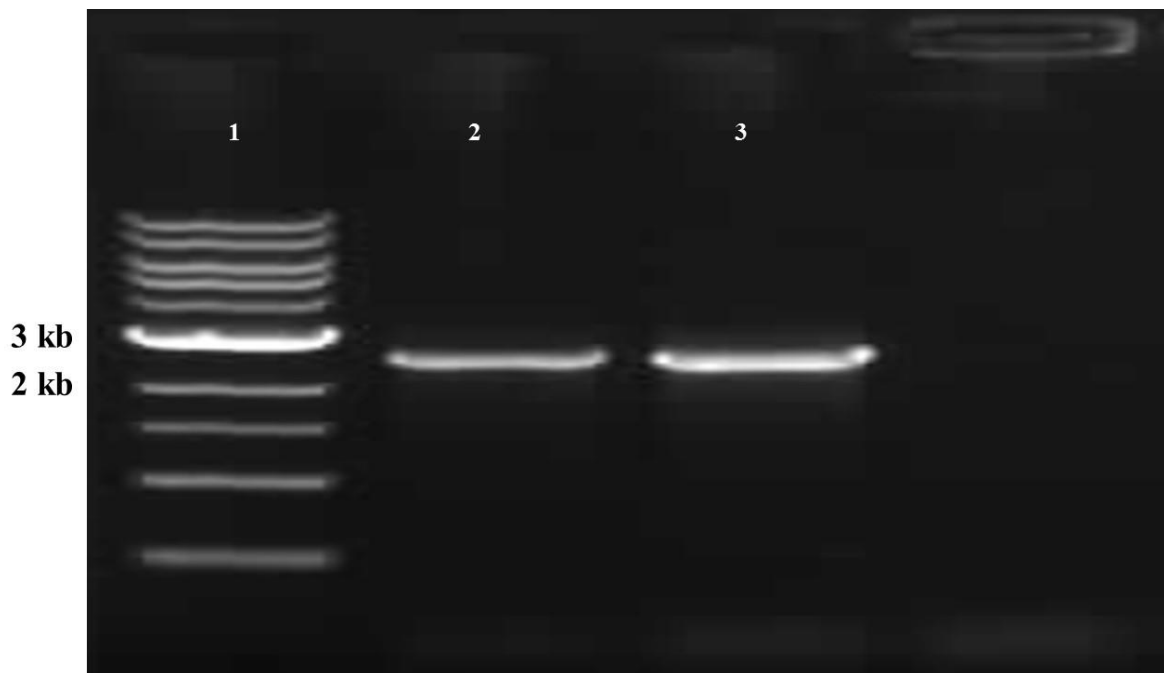
Figure 3.4 PCR amplification of *egtA* cDNA in the plasmid *PUC57*. Lane 1= 10 kb NEB DNA ladder, lanes 2 & 3= *egtA* band (size 2.5 kb) amplified with high fidelity Taq, lane 4= negative control.

The PCR products of *egtA* cDNA (hereafter) 'egtA') amplification were cleaned using Qiagen PCR purification kit as per manufacturer's instructions prior to use. The cleaned PCR

product was digested to create the sticky ends, required when ligating the *egtA* insert. The vector *p426 GPD* was also digested to open the plasmid, linearizing it in preparation for ligation. Both insert and vector were digested with the restriction enzymes *spe1* and *xho1* for 3 h at 37 °C and separated using gel electrophoresis on an agarose gel to prevent religation of excised fragments during ligation (Figure 3.5 A & B). Fragments were then excised from a gel using Qiagen quick gel extraction kit as per manufacturer's instructions.
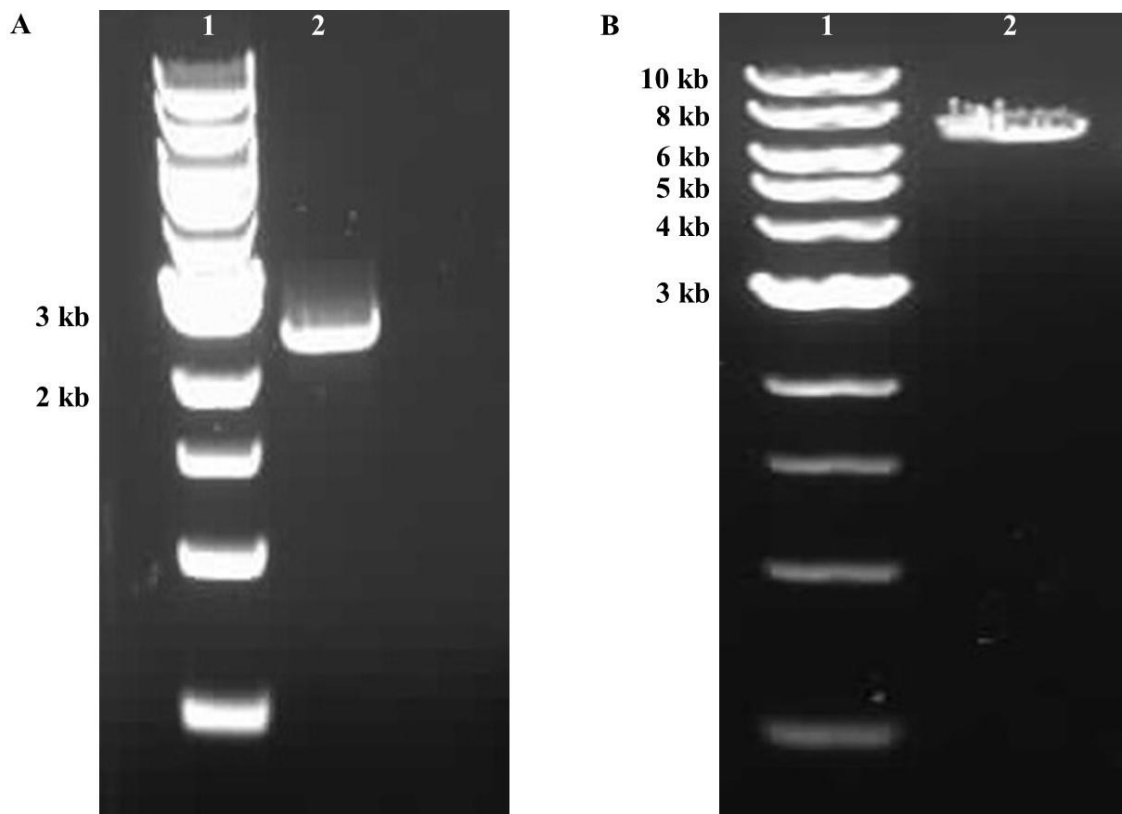
Figure 3.5 A-B Digestion product of insert *egtA* (A) and vector *p426 GPD* (B). A: Lane 1= 10 kb NEB DNA ladder, lane 2= digested *egtA*; B: Lane 1= 10 kb NEB DNA ladder, lane 2= digested *p426 GPD*.

After gel extraction of digested *egtA* and *p426 GPD* the DNA concentration of samples were measured using a Nanodrop (Mason). The *egtA* insert was then ligated into the vector *p426 GPD* as described in Section 2.2.3.5 and left overnight at 16 °C. Following this *p426 GPD-egtA* was transformed into *E. coli* cells as described in Section 2.2.4.5. *E. coli* with p*426 GPD-egtA* were selected by their ability to grow on LB-amp-agar plates. Plasmid DNA

of p*426 GPD-egtA* was purified from transformed *E. coli* as described in Section 2.2.5.1. Plasmid DNA of *p426 GPD-egtA* was then transformed into the *S. cerevisiae* strain BY4741 as described in Section 2.2.4.2. Successful transformants were selected by their ability to grow on –URA SC media. A colony PCR was carried out on selected colonies to further confirm that the transformation was a success, of the 5 colonies checked by PCR 4 contained *egtA* (Figure 3.6).
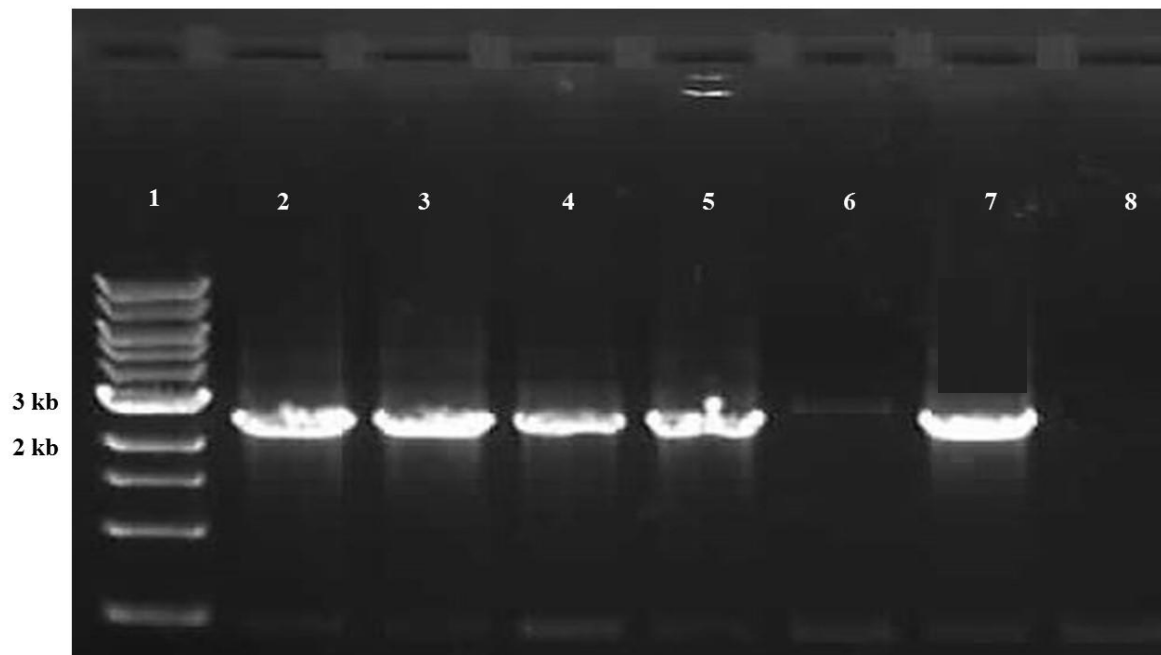
Figure 3.6 Confirmation of *egtA* in BY4741$^{p426\ GPD\text{-}egtA}$ by colony PCR. Lane 1= 10 kb NEB DNA ladder, lanes 2-5= *egtA* in *S. cerevisiae* BY4741$^{p426\ GPD\text{-}egtA}$ (size 2.5 kb) amplified with high fidelity taq, lane 6= BY4741 colony that did not contain *egtA*, lane 7= positive control *p426 GPD-egtA* (size 2.5 kb), lane 8= negative control.

3.3 Confirmation of expression of *EGTA* in the budding yeast *S. cerevisiae*

To confirm *egtA* could be expressed in *S. cerevisiae* a 6X Histidine tag (His tag) was generated on the N-terminus of EgtA in the vector *p426 GPD*. The template *p426 GPD-egtA* was amplified using high fidelity Taq and the primers EgtA N terminal His tag and EgtA R with the restriction sites *Spe1* and *Xho1* at the 5' and 3' end respectively. Following a

successful transformation of *p426 GPD-egtA* with an N-terminal His tag into the *S. cerevisiae* strain BY4741 successful transformants were screened colony PCR (Figure 3.7)
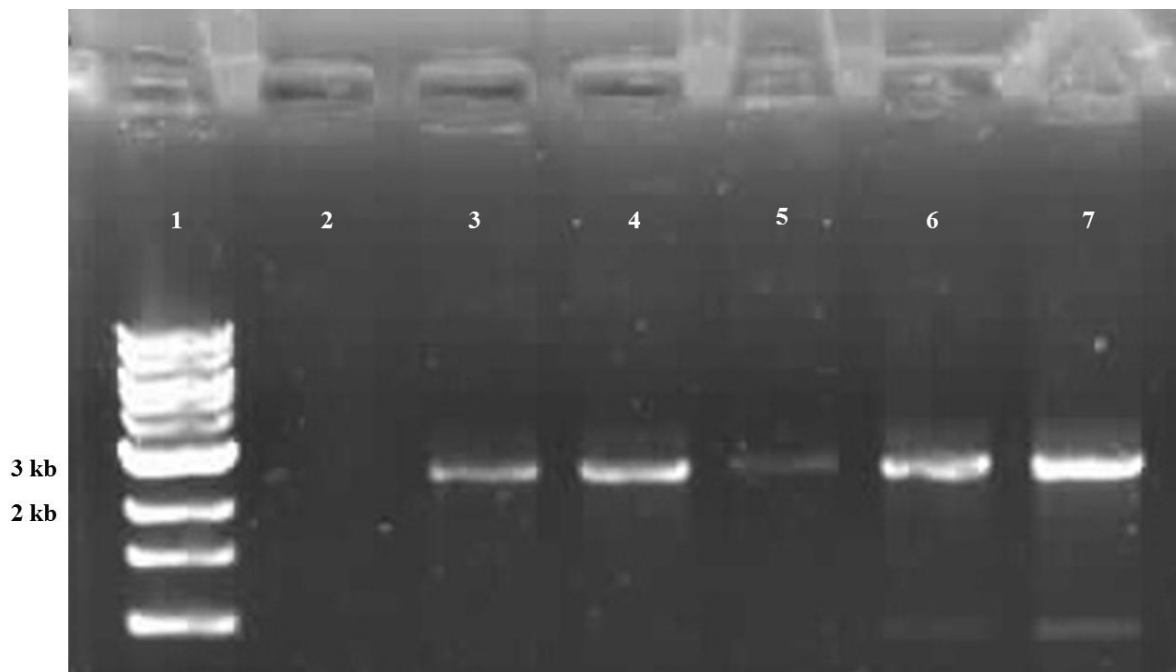
Figure 3.7 Presence of *egtA* confirmed in BY4741$^{p426\ GPD\text{-}egtA}$ by colony PCR. Lane 1= 10 kb NEB DNA ladder, lane 2= negative control, lanes 3, 4 & 5= *egtA* His tag in *S. cerevisiae* BY4741$^{p426\ GPD\text{-}egtA}$ (size 2.5 kb) amplified with high fidelity taq, lane 4= BY4741 colony that did not contain *egtA* His tag, lane 7= positive control *p426 GPD-egtA* (size 2.5 kb).

Western Blot analysis to confirm the expression of EgtA (Figure 3.8). Cultures of BY4741 $^{p426\ GDP\text{-}egtA\ His\ tag}$ were grown for 24 h and protein was extracted as described in Section 2.2.7.1. Protein was loaded onto a polyacrylamide gel as described in Section 2.2.7.4 and transferred onto a PVDF membrane as described in Section 2.2.7.5.
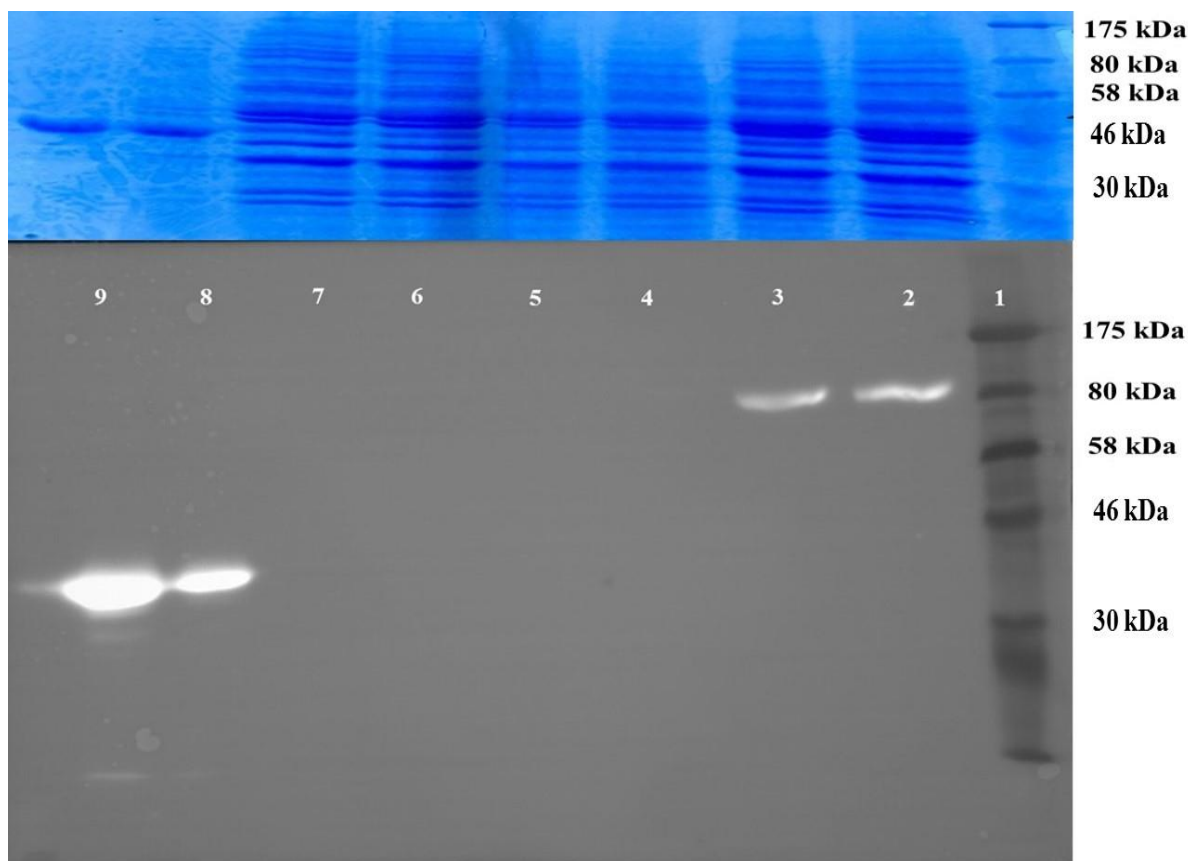
Figure 3.8 Western Blot confirming the expression of EgtA in BY4741$^{p426\ GPD\text{-}egtA\ \text{His tag}}$. Lane 1= NEB Prestained Protein ladder 175-7 kDa, lanes 2-3= EgtA His tag protein (96 kDa) from *S. cerevisiae* BY4741$^{p426\ GPD\text{-}egtA\ \text{His tag}}$ cell lysate, lanes 4-7= negative control BY4741$^{p426\ GPD\text{-}egtA}$ cell lysate, lane 7= positive control recombinant GliT His Tag (36 kDa) (Schrettl *et al*., 2010). Western blot visualized using a Syngene Bioimager.

To further confirm that EgtA was expressed protein analysis by mass spectrometry was carried out. Cell lysates were constructed from a 24 h culture and ran on a polyacrylamide gel. Bands were sampled from the polyacrylamide gel where EgtA was located and trypsin digested as described in Section 2.2.8.1. Samples were analysed on a Q-Exactive Orbitrap LC-MS system (Thermo Scientific) and identified peptides were analysed using Proteome Discoverer software (Figure 3.9). The product of the gene AFUA_2G15650, the Egt-1 homologue denoted as EgtA in this study was identified by having a high score and 69 unique peptides identified exclusively to it (Table 3.1).
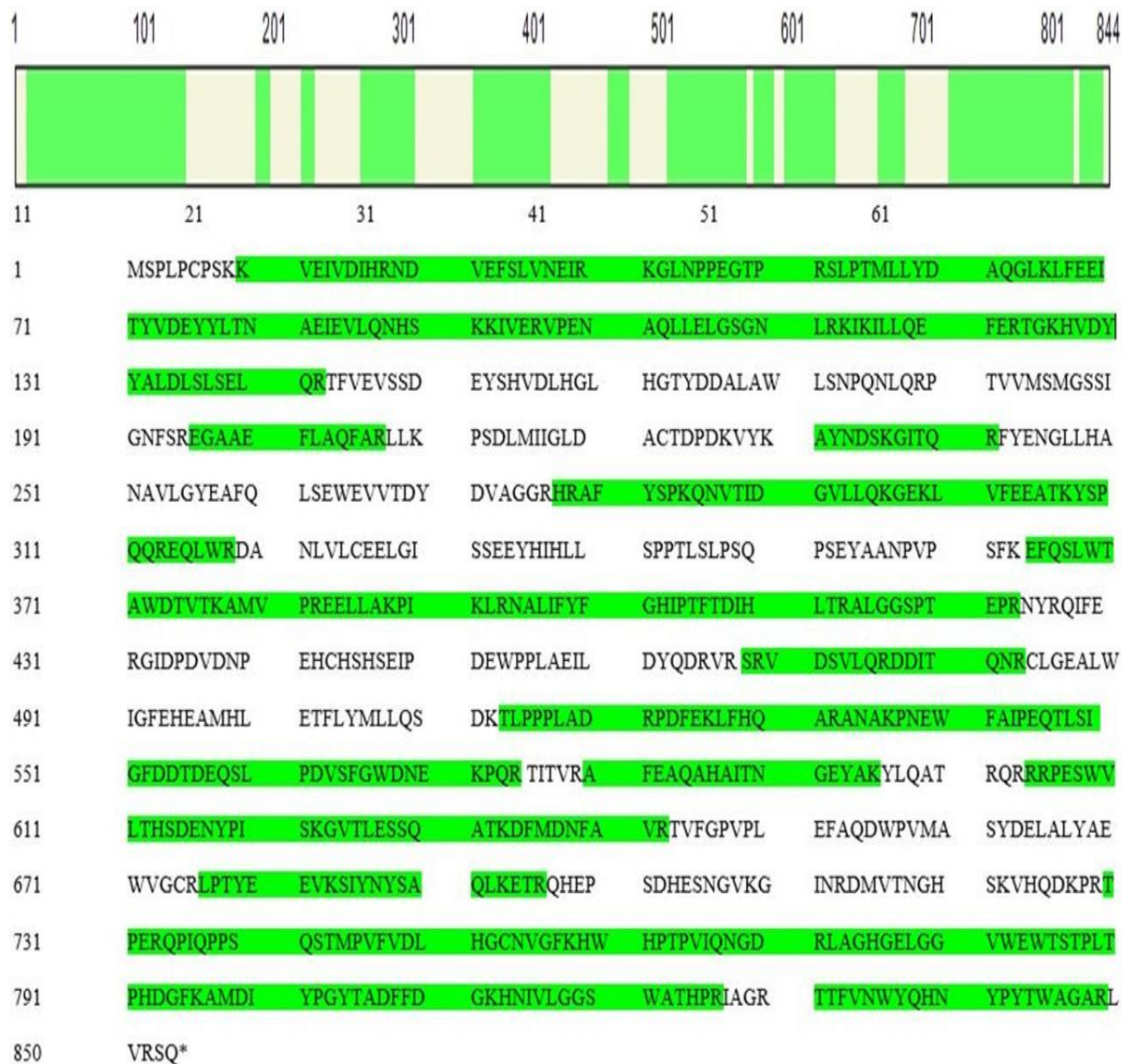
Figure 3.9 EgtA identified from protein MS analysis of *S. cerevisiae* BY4741*p426 GPD-egtA* His tag cell lysate. EgtA was confirmed to be produced by BY4741*p426 GPD-egtA* His tag with 61 % coverage. Both peptides form the N-and C-terminal are present highlighted in green indicating that EgtA is intact upon expression.

Table 3.1 AF293 _A. fumigatus_ proteins identified in BY4741[426 GPD-egtA His tag] using Proteome Discoverer

Accession	Score	Coverage %	Identified Proteins	Unique Peptides	Amino Acids	Molecular Weight (kDa)
AFUA_2G15650	756.34	61.37	1	69	844	96.2

3.3 Confirmation of ergothioneine production in the yeast _S. cerevisiae_ using LC-MS analysis

Ergothioneine was detected in _S. cerevisiae_ strain BY4741[p426 GPD-EgtA] by alkylation of EGT with the fluorescent alkylation agent 5'-Iodoacetamidofluorescein (5'-IAF) first used by Gallagher _et al_. (2012). Gallagher _et al_. (2012) demonstrated alkylated EGT was capable of being detected by RP-HPLC analysis when loaded onto a C-18 Agilent XDB-Eclipse column. Alkylation of EGT with 5'-IAF the molecules hydrophobicity allowing for its detection with a hydrophobic stationary phase which otherwise could not be used due to the hydrophilic of EGT (Gründemann 2012). This method exhibits high sensitivity for the detection of alkylated EGT (0.15 µM) and sensitivity can be increased in combination with LC-MS analysis (Sotgia _et al_., 2013).

Alkylated samples were analysed using a Q-Exactive Orbitrap LC-MS system as described in Section 2.2.9.6. Alkylated EGT was identified using its known fragmentation pattern (Figure 3.10 A-C), identified by Gallagher _et al_. (2012). EGT alkylated with 5'-IAF has been identified as having a single charged _m/z_ of 617 (M + H)$^+$ and a _m/z_ of 309 (M + H)$^{2+}$ when double protonated. The daughter ions _m/z_ 573 and _m/z_ 514 have also been detected using tandem mass spectrometry as well as their double protonated versions _m/z_ 287 and _m/z_ 257 respectively (Gallagher _et al_., 2012).
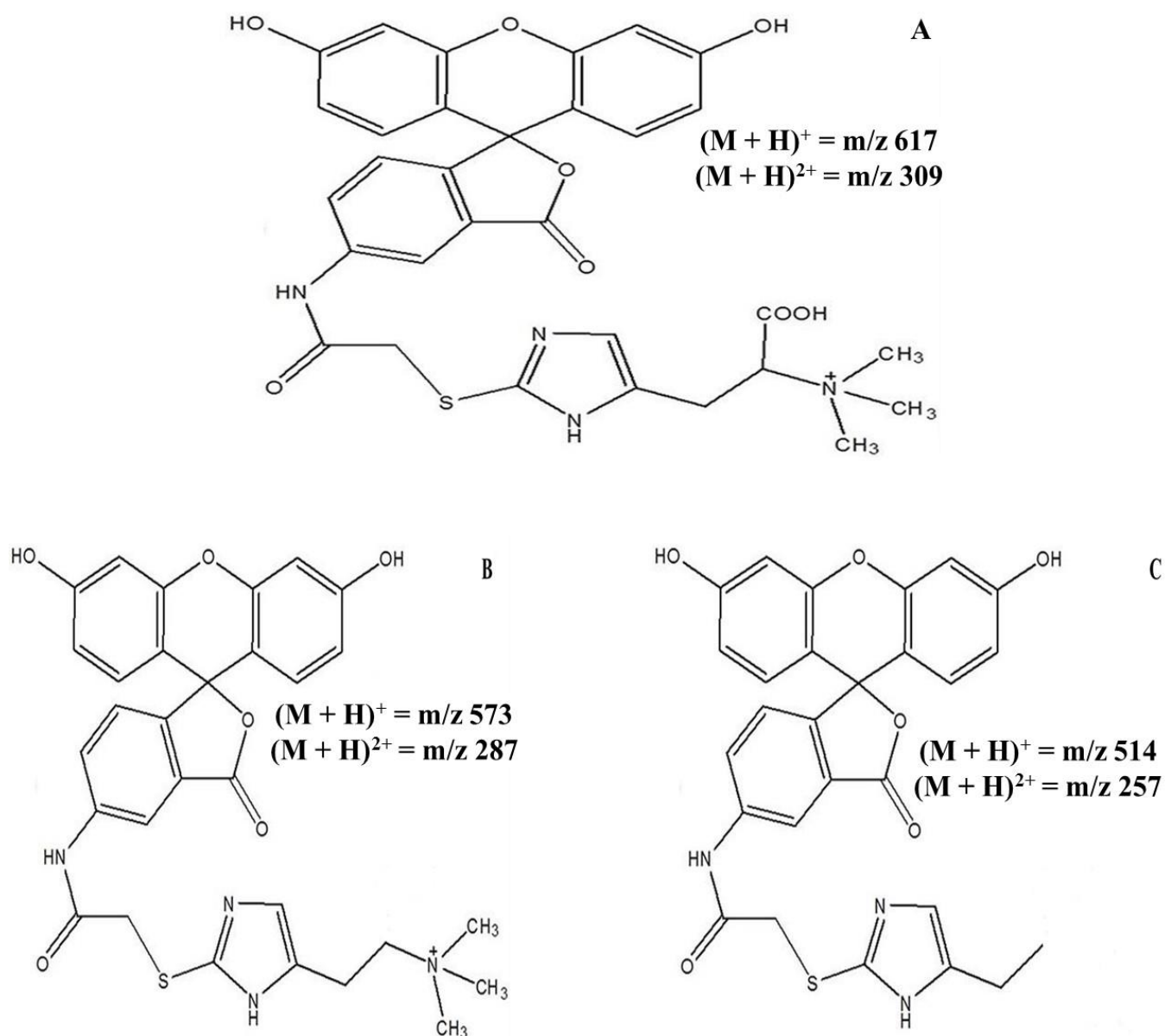
Figure 3.10 A-C Alkylated EGT with 5'-IAF and identified fragments. (A) The molecular ion EGT-AF $(M + H)^+ = m/z$ 617 and $(M + H)^{2+} = m/z$ 309 caused by double protonation of the molecular ion . (B) The daughter ion $(M + H)^+ = m/z$ 573 with a neutral loss of 44 from the loss of COO$^-$ from the molecular ion EGT-AF with the double protonated version $(M + H)^{2+} = m/z$ 287. (C) EGT-AF $(M + H)^+ = m/z$ 514 with a neutral loss of 103 from with the loss of COO$^-$ and $N(CH_3)_3^+$ and the double protonated version $(M + H)^{2+} = m/z$ 257.

Cultures of BY4741$^{p426\text{-}GPD\text{-}egtA}$ were grown for 24 h and cell lysates were prepared without the addition of DTT. Alkylated lysates were then examined for the presence of intracellular EGT by LC-MS analysis. Examination of the full scan mass spectra identified alkylated EGT in the double protonated form of the molecular ion *m/z* 309 at a retention time of 24 min (Figure 3.11). Tandem mass spectrometry of *m/z* 309 revealed the daughter ions *m/z* 257 and 287 further confirming alkylated EGT was present (Figure 3.12). Neither *m/z* 617 nor *m/z* 309 was detected in the negative control culture BY4741$^{p426\text{-}GPD}$ (Figure 3.13).
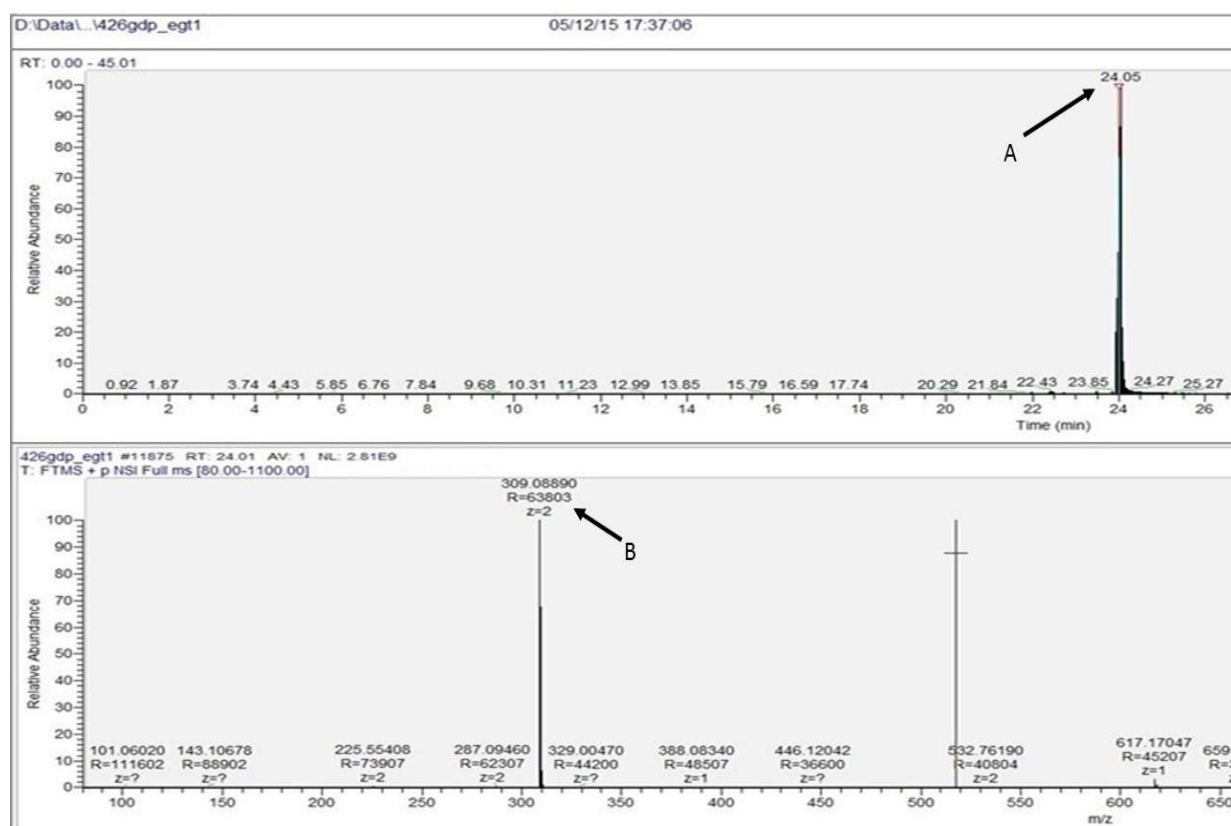
Figure 3.11 Identification of the double protonated form of alkylated EGT (M + H)$^{2+}$ = *m/z* 309 in BY4741$^{p426\text{-}GPD\text{-}egtA}$ cell lysate. Full scan (MS) of BY4741$^{p426\text{-}GPD\text{-}egtA}$ alkylated cell lysate identified at a retention time of 24 min (A) the double protonated form of alkylated EGT *m/z* 309 (B).
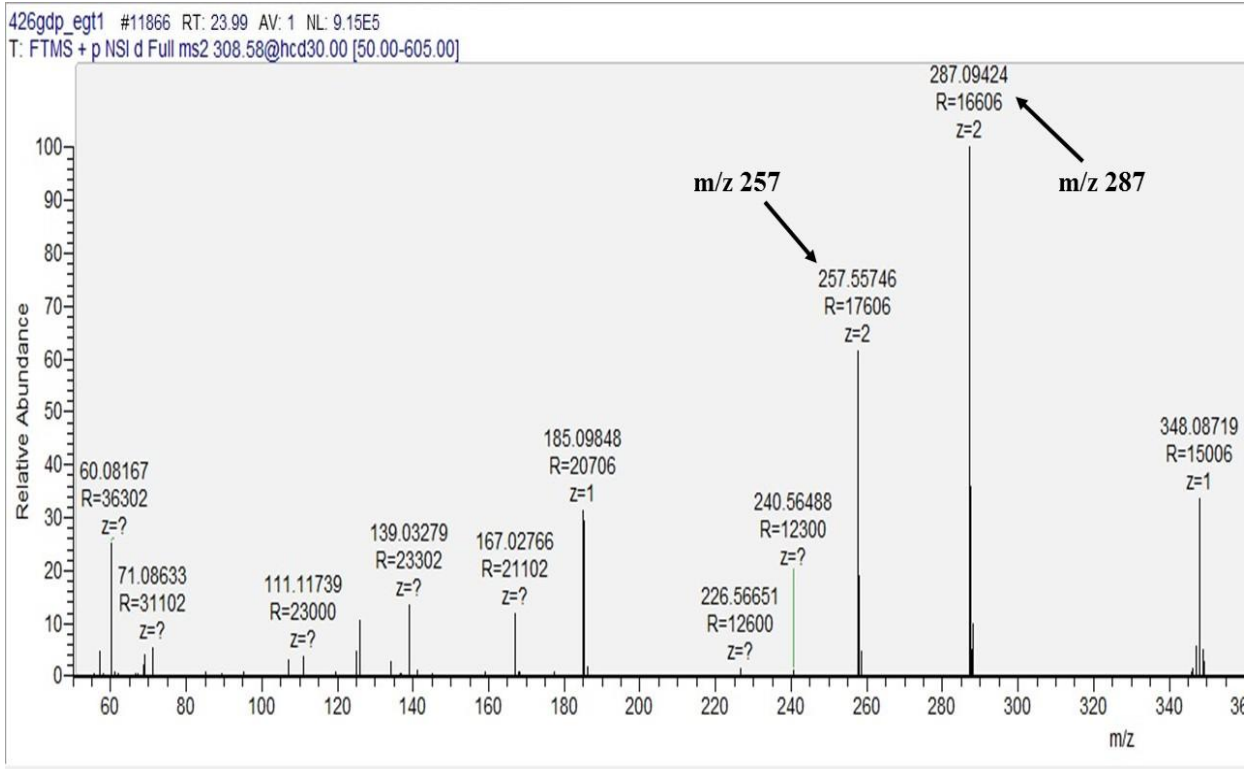
Figure 3.12 Tandem mass spectrometry of *m/z* 309 identifies the daughter ions *m/z* 287 and *m/z* 257 in cell lysate of BY4741$^{p426\text{-}GPD\text{-}egtA}$. MS2 of *m/z* 309 produced the predicted daughter ions *m/z* 287 and *m/z* 257 confirming the intracellular presence EGT.
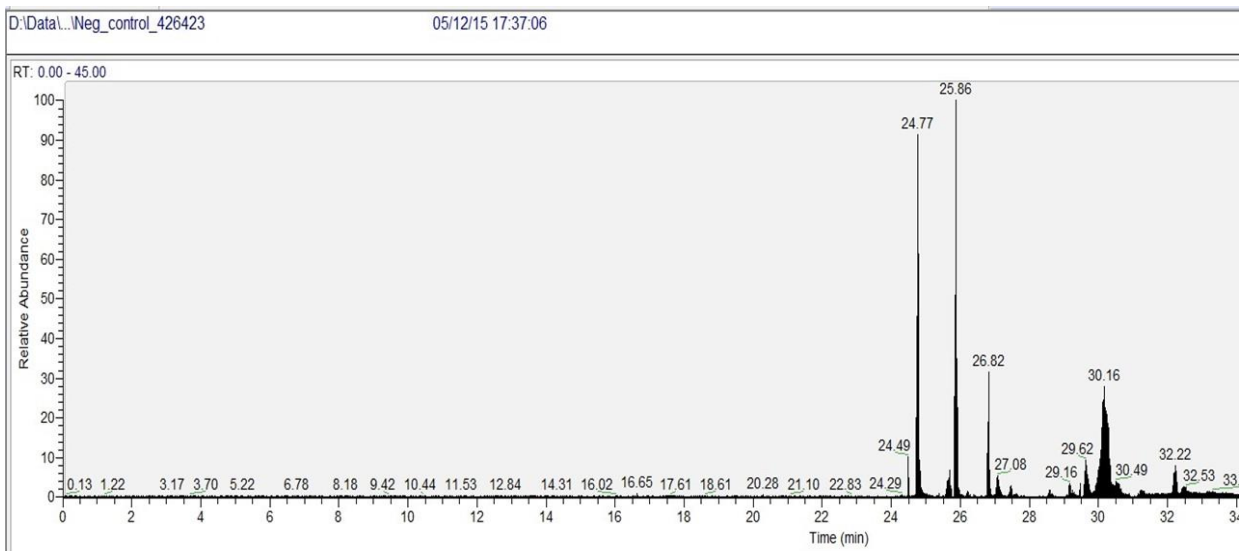
Figure 3.13 Full scan for *m/z* 309 and *m/z* 617 reveals neither is present in the control culture BY4741$^{p426\text{-}GPD}$. Full scan mass spectra of the control culture BY4741$^{p426\text{-}GPD}$ did not contain *m/z* 309 identified at a retention time of 24 min or *m/z* 617.

Culture supernatant was extracted and alkylated as described in Section 2.2.9.2. Alkylated supernatant was then examined for extracellular EGT using the Q-Exactive Orbitrap LC-MS system and identified using the known fragmentation pattern and *m/z* of alkylated EGT. Full scan mass spectra identified alkylated EGT again in its double protonated form at a retention time of 25.4 min in culture supernatants of BY4741$^{p426\ GPD-egtA}$ (Figure 3.14). Tandem mass spectrometry of m/z 309 revealed the daughter ions *m/z* 257 and 287 confirming *m/z* 309 was indeed alkylated EGT (Figure 3.15). Again *m/z* 617 and *m/z* 309 was not detected in the culture supernatants of negative control cultures of BY4741$^{p426-GPD}$.
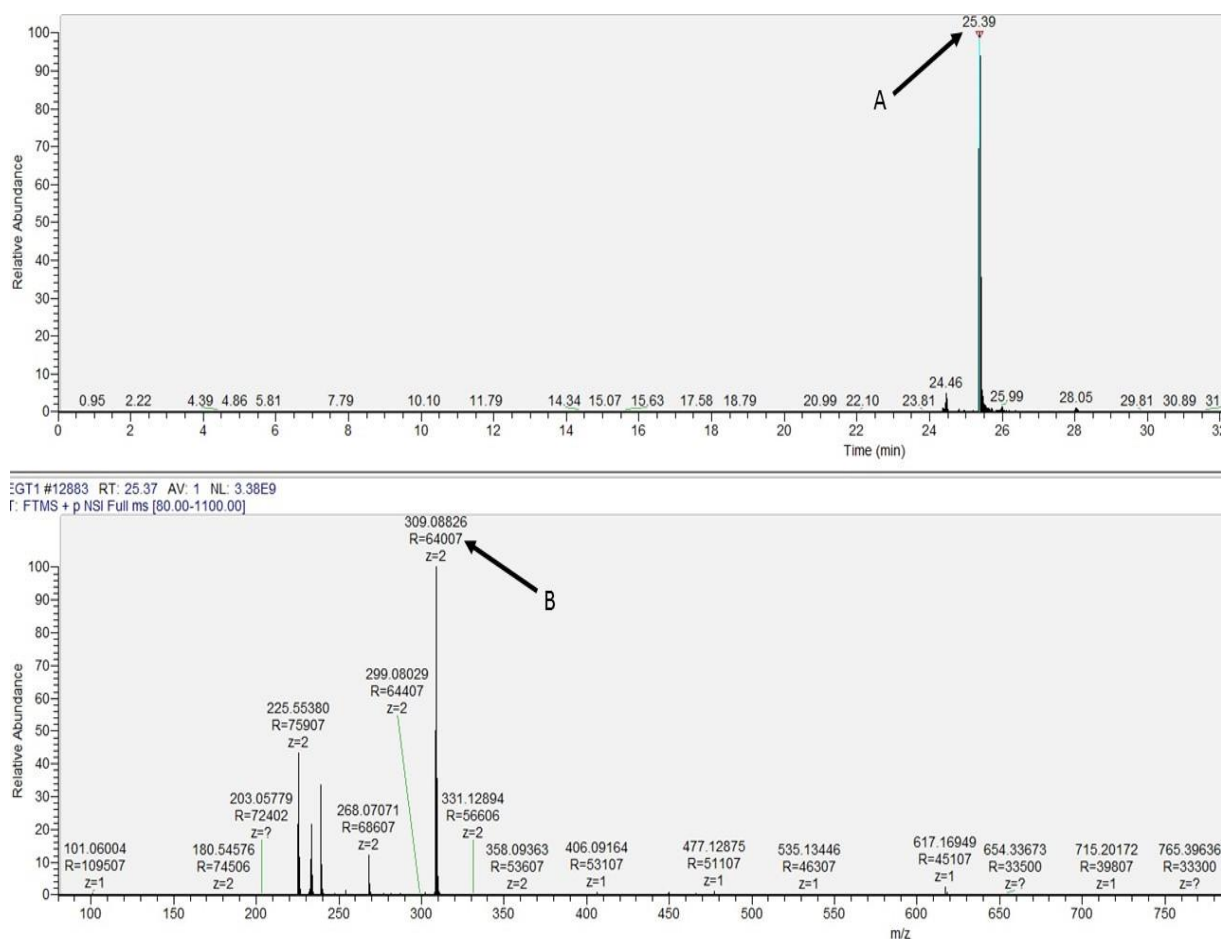
Figure 3.14 Identification of the double protonated form of alkylated EGT (M + H)$^{2+}$ = *m/z* 309 in BY4741$^{p426-GPD-egtA}$ culture supernatant. Full scan MS of BY4741$^{p426-GPD-egtA}$ identified at a retention time of 25.39 min. (A) Alkylated EGT *m/z* 309 (B) in the culture BY4741$^{p426-GPD-egtA}$ at a retention time of 25.39 min. (B) The double protonated form of alkylated EGT.
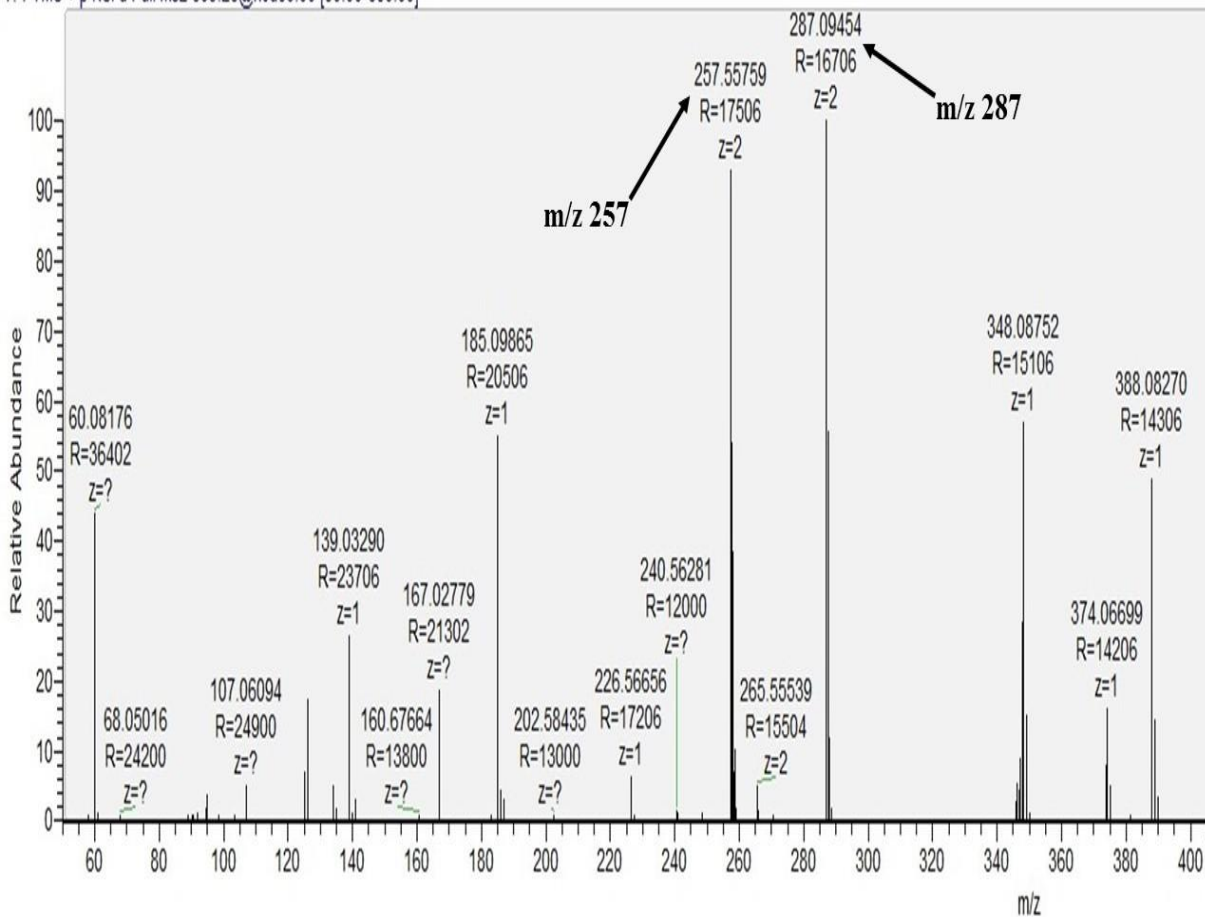
Figure 3.15 Tandem mass spectrometry of *m/z* 309 identifies the daughter ions *m/z* 287 and *m/z* 257 in culture supernatant. MS2 of *m/z* 309 produced the predicted daughter ions of *m/z* 309 confirming the presence alkylated EGT extracellularly.

3.4 Detection of ergothioneine in the yeast *S. cerevisiae* using RP-HPLC analysis

Alkylation of an EGT standard with 5'-IAF was seen to produce a peak with a retention time of approximately 13.7 min to 13.8 min varying slightly with room temperature (Figure 3.16), using an Agilent Eclipse XDB-C18 column and a Shimadzu Prominence HPLC system as described in Section 2.1.12.1.
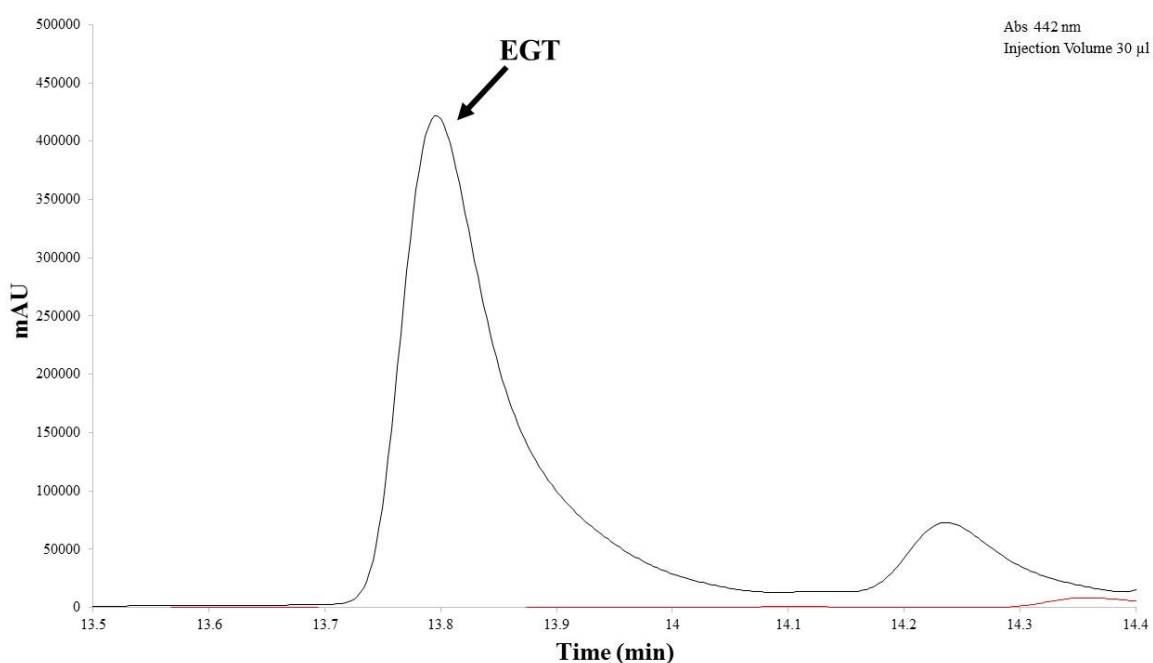
Figure 3.16 Detection of alkylated EGT standard (100 µg/ml) compared to PBS negative control. Alkylated EGT elutes from the stationary phase at a retention time of approximately 13.8 min (black) with no peak in PBS control (red).

Extracellular EGT levels were examined by preparing cultures in triplicate at the time points 24 h, 48 h, 72 h, 96 h and 120 h. Cell lysates were then prepared and alkylated with 5'-IAF as described in Section 2.2.9.2 and examined using RP-HPLC analysis as described in Section 2.2.9.4. Extracellular EGT was identified in BY4741$^{p426\text{-}GPD\text{-}egtA}$ culture supernatants by comparison with culture supernatant from the negative control BY4741$^{426\text{-}GPD}$. RP-HPLC analysis revealed the presence of an additional peak in BY4741$^{p426\text{-}GPD\text{-}egtA}$ supernatant with a retention time of 13.83 matching the retention time of the EGT standard (Figure 3.17).
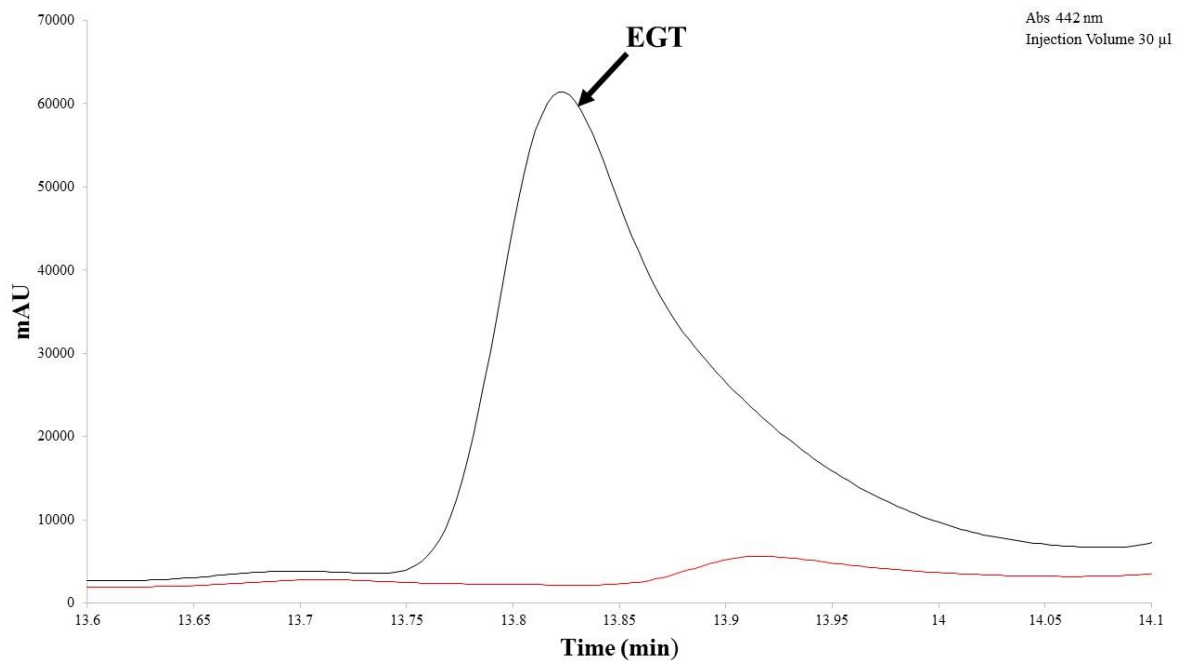
Figure 3.17 Detection of EGT in BY4741$^{p426\text{-}GPD\text{-}egtA}$ in culture supernatants using RP-HPLC analysis. Novel peak identified in alkylated culture supernatants of BY4741$^{p426\text{-}GPD\text{-}EgtA}$ (black) when compared to alkylated culture supernatant from BY4741$^{p426\text{-}GPD}$ (red) matches the retention time of alkylated EGT standard of 13.8 min.

Intracellular EGT levels were then investigated, by preparing cultures in triplicate at the time points of 24, 48 and 72 h. From these cell lysates were prepared and alkylated with 5'-IAF as described in Section 2.2.9.1. BY4741$^{p426\text{-}GPD\text{-}egtA}$ lysates were examined in comparison to BY4741$^{p426\text{-}GPD}$ for the presence of intracellular EGT. At the time point of 24 h EGT was identified to be co-eluting with a small peak with a retention time of 13.81 min noticed in the control BY4741$^{p426\text{-}GPD}$ (Figure 3.18). No EGT was identified in cell lysates from 48 h and 72 h cultures.
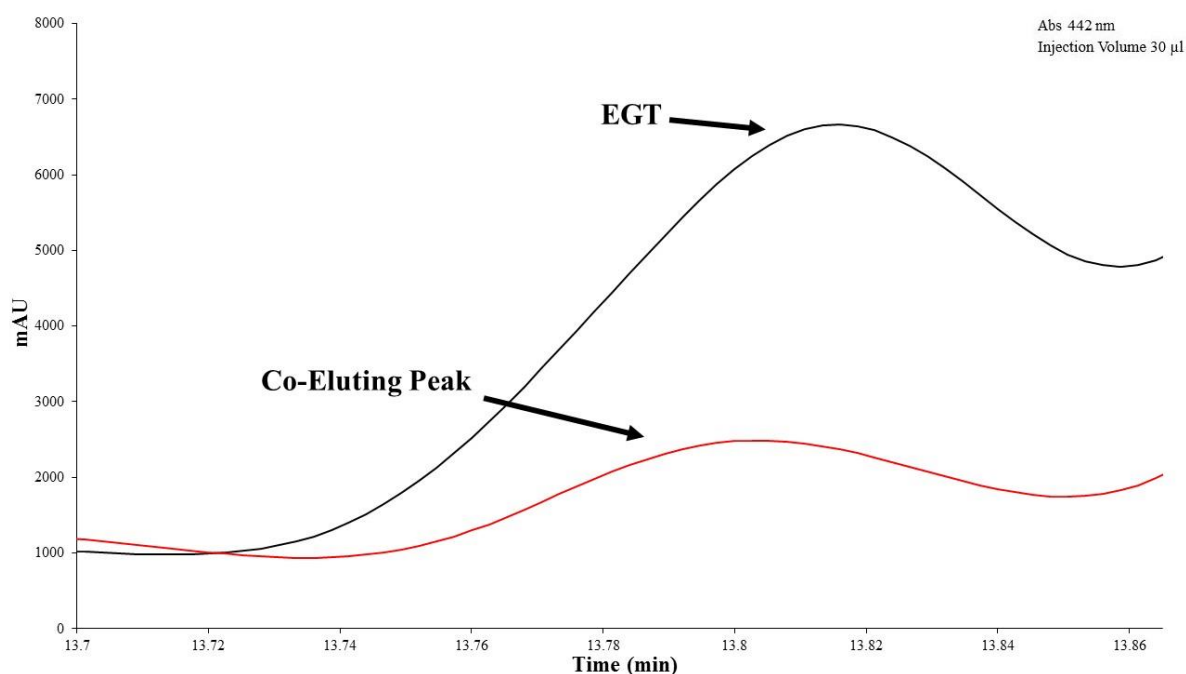
Figure 3.18 EGT in BY4741$^{426\text{-}GPD\text{-}egtA}$ in cell lysates using RP-HPLC analysis. Peak of BY4741$^{p426\text{-}GPD\text{-}EgtA}$ cell lysate (black) when compared to alkylated cell lysate from BY4741$^{p426\text{-}GPD}$ (red) which matches the retention time of alkylated EGT (13.8 min). A small peak can be seen to co-elute with EGT in cell lysates of BY4741$^{p426\text{-}GPD}$.

3.5 Quantification of EGT in the yeast *S. cerevisiae* using RP-HPLC analysis shows a greater abundance of EGT in culture supernatant

A standard curve was constructed as described in Section 2.2.9.3 to enable determination of the quantity of EGT in BY4741$^{426\text{-}GPD\text{-}egtA}$. EGT was measured in terms of the peak area produced by the quantity of EGT loaded onto the column (Figure 3.19). The quantity EGT in culture supernatants of 24 h, 48 h, 72 h, 96 h and 120 h BY4741$^{426\text{-}GPD\text{-}egtA}$ cultures was calculated using the standard curve as described in Section 2.2.9.5.
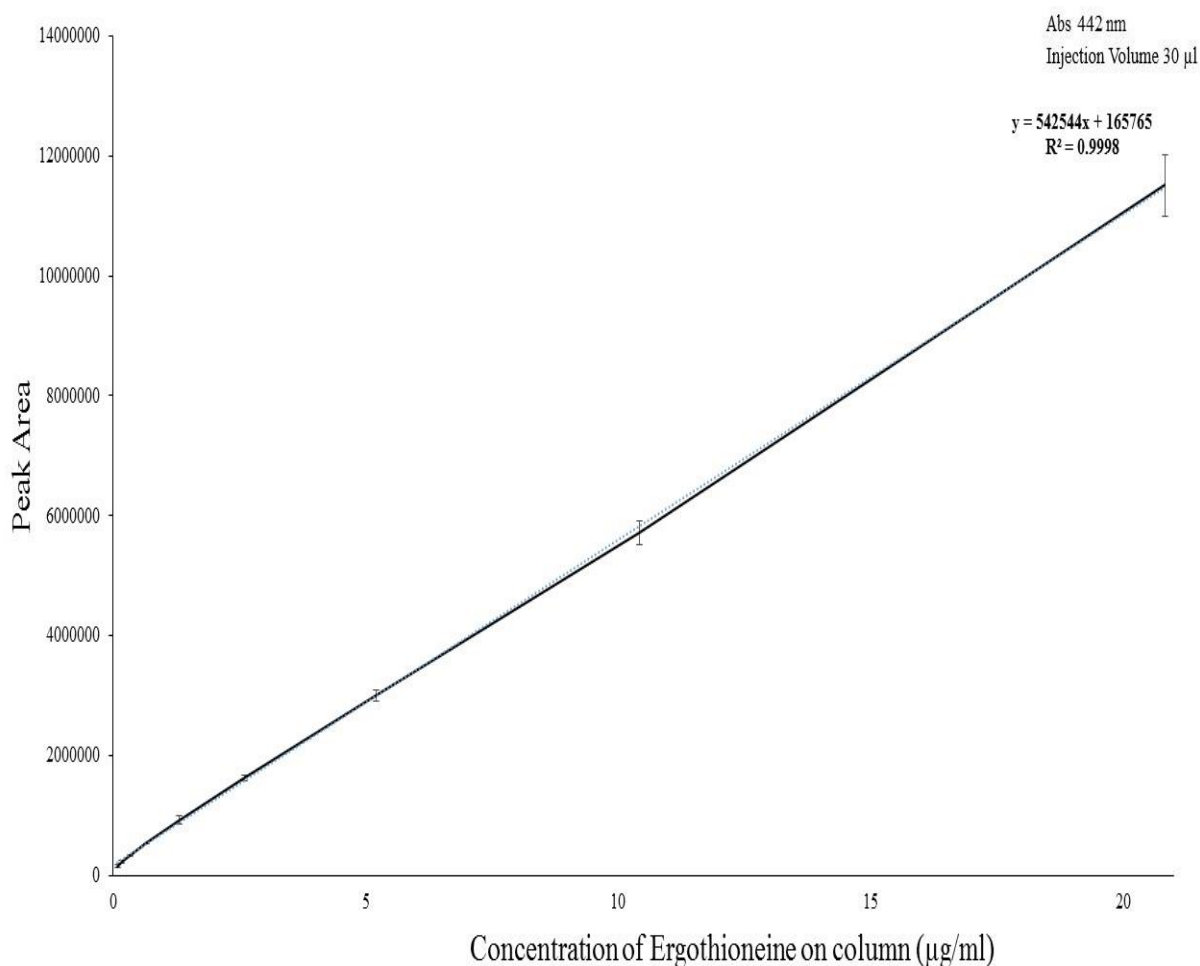
Figure 3.19 Standard curve of EGT. Standard curve generated using 9 EGT standards ranging from 0.08 µg/ml to 20.83 µg/ml of EGT loaded onto column. Accuracy of standards was gauged by the curves R^2 value which was 0.9998 indicating a high degree of accuracy

EGT was quantified using the equation produced from the standard curve as described in Section 2.2.9.6. A small amount of intracellular EGT was only detected at 24 h and present at a significantly higher level extracellularly at 24 h (P < 0.0001).The quantity of EGT in supernatant of BY4741$^{426\text{-}GPD\text{-}egtA}$ rose at the time points 48 h, 72 h and peaked at 96 h with 7.93 mg/L of EGT detected (Figure 3.20). This indicates that most EGT is either been effluxed out of cells or possibly leaking from cells at death phase as the cell membrane loses its integrity.
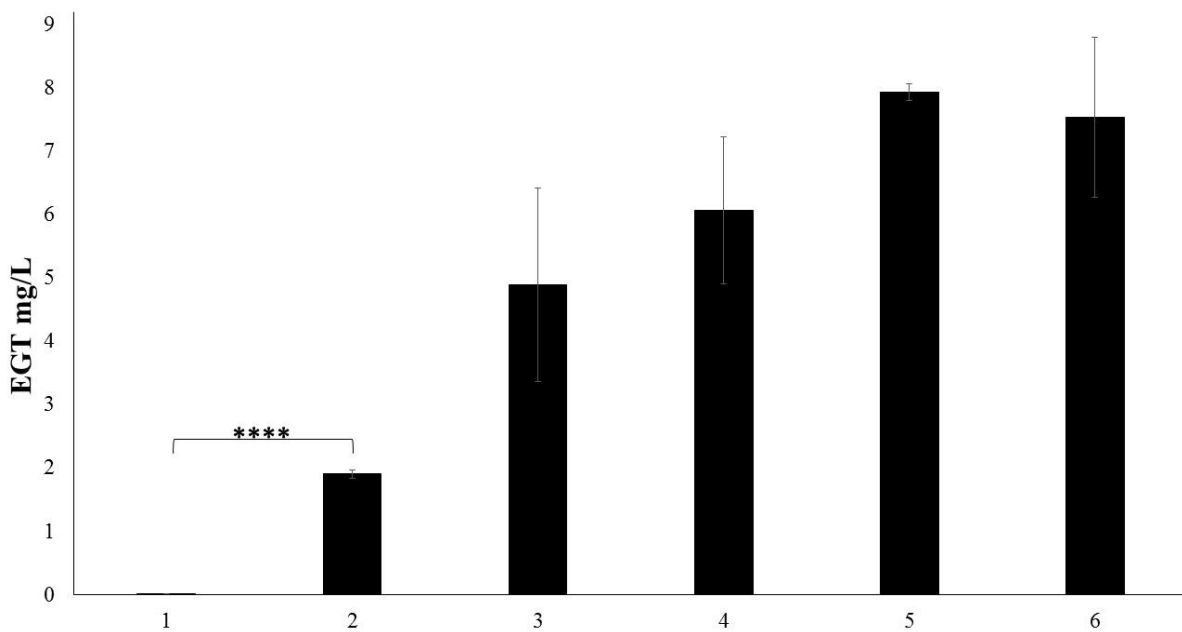
Figure 3.20 Quantification of EGT production (n = 2). Quantity of EGT in BY4741$^{426\text{-}GPD\text{-}egtA}$ grown in SC media. 1= Quantity of intracellular EGT (10.12 µg/L) after 24 h. 2= Quantity of extracellular EGT (1.91 mg/L) after 24 h. 3= Quantity of extracellular EGT (4.89 mg/L) after 48 h. 4= Quantity of extracellular EGT (6.07 mg/L) after 72 h. 5= Quantity of extracellular EGT (7.93 mg/L) after 96 h. 6= Quantity of extracellular EGT (7.53 mg/L) after 120 h.

3.6 Phenotypic response of *S. cerevisiae* ergothioneine producing strain to oxidative stress from hydrogen peroxide

The *S. cerevisiae* EGT producing strain BY4741$^{426\text{-}GPD\text{-}egtA}$ was investigated to see if production of EGT would increase growth when experiencing oxidative stress from the ROS stressor, hydrogen peroxide. However BY4741$^{426\text{-}GPD\text{-}egtA}$ did not confer any resistance to oxidative stress from hydrogen peroxide. BY4741$^{426\text{-}GPD\text{-}egtA}$ was observed to have increased sensitivity to hydrogen peroxide when compared to wildtype BY4741$^{426\text{-}GPD}$ at a concentration of 1-1.5 mM hydrogen peroxide (Figure 3.21 B and C). Both BY4741$^{426\text{-}GPD\text{-}egtA}$ and wildtype growth was abolished at 2 mM hydrogen peroxide (Figure 3.21 D).
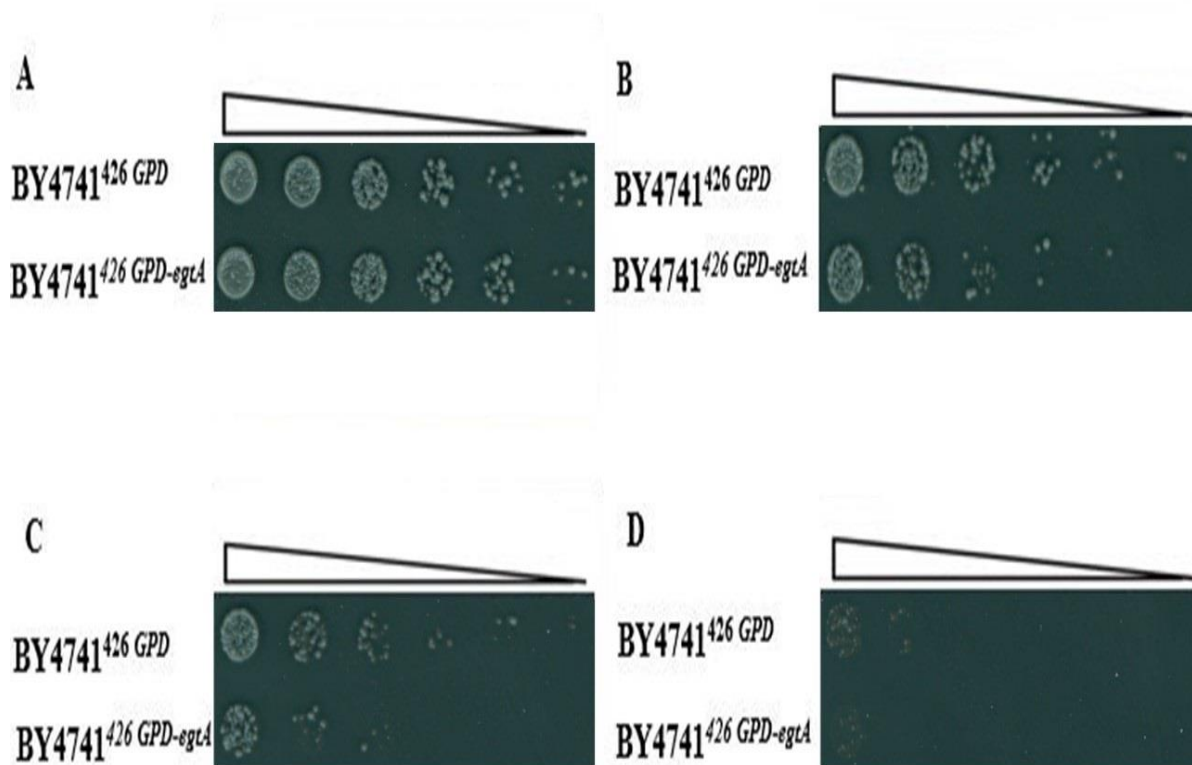
Figure 3.21 A-D Growth analysis of *S. cerevisiae* strains on synthetic complete media (SC) with hydrogen peroxide. Comparative growth analysis assay using strains BY4741$^{426\text{-}GPD}$ and BY4741$^{426\text{-}GPD\text{-}egtA}$. (A) Strains BY4741$^{426\text{-}GPD}$ and BY4741$^{426\text{-}GPD\text{-}egtA}$ grown on SC media. (B) Strains BY4741$^{426\text{-}GPD}$ and BY4741$^{426\text{-}GPD\text{-}egtA}$ grown on SC media with 1 mM hydrogen peroxide added. (C) Strains BY4741$^{426\text{-}GPD}$ and BY4741$^{426\text{-}GPD\text{-}egtA}$ grown on SC media with 1.5 mM hydrogen peroxide added. (D) Strains BY4741$^{426\text{-}GPD}$ and BY4741$^{426\text{-}GPD\text{-}egtA}$ grown on SC media with 2 mM hydrogen peroxide added.

BY4741$^{426\ GPD\text{-}egtA}$ did not confer any additional tolerance to ethanol, growth was maintained at wildtype level and abrogated completely at a concentration of 8 % ethanol (Figure 3.22).
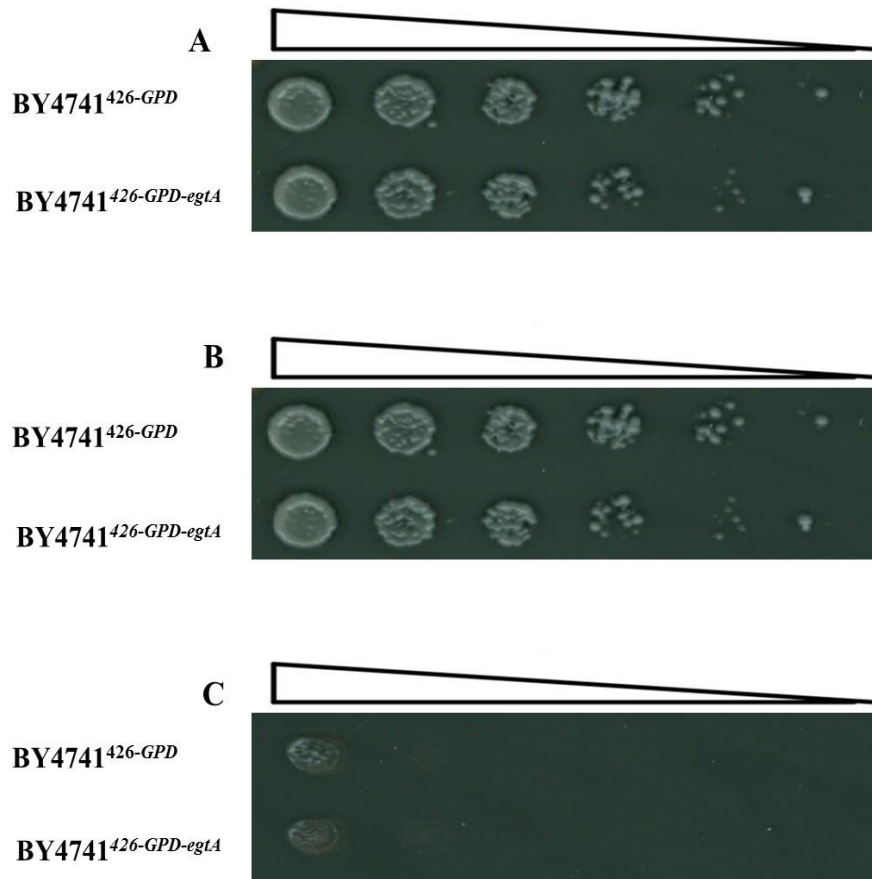
Figure 3.22 A-D Growth analysis of *S. cerevisiae* strains on synthetic complete media (SC) with ethanol. (A) Strains BY4741$^{426\text{-}GPD}$ and BY4741$^{426\text{-}GPD\text{-}egtA}$ grown on SC media. (B) Strains BY4741$^{426\text{-}GPD}$ and BY4741$^{426\text{-}GPD\text{-}egtA}$ grown on SC media with 4 % ethanol added. (C) Strains BY4741$^{426\text{-}GPD}$ and BY4741$^{426\text{-}GPD\text{-}egtA}$ grown on SC media with 8 % ethanol added.

3.7 BY4741$^{426\text{-}GPD\text{-}egtA}$ egtA mutant T213A shows increased production of EGT at 24 h but is not significant.

Phosphate-based signalling is critical to almost all major cellular processes and is ubiquitously present across Archaea, Prokaryotes, and Eukaryotes (Kannan *et al.*, 2007). EgtD in *M. tuberculosis* was identified to be negatively regulated by phosphorylation at Thr^{213} by PknD a serine protein kinase (Richard-Greenblatt *et al.*, 2015). The *S. cerevisiae* genome is predicted to contain 122 protein kinases (Zhu *et al.*, 2000). With the exception of two histidine protein kinases all of the yeast protein kinases are members of the Ser/Thr family (Zhu *et al.*, 2000). Thr^{213} was identified to be conserved in EgtA and was reasoned that it could be indiscriminately phosphorylated in *S. cerevisiae*. To investigate this site directed mutagenesis was used to changing Thr^{213} to Ala as described in Section 2.2.2.2. Conversion of Thr^{213} to Ala was confirmed by DNA sequence analysis as described in Section 2.2.2.3. The p426 GDP-*EgtA* T213A mutant was transformed into *S. cerevisiae* BY4741 and selected by their ability to grow on –URA SC media as well as carrying out a colony PCR (Figure 3.23).
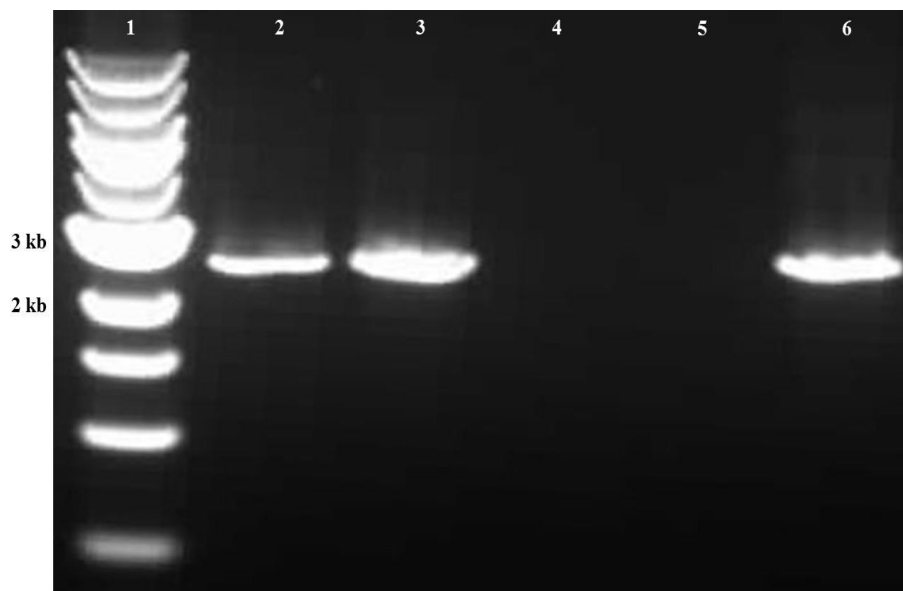
Figure 3.23 Presence of *egtA* T213A confirmed in BY4741 by colony PCR. Lane 1= 10 kb NEB DNA ladder, lanes 2 & 3= *egtA* T213A in BY4741 $^{p426\text{-}GPD\text{-}egtA\ T213A}$ (size 2.5 kb)

amplified with high fidelity Taq, lane 4 empty, lane 5= negative control, lane 6= positive control *p423-GPD-egtA* (size 2.5 kb).

RP-HPLC analysis determined BY4741 [p426-GPD-*egtA* T213A] produces EGT by identification of a peak at 13.84 min with an identical retention time to an EGT standard (Figure 3.24 A-B). This peak was present in both cell lysates and culture supernatant of BY4741 [p426-GPD-*egtA* T213A] and was not present in the control strain BY4741 [p426-GPD] at the time point of 24 h (Figure 3.24 C-D).
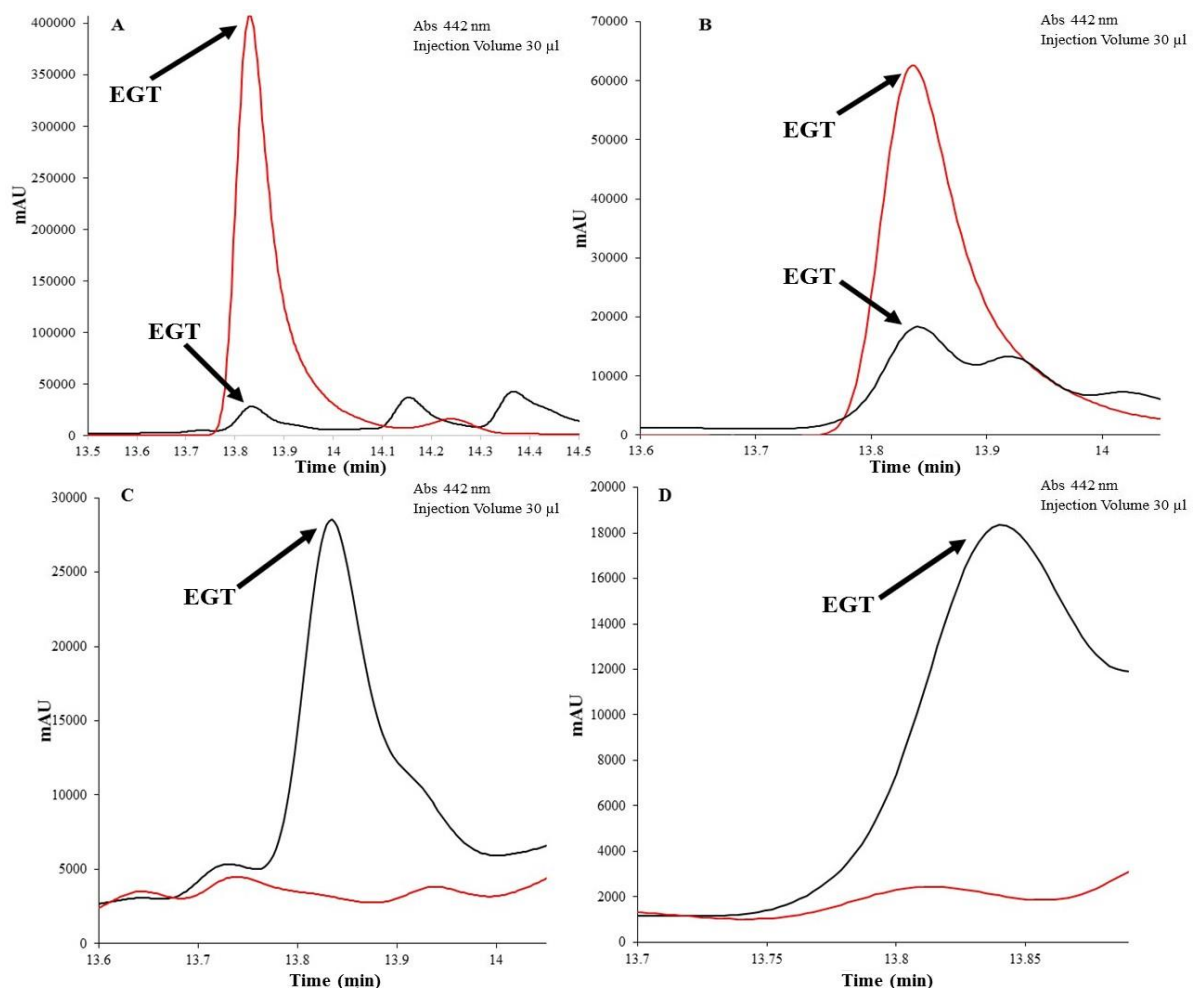
Figure 3.24 A-D EGT production by BY4741 [p426-GPD-*egtA* T213A]. (A) Extracellular EGT detected in culture supernatant (black) by seeing a peak at a retention time of 13.84 min compared to an EGT peak in an EGT standard, 13.84 min (red). (B) Intracellular EGT detected in cell lysate with a retention time of 13.84 min detected (black) compared to EGT standard, 13.84 min (red). (C) Extracellular EGT detected in culture supernatants. BY4741 [p426-GPD-*egtA* T213A] produces EGT seen by a peak at 13.85 min (black) compared to BY4741 [p426-GPD] (red)

which does not produce EGT. (D) Intracellular EGT detected in cell lysates. BY4741 $^{p426\text{-}GPD\text{-}egtA\ T213A}$ produces EGT seen by a peak at 13.84 min (black) compared to BY4741 $^{p426\text{-}GPD}$ (red) which does not produce EGT.

In triplicate 24 h cultures of BY4741 $^{p426\text{-}GPD\text{-}egtA\ T213A}$ were shown to have higher levels of EGT than BY4741 $^{p426\text{-}GPD\text{-}egtA}$ both extracellularly and intracellularly at 24 h but this was not statistically significant (Figure 3.25 A & B). However this trend was reversed in 72 h cultures with the extracellular EGT level of BY4741 $^{p426\text{-}GPD\text{-}egtA\ T213A}$ lower than that of BY4741 $^{p426\text{-}GPD\text{-}egtA}$ (Figure 3.25 C). Overall there was an increase in extracellular EGT in 72 h cultures of BY4741 $^{p426\text{-}GPD\text{-}egtA\ T213A}$ and BY4741 $^{p426\text{-}GPD\text{-}egtA}$ compared to their 24 h counterparts in keeping with previous observations.
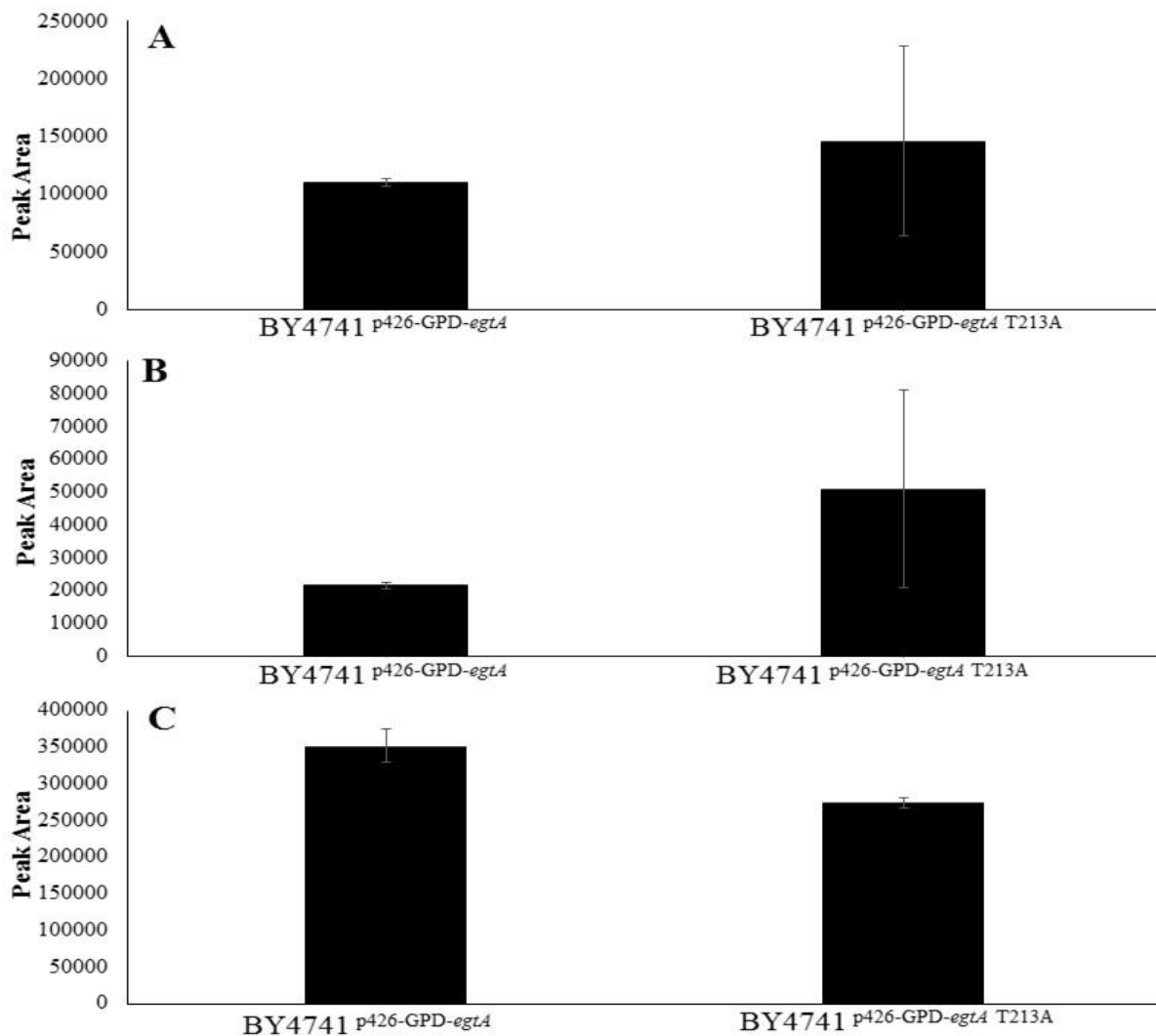
Figure 3.25 A-C Comparison of EGT production in BY4741 $^{p426\text{-}GPD\text{-}egtA\ T213A}$ to BY4741

p426-GPD-*egtA* (n = 2). (A) Peak areas of 24 h extracellular EGT in BY4741 [p426-GPD-*egtA* T213A] and BY4741 [p426-GPD-*egtA*]. (B) Peak areas of 24 h intracellular EGT in BY4741 [p426-GPD-*egtA* T213A] and BY4741 [p426-GPD-*egtA*]. (C) Peak areas of 72 h extracellular EGT in BY4741 [p426-GPD-*egtA* T213A] and BY4741 [p426-GPD-*egtA*].

3.8 Co-expression of *egtA* with the *egtB* candidate AFUA_2G13295 decreases the level of EGT in *S. cerevisiae*.

The *egtB* candidates AFUA_2G13295 (*egt2a*) and AFUA_3G14240 (*egt2b*) were selected due to their sequence homology with known cysteine desulfurases used in the EGT biosynthetic pathway. *Egt2a* is a possible homologue of the cysteine desulfurase gene SPBC660.12c determined to be *egt2* in *S. pombe* by Pluskal *et al*. (2014) sharing 29 % identity. Egt2a shares homology with mycobacterial EgtE as well as Egt2 identified in *N. crassa* sharing 45 % identity with *N. crassa* Egt2 (Bello *et al*. (2012). *Egt2b* is a mitochondrial cysteine desulfurase and a homologue of *nfs1* found in *S. cerevisiae* which we considered the enzyme most likely to be completing EGT biosynthesis in *S. cerevisiae*.

RNA was extracted from the *A. fumigatus* strain AF293 as described in Section 2.2.6.1 and reverse transcribed into cDNA as described in Section 2.2.6.4. *Egt2a* and *egt2b* were amplified from cDNA by PCR using high fidelity Taq with proof reading ability to ensure sequence integrity. *Egt2a* was amplified using the primer set egt2a F and egt2a R (Figure 3.26 A), for AFUA_3G14240 the primer set egt2bF and egt2b R (Figure 3.26 B) as described in Table 2.3. Cloning of both *egt2a* and *egt2b* used the cloning strategy *Spe1* and *EcoR1* at the 5' and 3' end respectively.
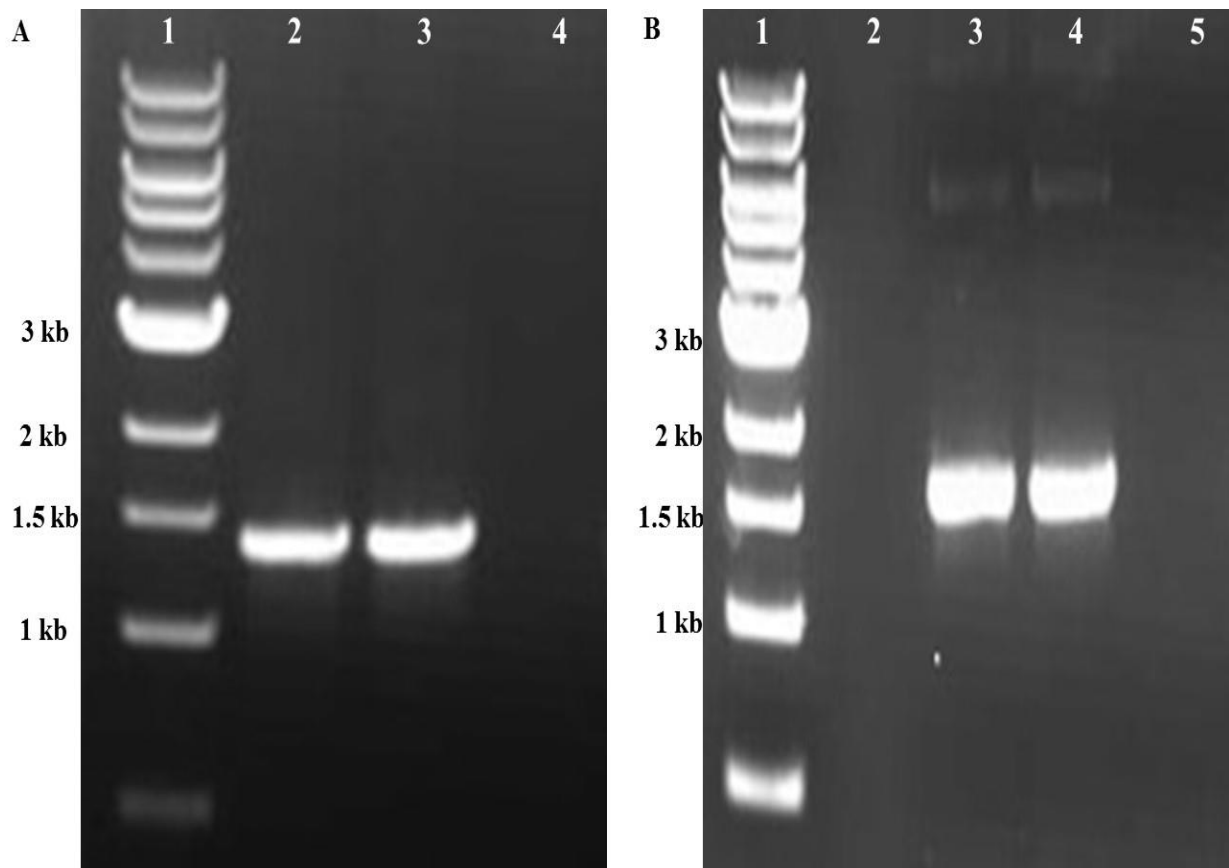
Figure 3.26 A-B Amplification of *egt2a* and *egt2b* from AF293 cDNA. (A) Lane 1= 10 kb NEB DNA ladder, lanes 2 & 3= *egt2a* (size 1.3 kb), lane 4= negative control. (B) Lane 1= 10 kb NEB DNA ladder, lane 2= empty, lanes 3 & 4= *egt2b* (size 1.55 kb), lane 5= negative control.

The PCR products of *egt2a* and *egt2b* were cleaned using Qiagen PCR purification kit as per manufacturer's instructions prior to use. The cleaned PCR products were then digested to create the sticky ends, required when ligating the *egtA* insert. The vector *p423-ADH* (Figure 3.27), was also digested in preparation for ligation.
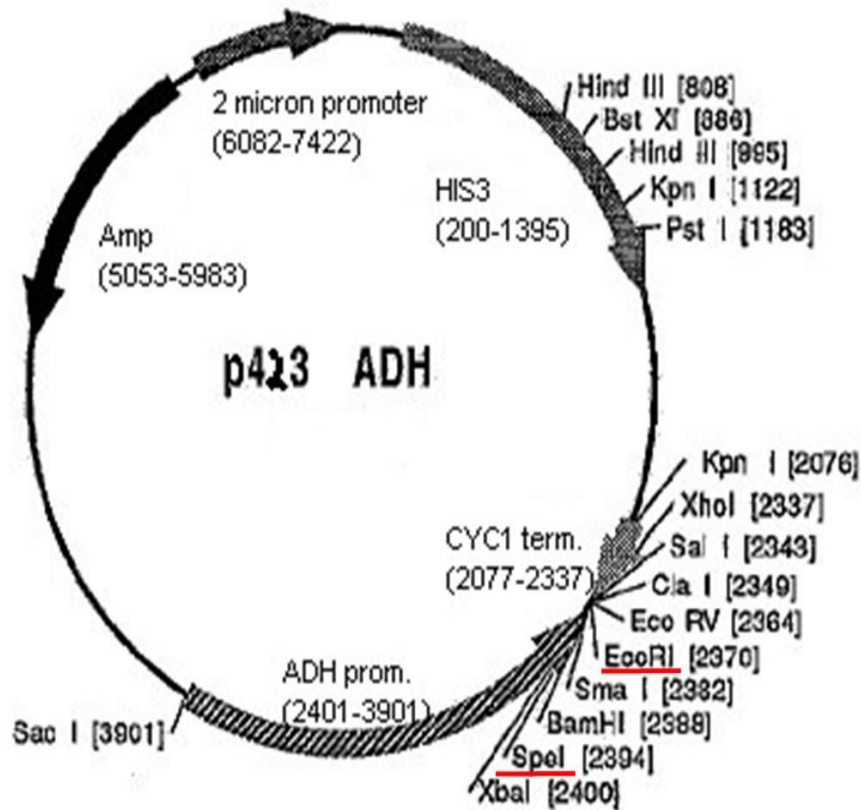
Figure 3.27 The 7.6 kb episomal *S. cerevisiae* shuttle vector *p423 ADH* used to express recombinant *egt2a* and *egt2b*. An *AmpR* gene for selection after cloning into *E. coli* is present along with a *HIS3* gene for selection after transformation into *S. cerevisiae* and the restriction enzyme sites *Spe1* and *EcoR1* used as part of the cloning strategy.

Both inserts and vector were digested with the restriction enzymes *Spe1* and *EcoR1* for 3 h at 37 °C and separated using gel electrophoresis on an agarose gel (Figure 3.28 A, B & C). Fragments were then excised from the agarose gel using Qiagen quick gel extraction kit as per manufacturer's instructions.
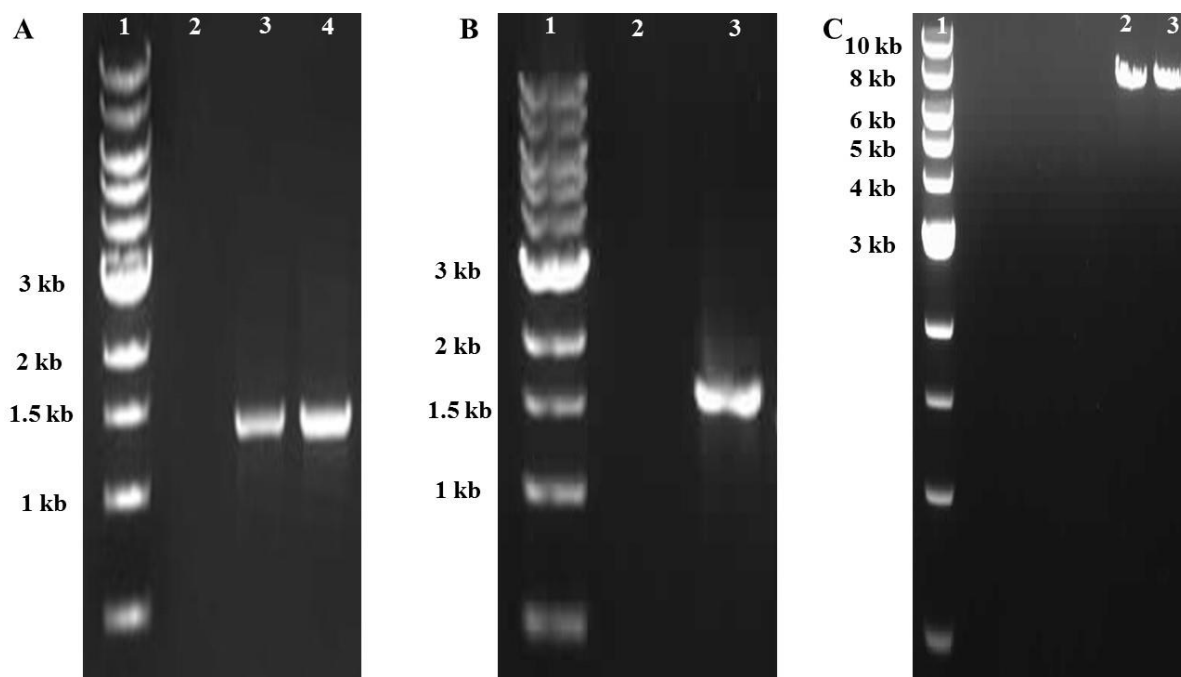
Figure 3.28 A-C Digestion of *egt2a*, *egt2b* and *p423 ADH* with the restriction enzymes *Spe1* and *EcoR1*. Lane 1= 10 kb NEB DNA ladder, (A) lane 2= empty, lanes 3 & 4= digest of *egt2a* (size 1.3 kb), (B) Lane 2= empty, lanes 3 = Digest of *egt2b* (size 1.55 kb), (C) Lanes 2 & 3= digest of *p426 GPD* (size 7.6 kb).

After gel extraction of digested inserts and vector the DNA concentration of samples was measured using a Nanodrop (Mason). The *egt2a* and *egt2b* inserts were then ligated separately into the vector *p423-ADH* as described in Section 2.2.3.5 and left overnight at 16 °C. The ligation products *p423-ADH-egt2a* and *p423-ADH-egt2b* were then transformed into *E. coli* cells as described in Section 2.2.4.5. *E. coli* cells with *p423 ADH-egt2a* and *p423 ADH-egt2b* were selected by their ability to grow on LB-amp-agar plates. *P423-ADH-egt2a* and *p423-ADH-egt2b* plasmid DNA was purified from transformed *E. coli* as described in Section 2.2.5.1. *P423-ADH-egt2a* and *p423-ADH-egt2b* plasmid DNA was then transformed into the *S. cerevisiae* strain BY4741*p426-GPD-egtA* as described in Section 2.2.4.2. An empty *p423-ADH* plasmid was transformed into BY4741*p426-GPD-egtA* for a better comparison. Successful transformants were selected by their ability to grow on –URA -HIS SC media. A colony PCR was carried out on selected colonies to further confirm that the transformation was a success (Figure 3.29).
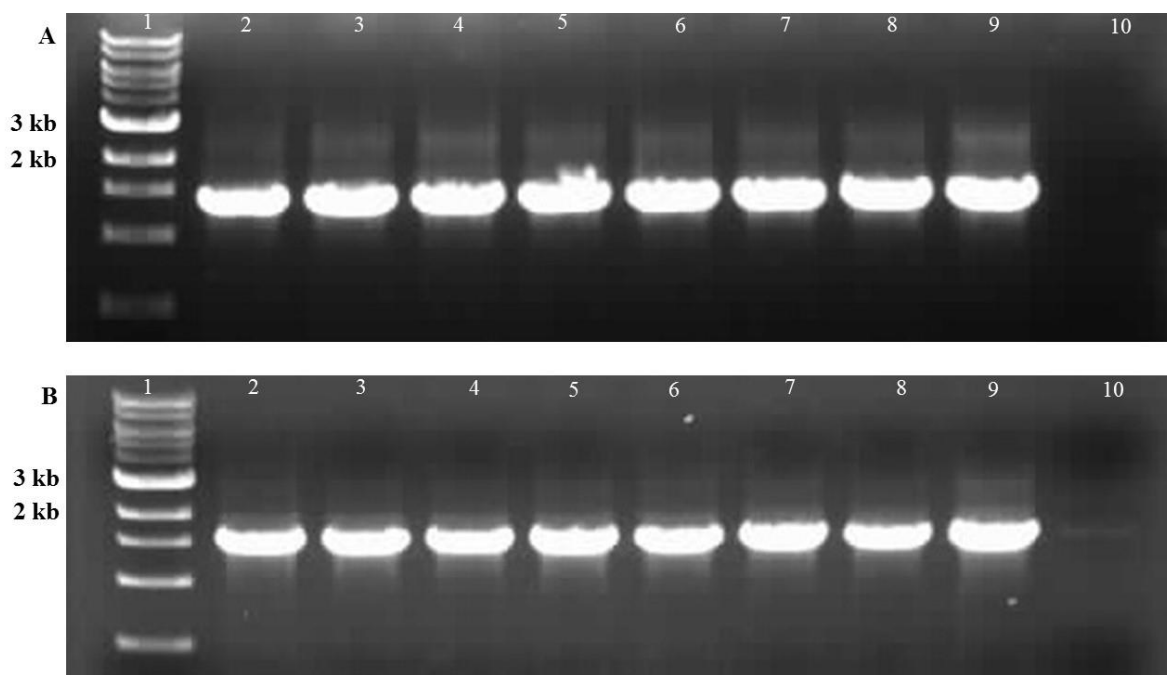
Figure 3.29 Successful transformation of *egt2a* and *egt2b* into BY4741$^{p426\text{-}GPD\text{-}egtA}$ confirmed by colony PCR. (A) Lane 1= 10 kb NEB DNA ladder, lanes 2-8 = *egt2a* (size 1.3 kb) from *S. cerevisiae* BY4741$^{p426\text{-}GPD\text{-}egtA\ p423\ ADH\text{-}egt2a}$ amplified with high fidelity taq, lane 9= positive control *egt2a* (size 1.3 kb) from *p423-ADH-egt2a*, lane 10= negative control. (B) Lane 1= 10 kb NEB DNA ladder, lanes 2-8 = *egt2b* (size 1.55 kb) from *S. cerevisiae* BY4741$^{p426\text{-}GPD\text{-}egtA\ p423\text{-}ADH\text{-}egt2b}$ amplified with high fidelity Taq, lane 9= positive control *egt2b* (size 1.55 kb) from *p423-ADH-egt2b*, lane 10= negative control.

Expression of *egt2a* was confirmed by generation of a His tag on the N-terminus of Egt2a in the vector *p423-ADH*. The same method was employed as in Section 3.3 using the appropriate primers listed in Table 2.3 and the template *p423-ADH* using the restriction sites *Spe1* and *Xho1* at the 5' and 3' end respectively. Following a successful transformation of BY4741 with *423 ADH-egt2a* and *423-ADH-egt2b* with an N terminal His tag successful transformants were screened by colony PCR as in Section 3.3. A western blot was preformed to confirm expression of *egt2a* and *egt2b*. Cultures of BY4741 $^{423\text{-}ADH\text{-}egt2a\ \text{His tag}}$ and BY4741 $^{423\ ADH\text{-}egt2b\ \text{His tag}}$ were grown for 24 h cell lysates and loaded onto a polyacrylamide gel and transferred onto a PVDF membrane. *Egt2a* was shown to be transcribed and expressed by BY4741 $^{423\text{-}ADH\text{-}egt2a\ \text{His tag}}$ (Figure 3.30). Unfortunately expression of Egt2b could not be detected when either an N- or C-terminal His tag was used.
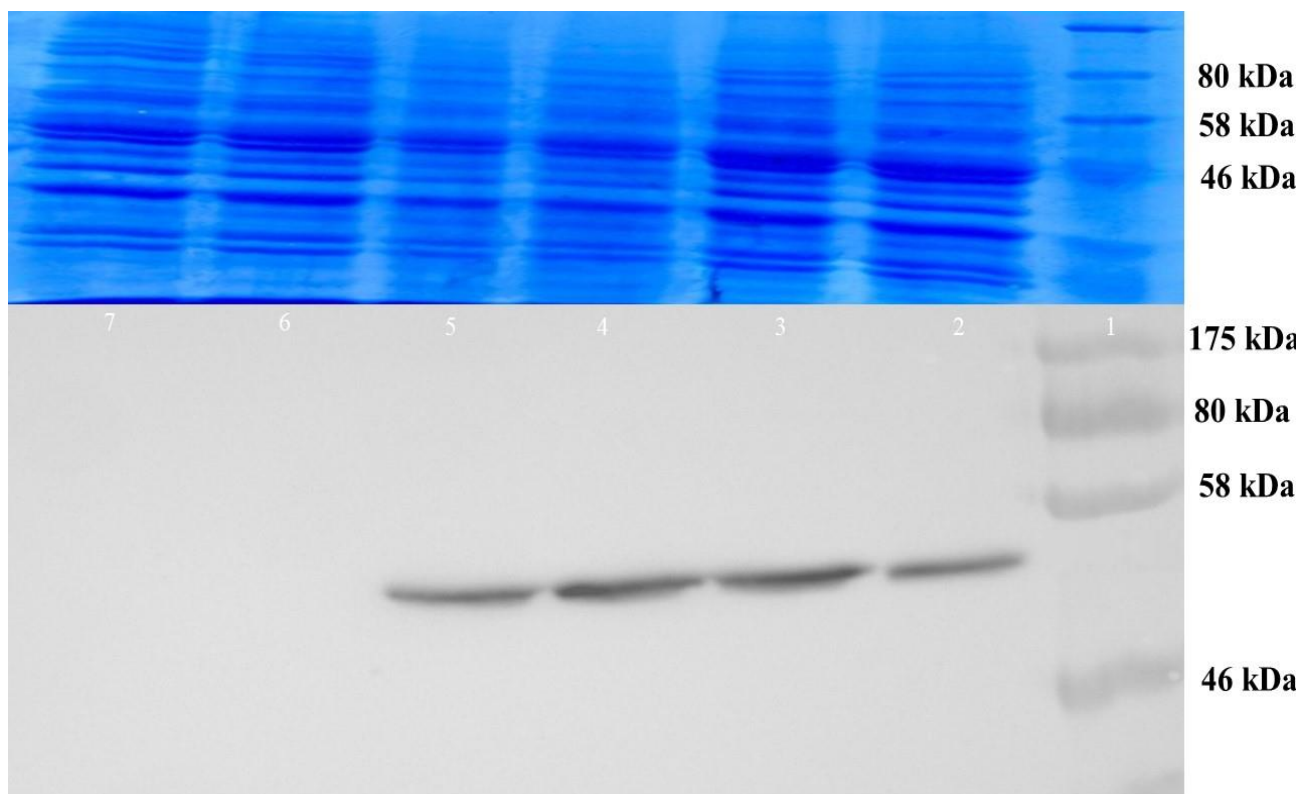
Figure 3.30 Western Blot confirming the expression of Egt2a in BY4741$^{p423\text{-}ADH\text{-}egt2a}$ **His tag.** Lane 1= NEB Prestained Protein ladder 175-7 kDa, lanes 2-3= Egt2a His tag protein (50 kDa) from *S. cerevisiae* BY4741$^{426\ GPD\text{-}egt2a\ His\ tag}$ cell lysate, lanes 6-7= negative control BY4741$^{426\text{-}GPD\text{-}egt2a}$ cell lysate.

EGT production was compared by looking at the peak area of EGT detected in culture supernatants as quantification of EGT had shown a greater abundance of EGT extracellularly (Section 3.5). EGT was confirmed to be produced in BY4741$^{p426\text{-}GPD\text{-}egtA\ p423\text{-}ADH\text{-}egt2a}$ (Figure 3.31 A-B).
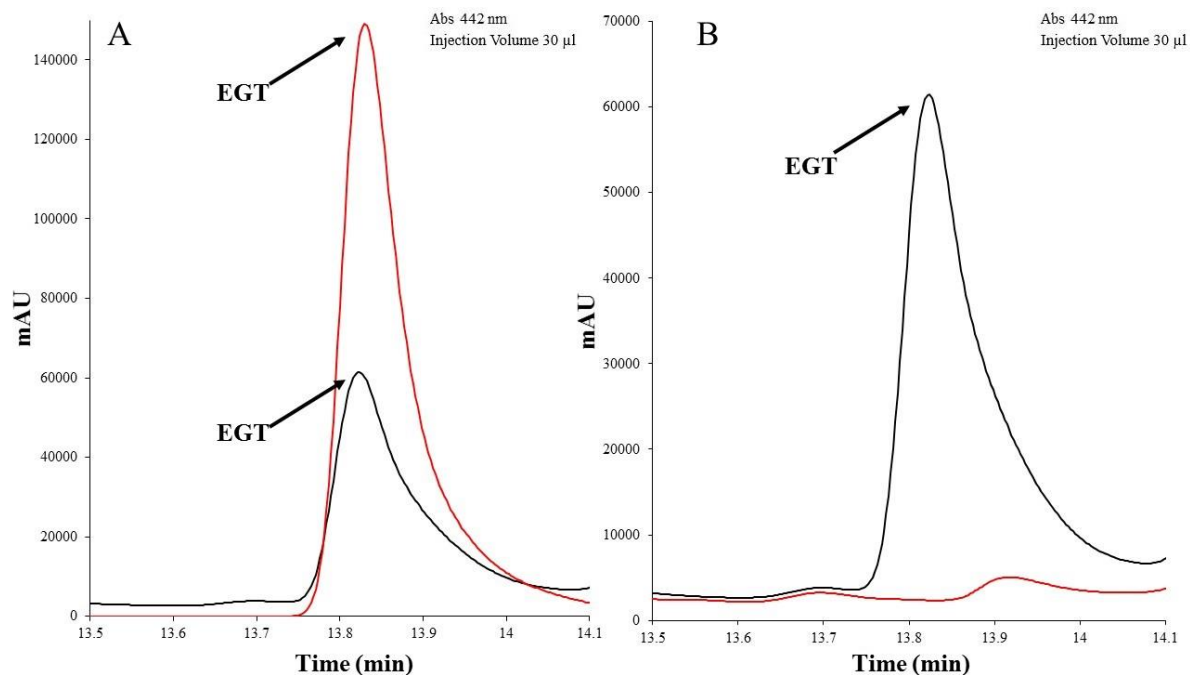
Figure 3.31 Confirmation of EGT production in BY4741$^{p426\text{-}GPD\text{-}egtA\ p423\text{-}ADH\text{-}egt2a}$. (A) EGT in BY4741$^{p426\text{-}GPD\text{-}egtA\ p423\text{-}ADH\text{-}egt2a}$ at a retention time of 13.84 min (black) compared to the EGT standard 13.85 min (red). (B) EGT in BY4741$^{p426\text{-}GPD\text{-}egtA\ p423\text{-}ADH\text{-}egt2a}$ at a retention time of 13.84 min (black) compared to the BY4741$^{p426\text{-}GPD\ p423\ ADH}$ no EGT is produced.

Surprisingly there was significantly less extracellular EGT detected in BY4741$^{p426\text{-}GPD\text{-}egtA\ p423\text{-}ADH\text{-}egt2a}$ when compared with BY4741$^{p426\text{-}GPD\text{-}egtA\ p423\ ADH}$ at 48 h and 72 h (Figure 3.32 A-B).
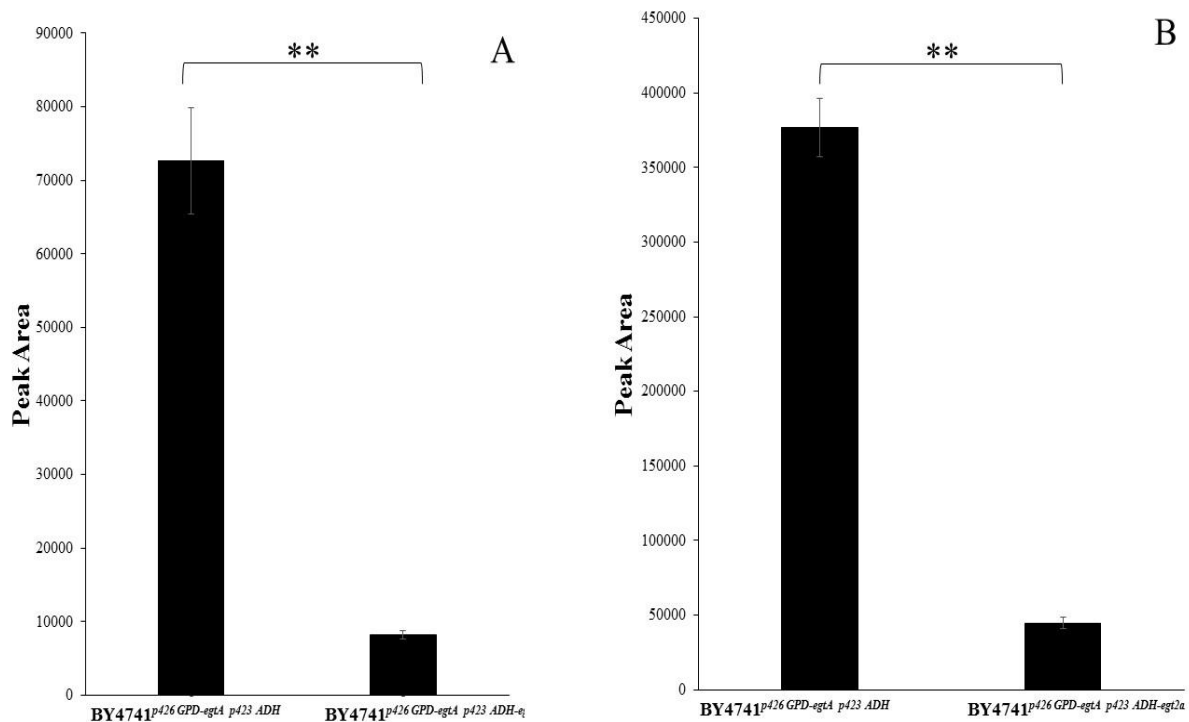
Figure 3.32 Significantly less extracellular EGT produced in BY4741$^{p426\text{-}GPD\text{-}egtA\ p423\text{-}ADH\text{-}egt2a}$ compared to BY4741$^{p426\text{-}GPD\text{-}egtA\ p423\text{-}ADH}$ (n = 2). (A) Peak areas of EGT in the supernatant of cultures grown for 48 h showing significantly higher levels (P = 0.0063) of EGT in BY4741$^{p426\text{-}GPD\text{-}egtA\ p423\ ADH}$ compared to BY4741$^{p426\text{-}GPD\text{-}egtA\ p423\text{-}ADH\text{-}egt2a}$. (B) Peak areas of EGT in the supernatant of cultures grown for 72 h showing significantly higher levels (P = 0.0018) of EGT in BY4741$^{p426\text{-}GPD\text{-}egtA\ p423\ ADH}$ compared to BY4741$^{p426\text{-}GPD\text{-}egtA\ p423\text{-}ADH\text{-}egt2a}$.

3.9 Reduction in expression of yeast *nfs1* or *S-adenosyl-L-homocysteine hydrolase* does not reduce production of EGT in *S. cerevisiae*

Native *S. cerevisiae nfs1* (*nfs1*) involvement in EGT biosynthesis was investigated. Yeast *nfs1* shares homology with both *egt2a* sharing 23 % identity, *egt2b* in particular shares a high degree of similarity (70 % identity). The strain R1158$^{Tet\ nfs1}$ (derived from BY4741) was purchased from Dharmacon with *Sc*NFS1 expression regulated by a TET off system by replacement of the native promoter with a CMV promoter and *tta* gene. Addition of doxycycline in a titratable manner allows for down-regulation of the promoter until the gene of   interest   is   no   longer   expressed   at   detectable   levels

S-adenosyl-L-homocysteine hydrolase (SAHH) is required in the metabolic pathway of sulphur-containing amino acids (Ulrey *et al*., 2005). SAHH plays an essential cellular role catalysing the breakdown of S-adenosyl-L-homocysteine (SAH) by catalysing the reversible hydrolysis of SAH into adenosine and homocysteine (Altintas & Sezgin 2004). This allows for homocysteine to undergo irreversible trans-sulfurization catalysed by pyridoxal phosphate containing enzymes to form cysteine or is converted back to methionine by the addition of a methyl group catalysed by methionine synthase (Altintas & Sezgin 2004). A methyl group from methionine becomes activated by adenosine triphosphate (ATP) with the addition of an adenosine to its methyl group to produce the universal methyl donor S-adenosyl methionine (SAM) (Boison 2013). Once the methyl group is removed from SAM it becomes SAH concluding the cycle (Figure 3.33).
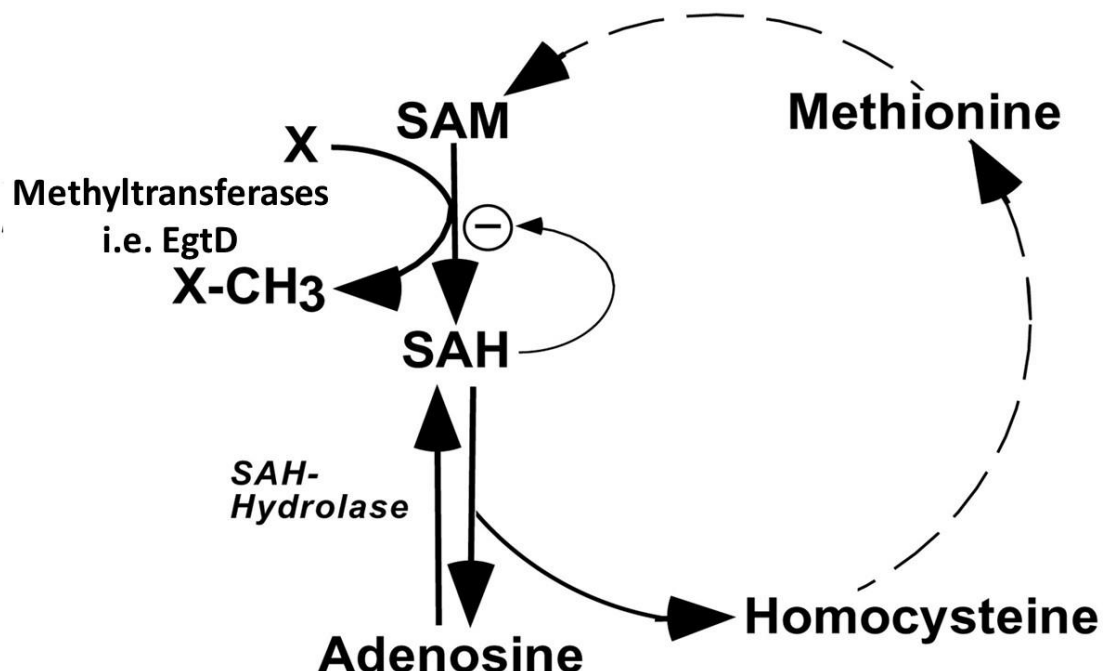
Figure 3.33 The methionine cycle. SAM the methyl donor to various methyltransferases such as EgtD, SAH formed from the removal of the methyl group from SAM which is

immediately broken down into adenosine and homocysteine catalysed by SAHH. Adapted from Boison (2013).

Seebeck (2010), identified SAM as the methyl donor in the reaction catalysed by mycobacterial EgtD a methyltransferase which tri-methylate's histidine to form hercynine. Elevated SAH levels, consequent to Hercynine biosynthesis, could inhibit the His tri-methylation reaction. Thus expression of *S. cerevisiae* SAHH was investigated for its affect on EGT production by regulation of SAHH expression through the TET off system. The strain R1158[Tet SAHH] (derived from BY4741) was purchased from Dharmacon with the native *S. cerevisiae* SAHH promoter replaced with a CMV promoter controlled by the tet trans-activator protein. Both R1158[Tet nfs1] and R1158[Tet SAHH] contain the *ura3* marker preventing transformation of the *p423-egtA* which also contains the *ura3* marker. The plasmid *p423-GPD* (Figure 3.34 A) was chosen instead containing a *his3* marker and digested with *Spe1* and *Xho1* using the same cloning strategy as described in Section 3.2 (Figure 3.34 B).
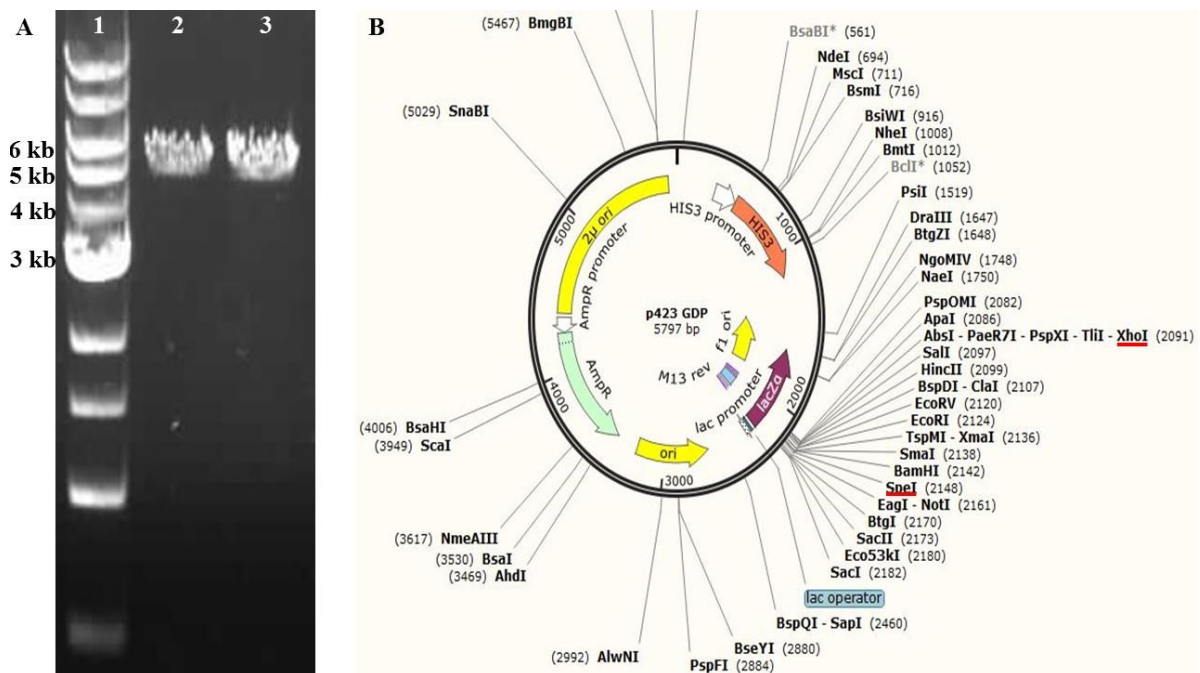
Figure 3.34 A & B Digest of the plasmid *p423 GPD*. (A) Lane 1= 10 kb NEB DNA ladder,

lanes 2 & 3= digested *p423 GPD* (size 5.9 kb). (B) Map of *p423 GPD* with the restriction sites *Spe1* and *Xho1* highlighted.

p*423-GPD-egtA* was ligated and transformed into *E. coli* cells and selected by their ability to grow on LB-amp-agar plates. P423-GPD-egtA was purified from *E. coli* containing p*423-GPD-egtA* as described in Section 2.2.5.1. *P423-GPD-egtA* plasmid DNA was then transformed into the *S. cerevisiae* strains R1158$^{Tet\ Nfs1}$ and R1158$^{Tet\ SAHH}$ as described in Section 2.2.4.2. Successful transformants were selected by their ability to grow on –Ura SC media. A colony PCR was also carried out on selected colonies of R1158$^{Tet\ Nfs1\ p423-GPD-egtA}$ and R1158$^{Tet\ SAHH\ p423-GPD-egtA}$ to confirm EgtA was present (Figure 3.32 A-B).
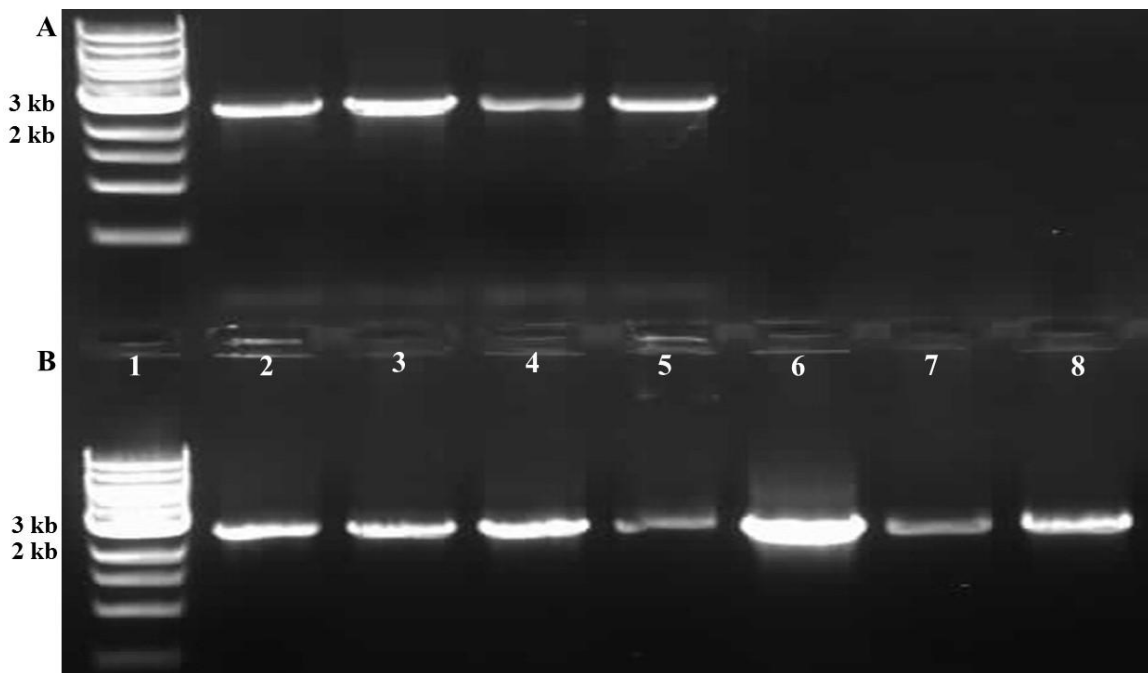
Figure 3.32A-B Colony PCR of R1158$^{Tet\ Nfs1\ p423-GPD-egtA}$ and R1158$^{Tet\ SAHH\ p423-GPD-egtA}$ confirming the presence of the *egtA* gene. (A) Lane 1= 10 kb NEB DNA ladder, lanes 2-4= *egtA* R1158$^{Tet\ Nfs1\ p423-GPD-egtA}$ (size 2.5 kb), lane 4= negative control, lanes 5-8 empty. (B) Lane 1= 10 kb NEB DNA ladder, lanes 2-7= *egtA* R1158$^{Tet\ SAHH\ p423-GPD-egtA}$ (size 2.5 kb), lane 8= positive control *p423-GPD-egtA* (size 2.5 kb).

EGT was confirmed to be produced by both strains R1158$^{Tet\ Nfs1\ p423\text{-}GPD\text{-}egtA}$ and R1158$^{Tet\ SAHH\ p423\text{-}GPD\text{-}egtA}$ using RP-HPLC analysis by comparison with an EGT standard and negative control (Figure 3.33A-D)
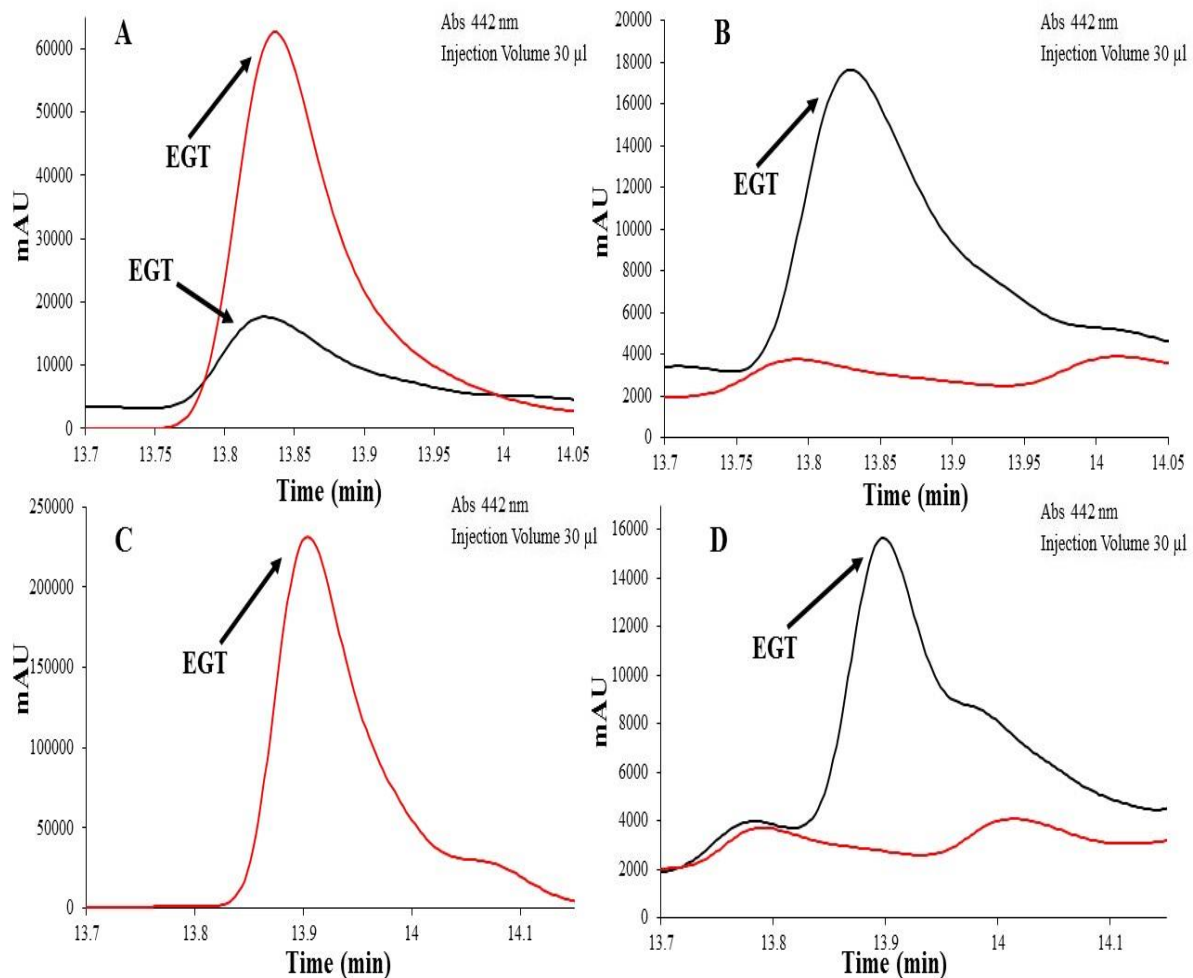
Figure 3.33 A-D EGT production identified in R1158$^{Tet\ Nfs1\ p423\text{-}GPD\text{-}egtA}$ and R1158$^{Tet\ SAHH\ p423\text{-}GPD\text{-}egtA}$. (A) EGT in R1158$^{Tet\ NFS1\ p423\text{-}GPD\text{-}egtA}$ at a retention time of 13.83 min (black) compared to the EGT standard 13.84 min (red). (B) EGT in R1158$^{Tet\ Nfs1\ p423\text{-}GPD\text{-}egtA}$ at a retention time of 13.83 m (black) compared to the negative control R1158$^{Tet\ Nfs1\ p423\text{-}GPD}$ no EGT is produced. (C) EGT standard 13.9 min (red) analysed with R1158$^{Tet\ Nfs1\ p423\text{-}GPD\text{-}egtA}$ but produced to large a peak to show on the same graph. (D) EGT in R1158$^{Tet\ Nfs1\ p423\text{-}GPD\text{-}egtA}$ at a retention time of 13.9 min (black) compared to the negative control R1158$^{Tet\ Nfs1\ p423\text{-}GPD}$ no EGT is produced.

Repression of *nfs1* and *SAHH* in the strains R1158$^{Tet\ Nfs1\ p423-GPD-egtA}$ and R1158$^{Tet\ SAHH}$ $^{p423-GPD-egtA}$ were assessed by examining each strains growth in the presence of varying concentrations of doxycycline in SC –His, -Ura agar. Addition of doxycycline caused reduced expression of Nfs1 and SAHH which was observed as the concentration of doxycycline gradually increased causing down regulation of the promoter until either Nfs1 or SAHH was no longer expressed. Both *nfs1* and *SAHH* are essential for growth, allowing repression of *nfs1* and *SAHH* to be visualized by observing the growth of R1158$^{Tet\ Nfs1\ p423-GPD-egtA}$ and R1158$^{Tet\ SAHH\ p423-GPD-egtA}$ in comparison to the control strain BY4741 $^{p423-GPD}$ (Figure 3.34 A-F). Growth of R1158$^{Tet\ Nfs1\ p423-GPD-egtA}$ decreased as doxycycline levels increased however a higher concentration of doxycycline was required in comparison to R1158$^{Tet\ SAHH\ p423-GPD-egtA}$ which was sensitive after as little as 0.5 µg/ml of doxycycline was added (Figure 3.34 A-D).

Growth analysis of R1158$^{Tet\ Nfs1\ p423-GPD-egtA}$ in the presence of doxycycline showed that a higher quantity of 100-150 µg/ml was required to slow growth without adversely affecting BY4741 $^{p423-GPD}$ (Figure 3.34 E-F). Growth analysis of R1158$^{Tet\ SAHH\ p423-GPD-egtA}$ demonstrated that a concentration range of (0.5 to 10 µg/ml was sufficient to induce a gradually diminished growth rate dependant on the doxycycline concentration.
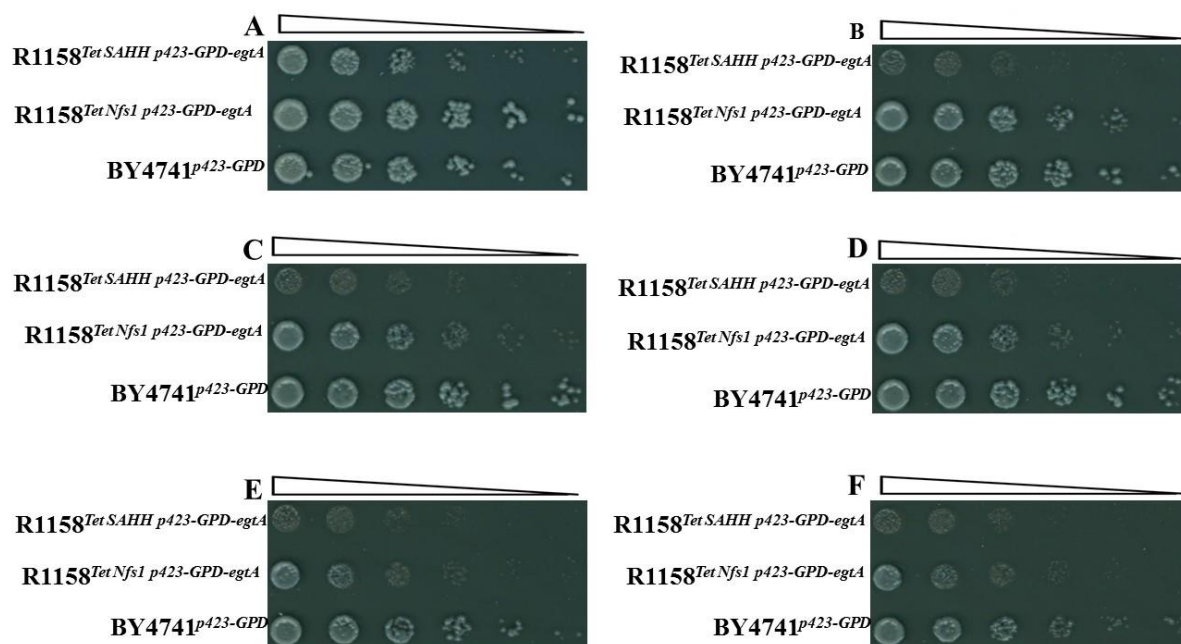
Figure 3.34 A-D Growth analysis of *S. cerevisiae* strains on synthetic complete media (SC) with doxycycline after 72 h. (A) Strains R1158$^{Tet\ SAHH\ p423-GPD-egtA}$, R1158$^{Tet\ Nfs1\ p423-GPD-egtA}$ and BY474 $^{p423-GPD}$ grown on SC media. (B) Strains R1158$^{Tet\ SAHH\ p423-GPD-egtA}$, R1158$^{Tet\ Nfs1\ p423-GPD-egtA}$ and BY4741$^{426-GPD}$ grown on SC media with 0.5 µg/ml of doxycycline added. (C) Strains R1158$^{Tet\ SAHH\ p423-GPD-egtA}$, R1158$^{Tet\ Nfs1\ p423-GPD-egtA}$ and BY4741$^{p423-GPD}$ grown on SC media with 4 µg/ml of doxycycline added. (E) Strains R1158$^{Tet\ SAHH\ p423-GPD-egtA}$, R1158$^{Tet\ Nfs1\ p423-GPD-egtA}$ and BY4741$^{p423-GPD}$ grown on SC media with 8 µg/ml of doxycycline added. (D) Strains R1158$^{Tet\ SAHH\ p423-GPD-egtA}$, R1158$^{Tet\ Nfs1\ p423-GPD-egtA}$ and BY4741$^{p423-GPD}$ grown on SC media with 100 µg/ml of doxycycline added. (F) Strains R1158$^{Tet\ SAHH\ p423-GPD-egtA}$, R1158$^{Tet\ Nfs1\ p423-GPD-egtA}$ and BY4741$^{p423-GPD}$ grown on SC media with 150 µg/ml of doxycycline added.

Cultures of R1158$^{Tet\ SAHH\ p423-GPD-egtA}$ were grown for 72 h in various concentrations of doxycycline which was determined by analysis of growth assays (Figure 3.34). RP-HPLC analysis of extracellular EGT levels in R1158$^{Tet\ SAHH\ p423-GPD-egtA}$ culture supernatant showed a significant decrease (P = 0.0281) of EGT levels in culture supernatant with a doxycycline concentration of 4 µg/ml and a significant (P = 0.0049) decrease of EGT levels in culture supernatant with a doxycycline concentration of 0.5 µg/ml (Figure 3.35 A). Cultures grown with a doxycycline concentration of 1, 2, 5 and 10 ug/ml all shown a decrease of EGT levels

in culture supernatant but was not statistically significant (Figure 3.35 B). This data suggests SAHH activity is required to prevent elevated SAH levels causing inhibition of EGT biosynthesis, via attenuation of methyltransferase activity of EgtA.
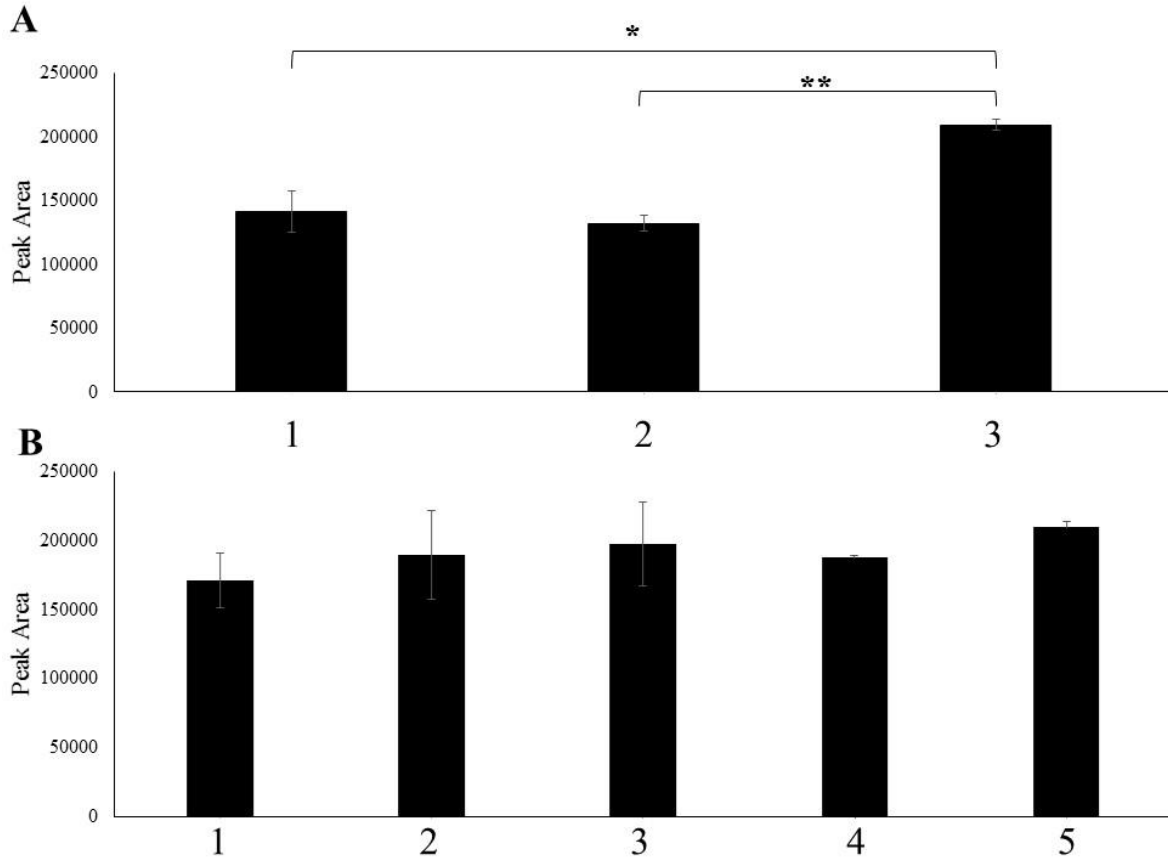
Figure 3.35 Repression of *SAHH* in R1158$^{Tet\ SAHH\ p423\text{-}GPD\text{-}egtA}$ decreases the level of EGT in 72 h cultures (n = 2). (A) Peak area of EGT in R1158$^{Tet\ SAHH\ p423\text{-}GPD\text{-}egtA}$ grown in SC media and with various concentrations of doxycycline. 1= 4 µg/ml of doxycycline added (Peak Area 141286). 2= 0.5 µg/ml of doxycycline added (Peak Area 209633). 3= No doxycycline added (Peak Area 168898). (B) 1= 1 µg/ml of doxycycline added (Peak Area 171599). 2= 2 µg/ml of doxycycline added (Peak Area 189819). 3= 5 µg/ml of doxycycline added (Peak Area 197559). 4= 10 µg/ml of doxycycline added (Peak Area 187732). 5= No doxycycline added (Peak Area 209633).

Cultures of R1158$^{Tet\ nfs1\ p423\text{-}GPD\text{-}egtA}$ were grown for 72 h in 100 and 150 µg/ml doxycycline which was determined by analysis of growth assays. RP-HPLC analysis of extracellular EGT levels in R1158$^{Tet\ nfs1\ p423\text{-}GPD\text{-}egtA}$ culture supernatant shown an increase in EGT levels of culture supernatants grown with a doxycycline when compared to R1158$^{Tet\ nfs1\ p423\text{-}GPD\text{-}egtA}$ grown without doxycycline. This increase was statistically significant (P = 0.0353) at a concentration of 100 ug/ml (Figure 3.36).
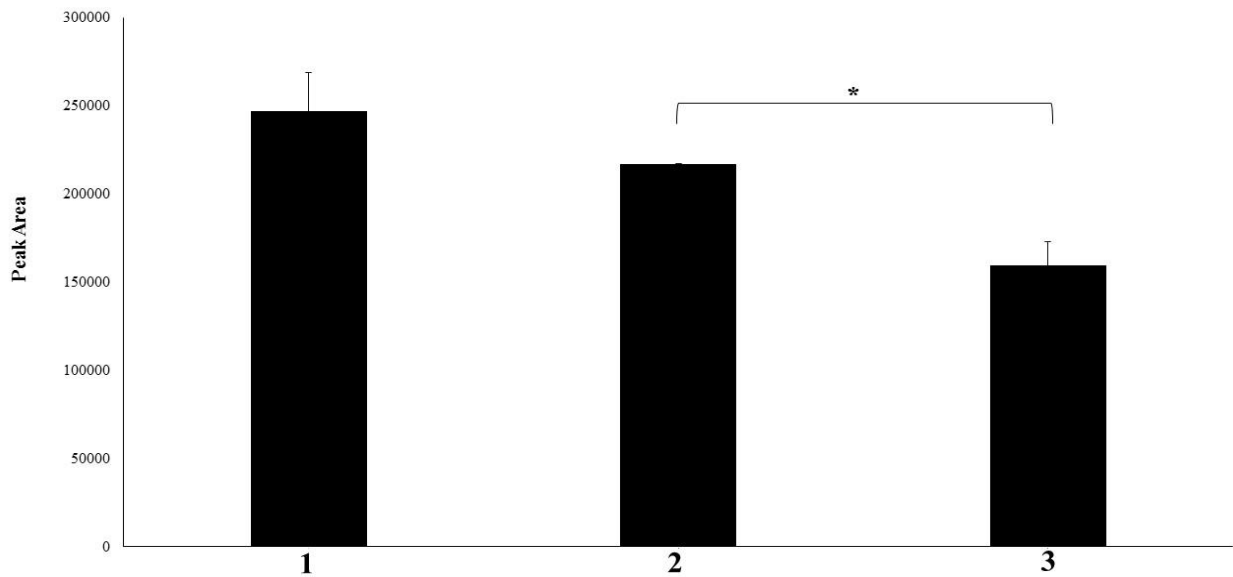
Figure 3.36 Repression of *nfs1* in R1158$^{Tet\ Nfs1\ p423\text{-}GPD\text{-}egtA}$ increases the level of EGT in 72 h cultures (n = 2). (A) Peak area of EGT in R1158$^{Tet\ nfs1\ p423\text{-}GPD\text{-}egtA}$ grown in SC media and various levels of doxycycline. 1= 100 µg/ml of doxycycline added (Peak Area 132369). 2= 150 µg/ml of doxycycline added (Peak Area 217091). 3= No doxycycline added (Peak Area 168898).

Chapter 4

Discussion

4.1 Discussion

EGT is an important NP which has potential uses in biotechnology, the cosmetics industry and the food industry as a preservative (Bao *et al*., 2010). EGT has been previously shown to demonstrate interesting biochemical properties such as antioxidant capabilities (Cheah & Halliwell, 2012). Identification of a putative EGT transporter OCTN1 expressed highly on the membranes of mammalian cells as well as on the membrane of mitochondria suggests EGT is an important biomolecule that may act as a cytoprotective (Halliwell *et al*., 2016; Gründemann, 2012; Paul & Snyder, 2009).

This body of work shows how transformation of the gene *egtA* from the saprotrophic fungus *A. fumigatus* into the *S. cerevisiae* strain BY4741 using an episomal vector, enables the de novo production of EGT. Expression of the *A. fumigatus* protein EgtA was confirmed by protein mass spectrometry and production of EGT was confirmed by both RP-HPLC and LC-MS analysis. By quantifying the level of EGT intracellularly and extracellularly, it was revealed that EGT builds up in the culture supernatant at far more significant level compared to the level of EGT seen in yeast cell lysates. EGT was seen to accumulate over time in the culture supernatant until the time point of 96 h was reached using a batch fermentation model making *S. cerevisiae* ideal for the production of EGT.

To further understand how EGT was being produced by the protein EgtA in *A. fumigatus* and *S. cerevisiae* proteins were identified that shared homology with other cysteine desulfurase identified to be involved in EGT biosynthesis (Qin *et al*., 2014; Pluskal *et al*., 2014). Co-expression of EgtA with AFUA_2G13295 (Egt2a) caused a significant decrease in EGT production *S. cerevisiae*. Interestingly decreasing the expression of the yeast Nfs1 a native cysteine desulfurase in S. cerevisiae caused an increase in EGT levels. This indicates EGT production by EgtA may be somehow affected by the cysteine desulfurase shown to be required to complete EGT biosynthesis (Seebeck, 2010; Qin *et al*., 2014; Pluskal *et al*., 2014).

Mutation of a conserved residue in EgtA known to be involved in the negative regulation of EGT production in *M. tuberculosis* showed this residue might also be phosphorylated in *S. cerevisiae* as EGT levels were seen to increase when Thr^{213} was changed to Ala. This work suggests that with further knowledge of EGT biosynthesis in *A. fumigatus* and genetic manipulation of the protein EgtA, *S. cerevisiae* can be used as a cellular factory for commercially viable production of EGT.

The gene AFUA_2G15650 from *A. fumigatus* was identified to be involved in production of EGT. Expression of recombinant EgtA in *S. cerevisiae* was determined to produce EGT by detection of alkylated EGT using RP-HPLC analysis. Alkylation of EGT with 5'-IAF and analysis using RP-HPLC first deployed by (Gallagher *et al*., (2012) has been shown to be an accurate and sensitive way of quantifying EGT. In this study a minimum of 51.58 µmol/L of EGT was detected in the production of an EGT standard curve however Sotgia *et al*., (2013) have used a similar method to detect as little as 0.15 µmol/L. Other derivatization agents have also been used to alkylate EGT such as 7-diethylamino-3-[4-(iodoacetamido) phenyl]-4-methylcoumarin which was shown to detect EGT at 0.10 µmol/L using HPLC analysis (Sotgia *et al*., 2014).

In recombinant *S. cerevisiae,* EGT was only detected intracellularly at 24 h and identified to be present at a significantly higher level extracellularly in 24 h cultures (P <0.0001) with 99.5 % of EGT in the culture supernatant of BY4741$^{p426-GPD-egtA}$. Larger quantities of EGT were seen to be present in 48 h and 72 h cultures and continued to rise peaking in the culture supernatant of 96 h cultures with 7.93 mg/L of EGT detected. This is not as large as the quantity of intracellular EGT detected by Pluskal *et al*., (2014) who managed to produce 266.3 mg/L of EGT detected in a *Schizosaccharomyces pombe* Egt-1 overexpression strain in a 20 day fermentation where the culture media was replaced with fresh media every 6-7 days. A longer term continuous fermentation would need to be carried out to confirm that BY4741$^{p426-GPD-egtA}$ could produce similar quantities of EGT. However, production of EGT in *S. cerevisiae* offers several advantages such as its extensive track record for expressing recombinant protein (Da Silva & Srikrishnan 2012). Another major advantage is how the vast majority of EGT being present in the culture supernatant. This allows for an easier extraction of EGT compared to extraction of EGT from intracellular sources and is more ideal for use in a continuous fermentation system.

Phenotypic analysis was conducted to determine if EGT increased the antioxidant capacity of *S. cerevisiae* to deal with oxidative agents such as hydrogen peroxide. BY4741$^{p426-GPD-egtA}$ exposed to increasing concentrations of the oxidant hydrogen peroxide was shown to have impaired growth compared to the control strain BY4741$^{p426-GPD}$. This was not completely unsurprising to see EGT production not increase the antioxidant capabilities of *S. cerevisiae* as a similar result had been seen by the fission yeast *S. pombe* by Pluskal *et al*., (2014). Here an *egt-1* overexpression strain producing greater quantities of EGT compared

to the wildtype strain showed no increased resistance to hydrogen peroxide or *tert*-butyl hydrogen peroxide seen by Bello *et al*., (2012) to cause sensitivity in the *N. crassa egt-1* deletion strain.

It may be that EGT acts as a supplementary antioxidant or has a highly specialized cellular function as suggested by Halliwell *et al*., (2016) such as involvement in tissue repair. Fungi and Bacteria that produce EGT also produce other antioxidants which have been demonstrated to have more effective antioxidant capabilities against a broad range of free radicals. An example of this would be the production of MSH the primary antioxidant of Mycobacteria (Rawat *et al*., 2002). Mutants of *M. tuberculosis* which cannot produce MSH or EGT have been characterised to have reduced antioxidant capabilities and greater sensitivity towards antibiotics such as erythromycin or rifampicin however MSH deficient strains have demonstrated a greater amount of sensitivity (Saini *et al*., 2015; Greenblatt *et al*., 2015).

The most likely reason for impaired growth in BY4741$^{p426-GPD-egtA}$ whilst under increased oxidative stress is the increased strain put on *S. cerevisiae* producing EGT under a constituent promoter and a high output origin of replication (2µ). *S. cerevisiae* already has a stable redox homeostasis mediated by production of high levels of GSH and enzymes such as superoxide dismutase and does not seem to require EGT (Steinman, 1980; Grant *et al*., 1996; Lu, 2013). This would also explain why *S. cerevisiae* does not produce EGT with all other fungal phyla identified as having an *egtA* homologue except for the Saccharomycotina sub-phylum (Jones *et al*., 2014). One cannot exclude the possibility that EGT biosynthesis in *S. cerevisiae* interferes with trans-sulfurization systems, and dissipates homocysteine levels by prioritization of SAM biosynthesis over provision of Cys for the formation of GSH. Levels of Cys for GSH biosynthesis may also be reduced by EGT biosynthesis (Figure 4.1).
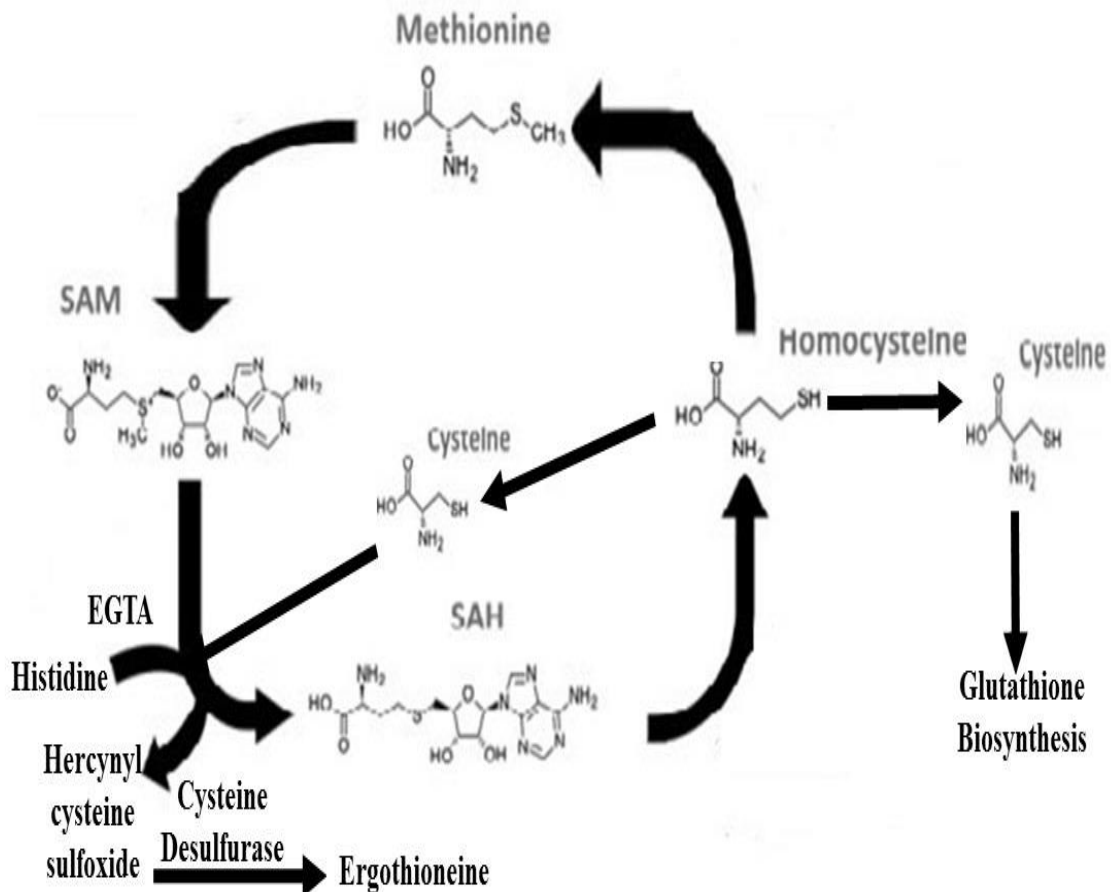
Figure 4.1 Production of EGT may interfere with GSH production in *S. cerevisiae*. Production of EGT may dissipate homocysteine levels by prioritizing SAM production. Cysteine may also be used for production of EGT instead of GSH. Adapted from Manzanares-miralles *et al.* (2016).

EgtA was investigated to determine whether phosphorylation of the conserved residue Thr^{213} might be causing down-regulation of EgtA activity as observed by Greenblatt *et al.*, (2015) in *M. tuberculosis*. A single base pair was mutated causing a change in the amino acid sequence (T213A) in BY4741$^{p426\text{-}GPD\text{-}egtA\ T213A}$. Cultures (24 h) of BY4741$^{p426\text{-}GPD\text{-}egtA\ T213A}$ which could no longer be phosphorylated showed an increased level of intracellular and extracellular EGT when compared to BY4741$^{p426\text{-}GPD\text{-}egtA}$ at a time point of 24 h but was not statistically significantly higher. This indicates that indiscriminate phosphorylation of Thr^{213} as seen in the egtA homologue egtD in *M. tuberculosis* is a possibility considering the array of protein kinases specifically Ser/Thr kinases *S. cerevisiae* (>122) (Zhu *et al.*, 2000; Greenblatt *et al.*, (2015). However examination of 72 h extracellular EGT levels showed a

discontinuation of this trend with BY4741$^{p426\text{-}GPD\text{-}egtA}$ containing a higher level of EGT compared to BY4741$^{p426\text{-}GPD\text{-}egtA\ T213A}$. This may indicate that indiscriminate phosphorylation may be more likely to occur in higher nutrient conditions such as those present in 24 h cultures as opposed to 72 h cultures whose cells have become quiescent due to less metabolic activity.

Co-expression of EgtA with Egt2a from *A. fumigatus* thought to be the cysteine desulfurase involved in the EGT biosynthetic pathway did not increase the level of EGT produced but significantly decreased it. It was observed in 48 h and 72 h culture supernatants of BY4741$^{p426\text{-}GPD\text{-}egtA\ p423\text{-}ADH\text{-}egt2a}$ that considerably less EGT was present when compared to the strain BY4741$^{p426\ GPD\text{-}egtA\ p423\ ADH}$. No EGT was detected in 24 h cultures. This surprising result indicates that expression of Egt2a interferes significantly with EGT production in *S. cerevisiae*. Even though a cysteine desulfurase has been shown to be required for EGT biosynthesis in both variations of the EGT biosynthetic process too much appears to effect EGT production in a negative manner. Another candidate AFUA_3G14240 (Egt2b) a homologue to the yeast cysteine desulfurase Nfs1 was investigated but transcription of Egt2b with a 6 X histidine tag at the N- or C-terminal end could not be detected by western blot analysis leading to the conclusion it could not be expressed in *S. cerevisiae*.

BLAST analysis of EgtA shown homology with 32 % identity with *S. pombe* Egt-1 (SPBC1604) and 49 % identity with *N. crassa* Egt-1 (NCU04343) were identical to EgtA. Domain analysis shown EgtA does not contain any additional domains that could carry out desulfurase activity (Figure 3.1). EGT biosynthesis in Mycobacteria, *N. crassa* and *S. pombe* have all shown the requirement of a cysteine desulfurase to complete EGT biosynthesis. Since expression of *A. fumigatus* EgtA alone in *S. cerevisiae* was capable of producing EGT a native protein was believed to be catalysing the desulfurization of cysteine. BLAST analysis confirmed no homologue of Egt2a was present in *S. cerevisiae* however a homologue of the A. fumigatus cysteine desulfurase Egt2b denoted as Nfs1 was present. Nfs1 in *S. cerevisiae* was therefore deemed to be the most likely candidate to be carrying out the desulfurization of cysteine from hercynyl cysteine sulfoxide.

Repression of yeast Nfs1 using a Tet off system did not cause a decrease in EGT as expected but a gradual increase instead which was statistically significant ($P < 0.05$). This is interesting as co-expression of the cysteine desulfurase candidate Egt2a was expected to increase or maintain EGT levels but instead was seen to cause a significant decrease ($P < 0.005$) in EGT. These results further suggest that cysteine desulfurase, although required to

produce EGT, also may act as a negative factor of EGT production (Figure 4.2 A & B). This result is also interesting as yeast Nfs1 has been shown to be located mainly inside the mitochondrial inner membrane and only low amounts have been reported in the nucleus and cytosol (Kispal *et al*., 1999). This low amount of Nfs1 in the cytosol may actually be providing the perfect level of Nfs1 for EGT production when produced under its native promoter (Muhlenhoff *et al*., 2004).
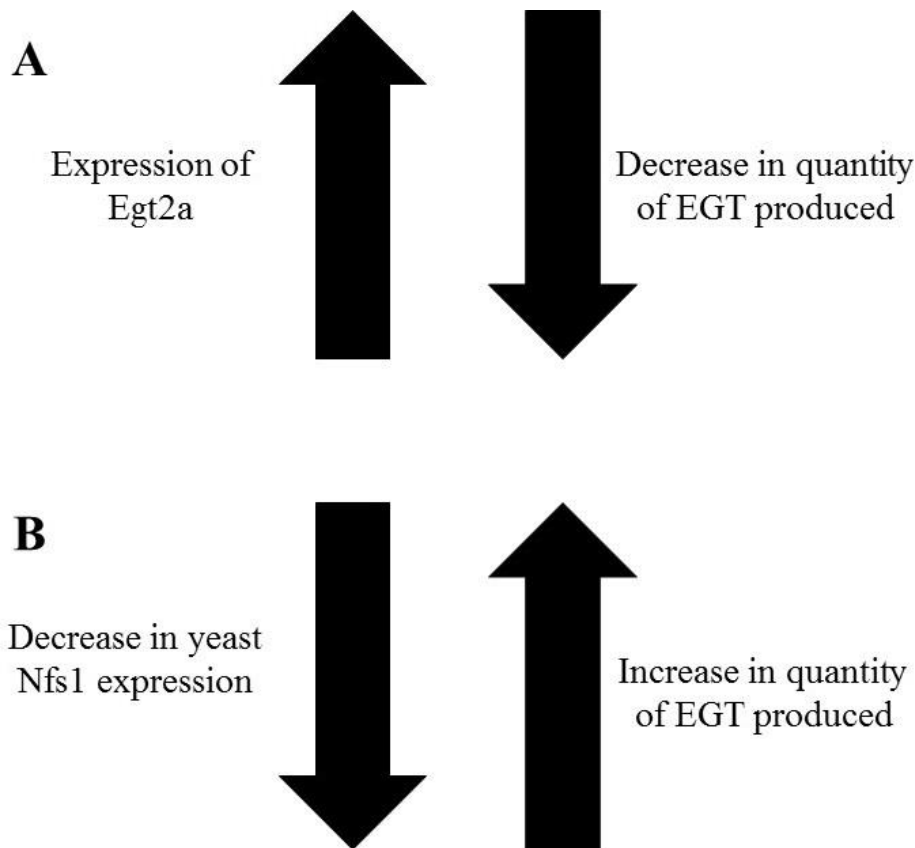
Figure 4.2 A & B Effects of cysteine desulfurase expression on EGT production. (A) Expression of the *A. fumigatus* cysteine desulfurase Egt2a caused a decrease in EGT production in *S. cerevisiae*. (B) Decreased expression of native yeast cysteine desulfurase Nfs1 using a TET off system was shown to increase EGT production.

Repression of SAHH was seen to cause a decrease in EGT levels which was significant (P = 0.0049) when repressed with a low level of doxycycline 0.5 µg/ml and significant (P = 0.0281) when repressed with 4 µg/ml. However no trend was evident correlating SAHH repression with a decrease in EGT as 1 and 2 µg/ml of doxycycline did show a decrease of EGT levels in culture supernatant but was not statistically significant. This

suggests a decrease in SAHH expression does negatively affects EGT production most likely by EGTA tri-methyltransferase inhibition or by somehow causing a lack of the methyl donor S-adenosyl methionine (SAM) required for the methylation of histidine by EgtA and would need to be monitored in any future system used to produce EGT.

The production of EGT in *S. cerevisiae* highlights the potential of using yeast as a cellular factory for the production of nutritional or industrial important natural products. *S. cerevisiae* showed no toxicity in producing such large amounts of EGT and its secretion of EGT makes it ideal for the use of a continuous fermentation system for the production of EGT which may allow it to become commercially viable way to produce EGT. This work also shows the need for a greater *in vivo* understanding of the function of EGT. Although EGT has been demonstrated to have antioxidant and cytoprotective properties in other fugal species this is not conclusive and stresses the need for EGT to be investigated further.

In an attempt to identify the cysteine desulfurase enzyme required to complete EGT biosynthesis in *A. fumigatus* co-expression of Egt2a with EgtA was shown to significantly reduce EGT levels. This indicates production of EGT by EgtA may be hindered if too large a quantity of the cysteine desulfurase is present and may be a way of regulating EGT production in *A. fumigatus*. This was again elucidated to when reduced expression of the yeast cysteine desulfurase Nfs1 caused an increase in EGT levels.

Alteration of the expression of the enzymes Nfs1 and SAH hydrolase have been shown to have a positive and negative effect on EGT production. Modifications to EgtA has also been shown to have an impact on EGT production by changing the conserved residue Thr[213] to Ala suggesting indiscriminate phosphorylation of EgtA may occur in *S. cerevisiae*. This indicates that higher yields of EGT may be attainable through further modification of *S. cerevisiae* and EgtA by genetic manipulation.

4.2 Future Work

Now that recombinant expression of EgtA in *S. cerevisiae* has been confirmed to produce EGT a continuous fermentation should be conducted using the EGT producing *S. cerevisiae* strain to determine how large a quantity of EGT can be produced. The conditions for fermentation should also be optimized such as pH, temperature and fermentation time. Media conditions should also be optimized including nitrogen source, carbon source and investigate the supplementation of media with histidine and or cysteine the precursor amino acids to EGT. Other vectors may be looked but referring to the literature has indicated that the *GPD* promoter and 2μ origin of replication used in the plasmid *p426 GPD* to express EGT may be the strongest available (Blazeck *et al*., 2012; Romanos *et al*., 1992). The use of different yeast strains to express recombinant EgtA should be investigated to see if this can increase EGT production.

An in vivo study could be carried out using purified histidine tagged EgtA and either Egt2a or native yeast Nfs1 to confirm their role in the production of EGT. A similar study was used by Seebeck, (2010) to confirm the role of the 5 gene EGT cluster in the mycobacteria (Vit *et al*., 2015). A study such as this could also be used investigate whether EgtA requires the same co-factors $FeSO_4$ and SAM. Further work should also be carried out in understanding the role Egt2a plays in EGT production in *A. fumigatus* perhaps by creating an overexpression mutant and a Δegt2a mutant.

In *A. fumigatus* other sulphur containing metabolites could be studied to identify whether Egt2A and Nfs1 play a role in there synthesis. In *S. cerevisiae* strains producing EGT, the levels of GSH should be checked to observe whether EGT biosynthesis is interfering with GSH biosynthetic machinery.

The intermediates produced by EgtA in the EGT biosynthetic process have not yet been identified partly due to the labelling technique used to identify EGT is not suitable for their identification. To detect intermediates normal phase-HPLC analysis should be considered as well as perhaps using other labelling techniques targeting the quaternary amine group present on all of the intermediates known intermediates. This could be carried out by perhaps using dansyl chloride which has been seen to label primary, secondary and tertiary amine groups. Dansylated derivatives have also been shown to be detectable using a Zorbax Eclipse XDB C18 as used in this study (Bartzatt, 2001; Meseguer Lloret *et al*., 2004; Onal, 2007). The Egt-1 overexpression mutant in S. pombe was identified to produce selenoneine

when fed Na$_2$SeO$_4$ (Pluskal *et al*., 2014). This should be investigated in the *S. cerevisiae* producing EGT strain as this relatively unknown compound may also have potential nutraceutical activity. However an alternative means will be needed to detect selenoneine as alkylation by 5'-IAF would be unsuitable however normal phase-HPLC would be ideal. In conclusion, the scene is now set for future studies to explore the biosynthesis, and exploit the potential, of EGT production by *S. cerevisiae*.

Chapter 5

Bibliography

5.1 Bibliography

Addgene, 2014. *Plasmids 101 : A Desktop Resource*. USA: Addgene , 1st ed, pp.57.

Agarwal, R. 2009. Allergic bronchopulmonary aspergillosis. *Chest*, 135(3), pp.805–826.

Fairlamb, A. H., Blackburn, P., Ulrich, P., Chait, B. T. and Cerami, A. 1985. Trypanothione: a novel bis(glutathionyl)spermidine cofactor for glutathione reductase in trypanosomatids. *Science*, 227(4693), pp.1485–1487.

Altintas, E. and Sezgin, O. 2004. S-adenosylhomocysteine hydrolase, S-adenosylmethionine, S-adenosylhomocysteine: Correlations with ribavirin induced anemia. *Medical Hypotheses*, 63(5), pp.834–837.

Amitani, R., Taylor, G., Elezis, E.N., Llewellyn-Jones, C., Mitchell, J., Kuze, F., Cole, P.J. and Wilson, R. 1995. Purification and Characterization of Factors Produced by *Aspergillus fumigatus* Which Affect Human Ciliated Respiratory Epithelium. *Infection and Immunity*, 63(9), pp.3266–3271.

Ardiani, A., Higgins, J.P. and Hodge, J.W. 2010. Vaccines based on whole recombinant Saccharomyces cerevisiae cells. *FEMS Yeast Research*, 10(8), pp.1060–1069.

Bacher, P. Giersiefer, S., Bach, M., Fork, C., Schömig, E, and Gründemann, D. 2009. Substrate discrimination by ergothioneine transporter SLC22A4 and carnitine transporter SLC22A5: Gain-of-function by interchange of selected amino acids. *Biochimica et Biophysica Acta - Biomembranes*, 1788(12), pp.2594–2602.

Bao, H.N., Osako, K. and Ohshima, T. 2010. Value-added use of mushroom ergothioneine as a colour stabilizer in processed fish meats. *Journal of the Science of Food and Agriculture*, 90(10), pp.1634–1641.

Bao, H.N., Ushio, H. and Ohshima, T. 2008. Antioxidative Activity and Antidiscoloration Efficacy of Ergothioneine in Mushroom (*Flammulina velutipes*) Extract Added to Beef and

Fish Meats. *Journal of Agricultural and Food Chemistry*, 56(21), pp.10032–10040.

Bartzatt, R., 2001. Fluorescent labeling of drugs and simple organic compounds containing amine functional groups, utilizing dansyl chloride in Na2CO3 buffer. *Journal of Pharmacological and Toxicological Methods*, 45(3), pp.247–253.

Bello, M.H., Mogannam, J.C., Morin, D., Epstein, L., 2014. Endogenous ergothioneine is required for wild type levels of conidiogenesis and conidial survival but does not protect against 254 nm UV-induced mutagenesis or kill. *Fungal Genetics and Biology*, 73, pp.120–127.

Bello, M.H., Barrera-Perez, V., Morin, D. and Epstein, L. 2012. The Neurospora crassa mutant Nc D Egt-1 identifies an ergothioneine biosynthetic gene and demonstrates that ergothioneine enhances conidial survival and protects against peroxide toxicity during conidial germination. *Fungal Genetics and Biology*, 49(2), pp.160–172.

Bene, J., Magyari, L., Talian, G., Komlosi, K., Gasztonyi, B., Tari, B., Varkonyl, A., Mozsik, G. and Melagh, B. 2006. Prevalence of SLC22A4, SLC22A5 and CARD15 gene mutations in Hungarian pediatric patients with Crohn's Disease. *World Journal of Gastroenterology*, 12(34), pp.5550–5553.

Berndt, C., Lillig, C.H. and Holmgren, A., 2008. Thioredoxins and glutaredoxins as facilitators of protein folding. *Biochimica et Biophysica Acta - Molecular Cell Research*, 1783(4), pp.641–650.

Biswas, S., Hwang J.W., Kirkham P.A. and Rahman I. 2013. Pharmacological and Dietary Antioxidant Therapies for Chronic Obstructive Pulmonary Disease. *Current Medicinal Chemistry*, 20(12), pp.1496–1530.

Blazeck, J., Garg, R., Reed, B., Alper, H.S., 2012. Controlling promoter strength and regulation in Saccharomyces cerevisiae using synthetic hybrid promoters. *Biotechnology and Bioengineering*, 109(11), pp.2884–2895.

Boison, D., 2013. Adenosine kinase: exploitation for therapeutic gain. *Pharmacological Reviews*, 65(3), pp.906–43.

Botta, C., Di Giorgio, C., Sabatier, A.S. and De Méo, M. 2008. Genotoxicity of visible light (400-800 nm) and photoprotection assessment of ectoin, l-ergothioneine and mannitol and

four sunscreens. *Journal of Photochemistry and Photobiology B: Biology*, 91(1), pp.24–34.

Brakhage, A.A. and Schroeckh, V. 2011. Fungal secondary metabolites - Strategies to activate silent gene clusters. *Fungal Genetics and Biology*, 48(1), pp.15–22.

Briggs, I., 1972. Ergothioneine in the central nervous system. *Journal of Neurochemistry*, 19(1), pp.27–35.

Celik, E. and Calık, P. 2012. Production of recombinant proteins by yeast cells. *Biotechnology Advances*, 30(5), pp.1108–18.

Cheah, I.K. and Halliwell, B. 2012. Ergothioneine; antioxidant potential , physiological function and role in disease. *Biochimica et Biophysica Acta - Molecular Basis of Disease*, 1822(5), pp.784–793.

Crossland, J., Mitchell, J. and Woodruff, G.N. 1966. The presence of ergothioneine in the central nervous system and its probable identity with the cerebellar factor. *The Journal of Physiology*, 182, pp.427–438.

Curran, B. and Bugeja, V. (2005). The Biotechnological Exploitation of Heterologous Protein Production in Fungi. In: *Fungi: Biology and Applications* 1st ed., Kavanagh, K. Wiley, England.

Daly, P. and Kavanagh, K. 2001. Pulmonary aspergillosis : clinical presentation , diagnosis and therapy . *British Journal of Biomedical Science*. , 58(3), pp. 197-205.

Davis, C., Carberry, S., Schrettl, M., Singh, I., Stephens, J.C., Barry, S.M., Kavanagh, K., Challis, G.L., Brougham D. and Doyle, S. 2011. The Role of Glutathione S-Transferase GliG in Gliotoxin Biosynthesis in Aspergillus fumigatus. *Chemistry & Biology*, 18(4), pp.542–552.

Delmotte, P. and Sanderson, M.J. 2006. Ciliary beat frequency is maintained at a maximal rate in the small airways of mouse lung slices. *American Journal of Respiratory Cell and Molecular Biology*, 35(1), pp.110–117.

Demain, A.L. and Vaishnav, P. 2009. Production of recombinant proteins by microbes and higher organisms. *Biotechnology Advances*, 27(3), pp.297–306.

Emani, C.S., Williams, M.J., Wiid, I.J., Hiten, N.F., Viljoen, A.J., Pietersen RD., van Helden,

P.D. and Baker, B. 2013. Ergothioneine is a secreted antioxidant in Mycobacterium smegmatis. *Antimicrobial Agents and Chemotherapy*, 57(7), pp.3202–3207.

Ey, J., Schömig, E. and Taubert, D. 2007. Dietary sources and antioxidant effects of ergothioneine. *Journal of Agricultural and Food Chemistry*, 55(16), pp.6466–6474.

Fahey, R.C. 2001. Novel Thiols in Prokaryoyes. *Annual Review in Microbiology*, 55, pp.333–356.

Fedorova, N.D. Khaldi, N., Joardar, V.S., Maiti, R., Amedeo, P., Anderson, M.J., Crabtree, J., Silva, J.C., Badger, J.H., Albarraq, A., Angiuoli, S., Bussey, H., Bowyer, P., Cotty, P.J., Dyer, P.S., Egan, A., Galens, K., Fraser-Liggett, C.M.,Haas, B.J., Inman, J.M., Kent, R., Lemieux, S., Malavazi, I., Orvis, J., Roemer, T., Ronning, C.M., Sundaram, J.P., Sutton, G., Turner, G., Venter, J.C., White, O.R., Whitty, B.R., Youngman, P., Wolfe, K.H., Goldman, G.H., Wortman, J.R., Jiang, B., Denning, D.W. and Nierman, W.C. 2008. Genomic islands in the pathogenic filamentous fungus Aspergillus fumigatus. *PLoS Genetics*, 4(4).

Fisher, S.A., Hampe, J., Onnie, C.M., Daly, M.J., Curley, C., Purcell, S., Sanderson, J., Mansfield, J., Annese, V., Forbes, A., Lewis, C.M., Schreiber, S., Rioux, J.D. and Mathew, C.G. 2006. Direct or indirect association in a complex disease the role of SLC22A4 and SLC22A5 functional variants in Crohn disease. *Human Mutation*, 27(7), pp.778–785.

Franzoni, F., Colognato, R., Galetta, F., Laurenza, I., Barsotti, M., Di Stefano, R., Bocchetti, R., Regoli, F., Carpi, A., Balbarini, A., Migliore, L. and Santoro, G. 2006. An in vitro study on the free radical scavenging capacity of ergothioneine: comparison with reduced glutathione, uric acid and trolox. *Biomedicine and pharmacotherapy*, 60(8), pp.453–7.

Funk, M., Niedenthal, R., Mumberg, D., Brinkmann, K., Rönicke, V. and Henkel, T. 2002. Vector systems for heterologous expression of proteins in Saccharomyces cerevisiae. *Methods in Enzymology*, 350, pp.248–257.

Galagan, J.E., Calvo, S.E., Cuomo, C., Ma L.J., Wortman, J.R., Batzoglou, S., Lee S.I., Baştürkmen, M., Spevak, C.C., Clutterbuck, J., Kapitonov, V., Jurka, J., Scazzocchio, C., Farman, M., Butler, J., Purcell, S., Harris, S., Braus, G.H.,Draht, O., Busch, S., D'Enfert, C., Bouchier, C., Goldman, G.H., Bell-Pedersen, D., Griffiths-Jones, S., Doonan, J.H.,Yu,

J., Vienken, K., Pain, A., Freitag, M., Selker, E.U., Archer, D.B., Peñalva, M.A., Oakley, B.R., Momany, M., Tanaka, T., Kumagai, T., Asai, K., Machida, M., Nierman, W.C., Denning, D.W., Caddick, M., Hynes, M., Paoletti, M., Fischer, R.,Miller, B., Dyer, P., Sachs, M.S., Osmani, S.A., and Birren B.W. 2005. Sequencing of Aspergillus nidulans and comparative analysis with A . fumigatus and A . oryzae. *Nature*, 438(12), pp.1105–1115.

Gallagher, L., Owens, R.A., Dolan, S.K,, O'Keeffe, G., Schrettl, M., Kavanagh, K., Jones, G.W. and Doyle, S. 2012. The Aspergillus fumigatus protein gliK protects against oxidative stress and is essential for gliotoxin biosynthesis. *Eukaryotic Cell*, 11(10), pp.1226–1238.

Geiser, D.M., Klich, M.A., Frisvad, J.C., Peterson, S.W. and Varga J. 2007. The current status of species recognition and identification in Aspergillus. *Studies in Mycology*, 59, pp.1–10.

Gellissen, G. Janowicz, Z.A., Weydemann, U., Melber, K., Strasser, A.W. and Hollenberg C.P. 1992. High-level expression of foreign genes in Hansenula polymorpha. *Biotechnology Advances*, 10(2), pp.179–189.

Godley, B.F., Shamsi, F.A., Liang, F.Q., Jarrett, S.G., Davies, S. and Boulton, M. 2005. Blue light induces mitochondrial DNA damage and free radical production in epithelial cells. *The Journal of Biologocal Chemistry*, 280(22), pp.21061–6.

Goncharenko, K.V., Vit, A., Blankenfeldt, W. and Seebeck, F.P. 2015. Structure of the Sulfoxide Synthase EgtB from the Ergothioneine Biosynthetic Pathway. *Angewandte Chemie*, pp.2821–2824.

González-Lobato, L., Real, R., Prieto, J.G., Alvarez, A.I. and M.G. 2010. Differential inhibition of murine Bcrp1 Abcg2 and human BCRP ABCG2 by the mycotoxin fumitremorgin C. *European Journal of Pharmacology*, 1(3), pp.41–48.

Grant, C.M., MacIver, F.H. and Dawes, I.W. 1996. Glutathione is an essential metabolite required for resistance to oxidative stress in the yeast Saccharomyces cerevisiae. *Current Genetics*, 29(6), pp.511–515.

Greenberger, P.A. 2002. Allergic bronchopulmonary aspergillosis. *Journal of Allergy and Clinical Immunology*, 110(5), pp.685–692.

Gruber, J., Fong, S., Chen, C.B., Yoong, S., Pastorin, G., Schaffer, S., Cheah, I. and Halliwell, B. 2013. Mitochondria-targeted antioxidants and metabolic modulators as

pharmacological interventions to slow ageing. *Biotechnology Advances*, 31(5), pp.563–592.

Gründemann, D., Harlfinger, S., Golz, S., Geerts, A., Lazar, A., Berkels, R., Jung, N., Rubbert, A. and Schömig, E. 2005. Discovery of the ergothioneine transporter. *Proceedings of the National Academy of Sciences of the United States of America*, 102(14), pp.5256–61.

Gründemann, D. 2012. The ergothioneine transporter controls and indicates ergothioneine activity - A review. *Preventive Medicine*, 54(5). S.71-74

Haas, H., Eisendle, M. and Turgeon, B.G. 2008. Siderophores in fungal physiology and virulence. *Annual review of phytopathology*, 46(1), pp.149–187.

Halliwell, B., Cheah, I.K. and Drum, C.L. 2016. Ergothioneine, an adaptive antioxidant for the protection of injured tissues A hypothesis. *Biochemical and Biophysical Research Communications*, 470(2), pp.245–250.

Halliwell, B. and Gutteridge, J.M.C., 2007. Antioxident defences synthesized *in vivo*. *In Free Radicals in Biology and Medicine*. Halliwell, B. and Gutteridge, J.M.C., 5th ed. Oxford, United Kingdom, pp.77–151.

Hand, C.E. and Honek, J.F. 2005. Biological Chemistry of Naturally Occurring Thiols of Microbial and Marine Origin. *Journal of Natual Products*, 68(2), pp.293–308.

Hand, C.E., Taylor, N.J. and Honek, J.F. 2005. Ab initio studies of the properties of intracellular thiols ergothioneine and ovothiol. *Bioorganic and Medicinal Chemical Letters*, 15(5) pp.1357–1360.

Hanlon, D.P. 1971. Interaction of ergothioneine with metal ions and metalloenzymes. *Journal of Medicinal Chemistry*, 14(11), pp.1084–1087.

Hatano, T., Saiki, S., Okuzumi, A., Mohney, R.P. and Hattori, N. 2015. Identification of novel biomarkers for Parkinson's disease by metabolomic technologies. *Journal of Neurology Neurosurgical and Psychiatry*, 87(3), pp.1–7.

Hofte, M. 1993. Classes of Microbial Siderophores. In *Iron Chelation in Plants and Soil Microorganisms*. Barton, L.L. and Hemming, B.C., Acedemic Press Inc, pp. 3-4.

Howard, S.J., Pasqualotto, A.C., Anderson, M.J., Leatherbarrow, H., Albarrag, A.M.,

Harrison, E., Gregson, L., Bowyer, P. and Denning, D.W. 2013. Major variations in Aspergillus fumigatus arising within aspergillomas in chronic pulmonary aspergillosis. *Mycoses*, 56(4), pp.434–441.

Hutchison, C.A., Phillips, S., Edgell, M.H., Gillam, S., Jahnke, P. and Smith, M. 1978. Mutagenesis at a specific position in a DNA sequence. *Journal of Biological Chemistry*, 253(18), pp.6551–6560.

Ingeber, D., Fujita, T., Kishimoto, S., Sudo, K., Kanamaru, T., Brem, H. and Folkman, J. 1990. Synthetic analogues of fumagillin that inhibit angiogenesis and suppress tumour growth. *Nature*, 348(6301), pp.555-557.

Inglis, D.O., Binkley, J., Skrzypek, M.S., Arnaud, M.B., Cerqueira, G.C., Shah, P., Wymore, F., Wortman, J.R. and Sherlock, G. 2013. Comprehensive annotation of secondary metabolite biosynthetic genes and gene clusters of Aspergillus nidulans, A. fumigatus, A. niger and A. oryzae. *BMC Microbiology*, 26(13), pp.91.

Jones, G.W., Doyle, S. and Fitzpatrick, D. 2014. The evolutionary history of the genes involved in the biosynthesis of the antioxidant ergothioneine. *Gene*, 549(1), pp.161–170.

Kaneko, I., Takechi, Y., Yamaoka, Y., Tanaka, Y., Fukuda, T., Fukumori, Y., Mayumi, T. and Hama, T. 1980. Qunatitive determination of ergothioneine in plasma and tissues by TLC-densitometry. *Chemical and Pharmalogical Bulletin*, 28, pp.3093–3097.

Kannan, N., Taylor, S.S., Zhai, Y., Venter, J.C. and Manning, G. 2007. Structural and functional diversity of the microbial kinome. *PLoS Biology*, 5(3), pp.0467–0478.

Kanno, T,, Uehara, T., Osawa, M., Fukumoto, H., Mine, S., Ueda, K., Hasegawa, H. and K.H. 2015. Fumagillin, a potent angiogenesis inhibitor, induces Kaposi sarcomaassociated herpesvirus replication in primary effusion lymphoma cells. *Biochem Biophys Res Commun*, 463(4), pp.1267–72.

Kaplowitz, N., Aw, T.Y., and Ookhtens, M., 1985. The Regulation of Hepatic Glutathione. *Annual Review of Pharmacology and Toxicology*, 25, pp.715–744.

Kato, Y., Kubo, Y., Iwata, D, Kato, S., Sudo, T., Sugiura, T., Kagaya, T., Wakayama, T., Hirayama, A., Sugimoto, M., Sugihara, K., Kaneko, S., Soga, T., Asano, M., Tomita, M., Matsui, T., Wada, M. and Tsuji, A. 2010. Gene knockout and metabolome analysis of

carnitine/organic cation transporter OCTN1. *Pharmaceutical Research*, 27(5), pp.832–840.

Kawano, H., Otani, M., Takeyama, K., Kawai, Y. and Mayumi, T, H.T., 1982. Studies on ergothioneine. VI. Distribution and fluctuations of ergothioneine in rats. *Chemical and Pharmaceutical Bulletin*, 30, pp.1760–1765.

Kennedy, J., Auclair, K., Kendrew, S.G., Park, C., Vederas, J.C. and Hutchinson, C.R. 1999. Modulation of Polyketide Synthase Activity by Accessory Proteins During Lovastatin Biosynthesis. *Science*, 284(5418), pp.1368–1372.

Khaldi, N., Seifuddin, F.T., Turner, G., Haft, D., Nierman, W.C., Wolfe, K.H. and Fedorova, N.D. 2010. SMURF: Genomic mapping of fungal secondary metabolite clusters. *Fungal Genetics and Biology*, 47(9), pp.736–741.

Khonde, P.L. and Jardine, A. 2015. Improved synthesis of the super antioxidant, ergothioneine, and its biosynthetic pathway intermediates. *Organic and Biomolecular Chemistry*, 13(5), pp.1415–9.

Kispal, G., Csere, P., Prohl, C. and Lill, R. 1999. The mitochondrial proteins Atm1p and Nfs1p are essential for biogenesis of cytosolic Fe/S proteins. *EMBO Journal*, 18(14), pp.3981–3989.

Knox, B.P. and Keller, N.P. 2015. Key Players in the Regulation of Fungal Secondary Metabolism. In *Biosynthesis and Molecular Geneticsof Fungal Secondary Metabolites, Volume 2*. Zeilinger, S., Martin, J.F. and Garcia-Estrada, C. 1st ed. pp.13–23

Van Laer, K., Hamilton, C.J. and Messens, J. 2013. Low-Molecular-Weight Thiols in Thiol–Disulfide Exchange. *Antioxidants & Redox Signaling*, 18(13), pp.1642–1653.

Lamhonwah, A.M. and Tein, I. 2006. Novel localization of OCTN1, an organic cation/carnitine transporter, to mammalian mitochondria. *Biochemical and Biophysical Research Communications*, 345(4), pp.1315–1325.

Latgé, J.P., 2001. The pathobiology of Aspergillus fumigatus. *Trends in Microbiology*, 9(8), pp.382–389.

Lee, S.-Y., Kinoshita, H., Ihara, F., Igarashi, Y. and Nihira, T. 2008. Identification of novel derivative of helvolic acid from Metarhizium anisopliae grown in medium with insect component. *Journal of Bioscience and Bioengineering*, 105(5), pp.476–80.

Li, S.M. 2011. Genome mining and biosynthesis of fumitremorgin-type alkaloids in ascomycetes. *The Journal of Antibiotics*, 64(1), pp.45–49.

Lin, M.T. and Beal, M.F. 2006. Mitochondrial dysfunction and oxidative stress in neurodegenerative diseases. *Nature*, 443(7113), pp.787–795.

Lin, S.-Y., Chien, S.C., Wang, S,Y. and Mau, J.L. 2015. Submerged Cultivation of Mycelium with High Ergothioneine Content from the Culinary-Medicinal Golden Oyster Mushroom, Pleurotus citrinopileatus (Higher Basidiomycetes). *International Journal of Medicinal Mushrooms*, 17(8), pp.749–761.

Lu, S.C., 2013. Glutathione synthesis. *Biochimica et Biophysica acta*, 1830(5), pp.3143–53.

Machida, M., Asai, K., Sano, M., Tanaka, T., Kumagai, T., Terai, G., Kusumoto, K., Arima, T., Akita, O., Kashiwagi, Y., Abe, K., Gomi, K., Horiuchi, H., Kitamoto, K, Kobayashi, T., Takeuchi, M., Denning, D.W., Galagan, J.E., Nierman, W.C., Yu J., Archer, D.B., Bennett, J.W., Bhatnagar, D., Cleveland, T.E., Fedorova, N.D., Gotoh, O., Horikawa, H., Hosoyama, A., Ichinomiya, M., Igarashi, R., Iwashita, K., Juvvadi, P.R., Kato, M., Kato, Y., Kin, T., Kokubun, A., Maeda, H., Maeyama, N., Maruyama, J., Nagasaki, H., Nakajima, T., Oda, K., Okada, K., Paulsen, I., Sakamoto, K., Sawano, T., Takahashi, M., Takase, K., Terabayashi, Y., Wortman, J.R., Yamada, O., Yamagata, Y., Anazawa, H., Hata, Y., Koide, Y., Komori, T., Koyama, Y., Minetoki, T., Suharnan, S., Tanaka, A., Isono, K., Kuhara, S., Ogasawara, N. and Kikuchi, H. 2005. Genome sequencing and analysis of Aspergillus oryzae. *Nature*, 438(7071), pp.1157–61.

Maeda, T., Hirayama, M., Kobayashi, D., Miyazawa, K. and Tamai, I. 2007. Mechanism of the Regulation of OCTN1 Transporter (SLC22A4) by Rheumatoid Arthritis-Associated Transcriptional Factor RUNX1 and Inflammatory Cytokines. *Drug Metababolism and Disposition,* 35(3), pp394–401.

Manzanares-Miralles, L., Sarikaya-Bayram, Ö., Smith, E.B., Dolan, S.K., Bayram, Ö., Jones, G.W. and Doyle S. 2016. Quantitative proteomics reveals the mechanism and consequence of gliotoxin-mediated dysregulation of the methionine cycle in Aspergillus niger. *Journal of Proteomics*, 131, pp.149–162.

Marr, K.A., Carter, R.A., Boeckh, M., Martin, P. and Corey, L. 2002. Invasive aspergillosis in allogeneic stem cell transplant recipients : changes in epidemiology and risk factors.

Survival, 100(13), pp.4358–4366.

Mattanovich, D., Branduardi, P., Dato, L., Gasser, B., Sauer, M. and Porro, D. 2012. Recombinant Protein Production in Yeasts. *Methods in Molecular Biology*, 824, pp.329–58.

Mayumi, T., Kawano, H., Sakamoto, Y., Suehisa, E., Kawai, Y. and Hama, T. 1978. Studies on ergothioneine. V. Determination by high performance liquid chromatography and application to metabolic research. *Chemical and Pharmaceutical Bulletin*, 26(12), pp.3772–8.

Medema, M.H., Blin, K., Cimermancic, P., de Jager, V., Zakrzewski, P., Fischbach, M.A., Weber, T., Takano, E. and Breitling, R. 2011. AntiSMASH: Rapid identification, annotation and analysis of secondary metabolite biosynthesis gene clusters in bacterial and fungal genome sequences. *Nucleic Acids Research*, 39(SUPPL. 2), pp.339–346.

Meseguer Lloret, S., Molins Legua, C., Verdú Andrés, J. and Campíns Falcó, P. 2004. Sensitive determination of aliphatic amines in water by high-performance liquid chromatography with chemiluminescence detection. *Journal of Chromatography*, 1035(1), pp.75–82.

Motohashi, N., Motohashi, N., Mori, I., Sugiura, Y. and Tanaka, H.
 1974. Metal complexes of ergothioneine. *Chemical and Pharmaceutical Bulletin*, 22(3), pp.654–657.

Muhlenhoff, U., Balk, J., Richhardt, N., Kaiser, J.T., Sipos K., Kispal, G. and Lill, R. 2004. Functional characterization of the eukaryotic cysteine desulfurase Nfs1p from Saccharomyces cerevisiae. *Journal of Biological Chemistry*, 279(35), pp.36906–36915.

Mumberg, D., Mailer, R. and Funk, M., 1995. Yeast vectors for the controlled expression of heterologous proteins in different genetic backgrounds. , 156, pp.119–122.

Nakamura, T., Sugiura, S., Kobayashi, D., Yoshida, K., Yabuuchi, H., Aizawa, S., Maeda, T. and Tamai, I. 2007. Decreased proliferation and erythroid differentiation of K562 cells by siRNA-induced depression of OCTN1 (SLC22A4) transporter gene. *Pharmaceutical Research*, 24(9), pp.1628–1635.

Narainsamy, K., Farci, S., Braun, E., Junot, C., Cassier-Chauvat, C. and Chauvat, F. 2015. Oxidative-stress detoxification and signaling in cyanobacteria: The crucial glutathione

synthesis pathway supports the production of ergothioneine and ophthalmate. *Molecular Microbiology*, 100(1), pp.15–24.

Nierman, W., Pain, A., Anderson, M.J., Wortman, J.R., Kim, H.S., Arroyo, J., Berriman, M., Abe, K., Archer, D.B., Bermejo, C., Bennett, J., Bowyer, P., Chen, D., Collins, M., Coulsen, R., Davies, R., Dyer P.S., Farman M., Fedorova N., Fedorova N., Feldblyum T.V., Fischer R., Fosker, N., Fraser A., García J.L., García M.J., Goble A., Goldman G.H., Gomi K., Griffith-Jones, S., Gwilliam R., Haas B., Haas H., Harris D., Horiuchi H., Huang J., Humphray S., Jiménez, J., Keller, N., Khouri, H., Kitamoto, K., Kobayashi, T., Konzack, S., Kulkarni, R., Kumagai, T., Lafon, A., Latgé, J.P., Li, W., Lord, A., Lu, C., Majoros, W.H., May, G.S., Miller, B.L., Mohamoud, Y., Molina, M., Monod, M., Mouyna, I., Mulligan, S., Murphy, L., O'Neil, S., Paulsen, I., Peñalva, M.A., Pertea, M., Price, C., Pritchard, B.L., Quail, M.A., Rabbinowitsch, E., Rawlins, N., Rajandream, M.A., Reichard, U., Renauld, H., Robson, G.D., Rodriguez, de Córdoba, S., Rodríguez-Peña, J.M., Ronning C.M., Rutter, S., Salzberg, S.L., Sanchez, M., Sánchez-Ferrero, J.C., Saunders, D., Seeger, K., Squares, R., Squares, S., Takeuchi, M., Tekaia, F., Turner, G., Vazquez de Aldana, C.R., Weidman, J., White, O., Woodward, J., Yu J.H., Fraser, C., Galagan, J.E., Asai K., Machida, M., Hall, N., Barrell, B. and Denning, D.W. 2005. Genomic sequence of the pathogenic and allergenic filamentous fungus Aspergillus fumigatus. *Nature*, 438(7071), pp.1151–6.

Nikodemus, D., Lazic, D., Bach, M., Bauer, T., Pfeiffer, C., Wiltzer, L., Lain, E., Schömig, E. and Gründemann, D. 2011. Paramount levels of ergothioneine transporter SLC22A4 mRNA in boar seminal vesicles and cross-species analysis of ergothioneine and glutathione in seminal plasma. *Journal of Physiology and Pharmacology*, 62(4), pp.411–419.

Nordberg, J. and Arnér, E.S. 2001. Reactive oxygen species, antioxidants, and the mammalian thioredoxin system. *Free Radical Biology and Medicine*, 31(11), pp.1287–1312.

Norins, A.L. 1962. Free Radical Formation in the Skin Following Exposure to Ultraviolet Light. *Journal of Investigative Dermatology*, 39(5), pp.445–448.

O'Keeffe, G.O. and Doyle, S. 2011. Functional Characterisation of the Eukaryotic Translation Elongation Factor 1Bγ in Aspergillus fumigatus ; A Proteomic Systems Approach.

Omara, W.A., Rash, B.M., Hayes, A., Wickham, M.S., Oliver, S.G. and Stateva, L.I. 2010. Conditional cell-wall mutants of Saccharomyces cerevisiae as delivery vehicles for

therapeutic agents in vivo to the GI tract. *Journal of Biotechnology*, 147(2), pp.136–143.

Onal, A., 2007. A review: Current analytical methods for the determination of biogenic amines in foods. *Food Chemistry*, 103(4), pp.1475–1486.

Park, E.J., Lee, W.Y., Kim, S.T., Ahn, J.K. and Bae, E.K. 2010. Ergothioneine accumulation in a medicinal plant Gastrodia elata. *Journal of medicinal Plants Research*, 4(12), pp.1141–1147.

Patterson, T.F. Kirkpatrick, W.R., White, M., Hiemenz, J.W., Wingard, J.R., Dupont, B., Rinaldi, M.G., Stevens, D.A. and Graybill, J.R. 2000. Invasive aspergillosis. Disease spectrum, treatment practices, and outcomes. *Medicine*, 79(4), pp.250–60.

Paul, B.D. and Snyder, S.H. 2009. The unusual amino acid L-ergothioneine is a physiologic cytoprotectant. *Cell Death and Differentiation*, 17(7), pp.1134–1140.

Payne, G.A., Nystrom, G.J., Bhatnagar, D., Cleveland, T.E. and Woloshuk, C.P. 1993. Cloning of the af-2 Gene Involved in Aflatoxin Biosynthesis from Aspergillus flavus. *Applied and Environmental Microbiology*, 59(1), pp.156–162.

Pel, H.J., de Winde, J.H., Archer, D.B., Dyer, P.S., Hofmann, G., Schaap P.J., Turner, G., de Vries, R.P., Albang, R., Albermann, K., Andersen, M.R., Bendtsen, J.D., Benen, J.A., van den Berg, M., Breestraat, S., Caddick, M.X., Contreras, R., Cornell, M., Coutinho, P.M., Danchin, E.G., Debets, A.J., Dekker, P., van Dijck, P.W., van Dijk, A., Dijkhuizen, L., Driessen, A.J., d'Enfert, C., Geysens, S., Goosen, C., Groot, G.S., de Groot, P.W., Guillemette, T., Henrissat, B., Herweijer, M., van den Hombergh, J.P., van den Hondel, C.A.,van der Heijden, R.T., van der Kaaij, R.M., Klis, F.M., Kools, H.J., Kubicek, C.P., van Kuyk, P.A., Lauber, J., Lu, X., van der Maarel, M.J., Meulenberg, R., Menke, H., Mortimer, M.A., Nielsen, J., Oliver, S.G., Olsthoorn, M., Pal, K., van Peij, N.N., Ram, A.F., Rinas, U., Roubos, J.A., Sagt, C.M., Schmoll, M., Sun, J., Ussery, D., Varga, J., Vervecken, W., van de Vondervoort, P.J., Wedler, H., Wösten, H.A., Zeng, A.P., van Ooyen, A.J., Visser, J. and Stam, H. 2007. Genome sequencing and analysis of the versatile cell. *Nature Biotechnology*, 25(2), pp.221–231.

Peltekova, V.D. Wintle, R.F., Rubin, L.A., Amos, C.I., Huang, Q., Gu X., Newman, B., Van Oene M., Cescon, D., Greenberg, G., Griffiths, A.M., St George-Hyslop, P.H. and Siminovitch, KA. 2004. Functional variants of OCTN cation transporter genes are associated

with Crohn disease. *Nature Genetics*, 36(5), pp.471–475.

Pendleton, M. and Denning, D.W. 2012. Multifocal pulmonary aspergillomas: Case series and review. *Annals of the New York Academy of Sciences*, 1272(1), pp.58–67.

Pfeiffer, C., Bauer, T., Surek, B., Schömig, E. and Gründemann, D.
 2011. Cyanobacteria produce high levels of ergothioneine. *Food Chemistry*, 129(4), pp.1766–1769.

Pike CJ, Walencewicz AJ, Glabe CG, C.C., 1991. In vitro aging of ß-amyloid protein causes peptide aggregation and neurotoxicity. *Brain Research*, 563(1-2), pp.311–4.

Markova, Nelli., Yarosh, D., Smiles, K. and Karaman-Jurukovska, N. 2009. The natural antioxident L-ergothioneine is integral to the skins defence against ultraviolet -induced oxidative damage. P3120. *The Journal of the American Acedamy of Dermatology*, AB.156.

Pluskal, T., Ueno, M. and Yanagida, M. 2014. Genetic and Metabolomic Dissection of the Ergothioneine and Selenoneine Biosynthetic Pathway in the Fission Yeast , S . pombe , and Construction of an Overproduction System. *PLoS One*, 9(5), e105177.

Qin, L., Li, B., Guan, J. and Zhang, G. 2009. In vitro synergistic antibacterial activities of helvolic acid on multi-drug resistant Staphylococcus aureus. *Natural Product Research*, 23(4), pp.309–318.

Hu, W., Song, H., Her, A.S., Bak, D.W., Naowarojna, N., Sean J. Elliott, S.J., Qin, L., Chen, X. and Liu, P., 2014. Bioinformatic and Biochemical Characterizations of C − S Bond Formation and Cleavage Enzymes in the Fungus Neurospora crassa Ergothioneine Biosynthetic Pathway. Organic Letters, 16(20) pp.5382–85.

Rabindran, S.K., Ross, D.D., Doyle, L.A., Yang, W. and Greenberger, L.M. 2000. Fumitremorgin C Reverses Multidrug Resistance in Cells Transfected with the Breast Cancer Resistance Protein. *Cancer Research* , pp.47–50.

Rahman, I., Gilmour, P.S., Jimenez, L.A., Biswas, S.K., Antonicelli, F. and Aruoma, O.I. 2003. Ergothioneine inhibits oxidative stress- and TNF-α-induced NF-κ B activation and interleukin-8 release in alveolar epithelial cells. *Biochemical and Biophysical Research Communications*, 302(4), pp.860–864.

Rawat, M., Newton G.L., Ko, M., Martinez, G.J., Fahey, R.C. and Av-Gay, Y. 2002.

Mycothiol-Deficient Mycobacterium smegmatis Mutants Are Hypersensitive to Alkylating Agents , Free Radicals , and Antibiotics. *Antimicrobial Agents and Chemotherapy*, 46(11), pp.3348–3355.

Richard-Greenblatt, M., Bach, H., Adamson, J., Peña-Diaz, S., Li, W., Steyn, A.J. and Av-Gay, Y. 2015. Regulation of ergothioneine biosynthesis and its effect on Mycobacterium tuberculosis growth and infectivity. *Journal of Biological Chemistry*, 290(38), pp.23064–23076.

Romanos, M.A., Scorer, C.A. and Clare, J.J., 1992. Foreign Gene Expression in Yeast : a Review. *Yeast*, 8(6), pp.423–488.

Rosales-Mendoza, S., Angulo, C. and Meza, B. 2015. Food-Grade Organisms as Vaccine Biofactories and Oral Delivery Vehicles. *Trends in Biotechnology*, 34(2), pp.124–36

Rougee, M, Bensasson, R.V., Land, E.J. and Pariente, R. 1988. Deactivation of singlet molecular oxygen by thiols and related compounds, possible protectors against skin photosensitivity. *Photochemistry and Photobiology*, 47(4), pp.485–9.

Saha, R., Saha, N., Donofrio, R.S. and Bestervelt, L.L. 2013. Microbial siderophores: A mini review. *Journal of Basic Microbiology*, 53(4), pp.303–317.

Saini, V., Cumming, B.M., Guidry, L., Lamprecht, D.A, Adamson, J.H., Reddy, V.P. Chinta, K.C., Mazorodze, J.H., Glasgow, J.N., Richard-Greenblatt, M., Gomez-Velasco, A., Bach, H., Av-Gay, Y., Eoh, H., Rhee, K. and Steyn, A.J. 2015. Ergothioneine Maintains Redox and Bioenergetic Homeostasis Essential for Drug Susceptibility and Virulence of Mycobacterium tuberculosis. *Cell Reports*, 14(3), pp.572–585.

Sanchez, J.F. Somoza, A.D., Keller, N.P. and Wang, C.C. 2012. Advances in Aspergillus secondary metabolite research in the post-genomic era. *Natural product reports*, 29(3), pp.351–371.

Santiago, J.L., Martínez, A., de la Calle, H., Fernández-Arquero, M., Figueredo, M.A., de la Concha, E.G. and Urcelay, E. 2006. Evidence for the association of the SLC22A4 and SLC22A5 genes with type 1 diabetes: a case control study. *BMC Medical Genetics*, 23(7), pp.54.

Schafer, F.Q. and Buettner, G.R., 2001. Redox environment of the cell as viewed through the

redox state of the glutathione disulfide/glutathione couple. *Free Radical Biology and Medicine*, 30(11), pp.1191–1212.

Schrettl, M., Bignell, E., Kragl, C., Sabiha, Y., Loss, O., Eisendle, M., Wallner, A., Arst, H.N. Jr., Haynes, K., and Haas, H. 2007. Distinct roles for intra- and extracellular siderophores during Aspergillus fumigatus infection. *PLoS Pathogens*, 3(9), pp.1195–1207.

Schrettl, M., Carberry, S., Kavanagh, K., Haas, H., Jones, G.W., O'Brien, J., Nolan, A., Stephens, J., Fenelon, O. and Doyle S. 2010. Self-protection against gliotoxin-a component of the gliotoxin biosynthetic cluster, gliT, completely protects Aspergillus fumigatus against exogenous gliotoxin. *PLoS Pathogens*, 6(6), e1000952.

Seebeck, F.P., 2010. In Vitro Reconstitution of Mycobacterial Ergothioneine Biosynthesis. *J Am Chem Soc*, 132(19), pp.6632–6633.

Servillo, L., Castaldo, D., Casale, R., D'Onofrio, N., Giovane, A., Cautela, D., Balestrieri, M.L. 2015. Free Radical Biology and Medicine An uncommon redox behavior sheds light on the cellular antioxidant properties of ergothioneine. *Free Radical Biology and Medicine*, 79, pp.228–236.

Shires, T.K., Brummel, M.C., Pulido, J.S. and Steginck, L.D. 1997. Ergothioneine distribution in bovine and porcine ocular tissues. *Comparative Biochemistry and Physiology - Pharmacology Toxicology and Endocrinology*, 117(1), pp.117–120.

Da Silva, N.A. and Srikrishnan, S. 2012. Introduction and expression of genes for metabolic engineering applications in Saccharomyces cerevisiae. *FEMS Yeast Research*, 12(2), pp.197–214.

Song, H., Hu, W., Naowarojna. N., Her, A.S., Wang, S., Desai, R., Qin, L., Chen, X. and Liu, P. 2015. Mechanistic studies of a novel C-S lyase in ergothioneine biosynthesis : the involvement of a sulfenic acid intermediate. *Nature Publishing Group*, (July), pp.1–13.

Song, T.Y., Chen, C.L., Liao, J.W., Ou, H.C. and Tsai, M.S. 2010. Ergothioneine protects against neuronal injury induced by cisplatin both in vitro and in vivo. *Food and Chemical Toxicology*, 48(12), pp.3492–3499.

Sotgia, S., Pisanu, E., Pintus, G., Erre, G.L., Pinna, G.A., Deiana, L., Carru, C. and Zinellu, A. 2013. Plasma L-Ergothioneine Measurement by High-Performance Liquid Chromatography and Capillary Electrophoresis after a Pre-Column Derivatization with 5-

Iodoacetamidofluorescein (5-IAF) and Fluorescence Detection. *PLoS ONE*, 8(7), pp.1–6.

Sotgia, S., Pisanu, E., Cambedda, D., Pintus, G., Carru, C. and Zinellu, A. 2014. Ultra-Performance Liquid Chromatographic Determination of L-Ergothioneine in Commercially Available Classes of Cow Milk. *Journal of Food Science*, 79(9), pp.C1683–C1687.

Speisky, H., Gómez, M., Carrasco-Pozo, C., Pastene, E., Lopez-Alarcón, C. and Olea-Azar C. 2008. Cu(I)-Glutathione complex: A potential source of superoxide radicals generation. *Bioorganic and Medicinal Chemistry*, 16(13), pp.6568–6574.

Staud, F. and Pavek, P. 2005. Breast cancer resistance protein (BCRP/ABCG2). *The International Journal of Biochemistry and Cell Biology*, 37(4), pp.720–5.

Steinman, H.M. 1980. The amino acid sequence of copper-zinc superoxide dismutase from bakers' yeast. *The Journal of Biological Chemistry*, 255(14), pp.6758–6765.

Sullivan, D., Moran, G. and Coleman, D. (2005). The Biotechnological Exploitation of Heterologous Protein Production in Fungi. In: *Fungi: Biology and Applications* 1st ed., Kavanagh, K. Wiley, England.

Tanret, C. 1909. Sur une base nouvelle retirée du seigle ergoté, l'ergothioneine. *French Academy of. Science*, 49, pp.222–224.

Taubert, D., Jung, N., Goeser, T. and Schömig E. 2009. Increased ergothioneine tissue concentrations in carriers of the Crohn's disease risk-associated 503F variant of the organic cation transporter OCTN1. *Gut*, 58(2), pp.312–4.

Taubert, D., Lazar, A., Grimberg, G., Jung, N., Rubbert, A., Delank, K.S., Perniok, A., Erdmann, E. and Schomig, E. 2006. Association of rheumatoid arthritis with ergothioneine levels in red blood cells: a case control study. *The Journal of Rheumatology,* 33(11), pp.2139–2145.

Thompson, G.R. and Patterson, T.F. 2008. Pulmonary aspergillosis. *Seminars in Respiratory and Critical Care Medicine*, 29(2), pp.103–110.

Tillie-Leblond, I. and Tonnel, A. 2005. Allergic bronchopulmonary aspergillosis. *Allergy*, 60(8), pp.1004–1013.

Tokuhiro, S., Yamada, R., Chang, X., Suzuki, A., Kochi, Y., Sawada, T., Suzuki,

M., Nagasaki, M., Ohtsuki, M., Ono, M., Furukawa, H., Nagashima, M., Yoshino, S., Mabuchi, A., Sekine, A., Saito, S., Takahashi, A., Tsunoda, T., Nakamura, Y. and Yamamoto, K. 2003. An intronic SNP in a RUNX1 binding site of SLC22A4, encoding an organic cation transporter, is associated with rheumatoid arthritis. *Nature Genetics*, 35(4), pp.341–348.

Tomimoto, K., Fujita, Y., Iwaki, T., Chiba, Y., Jigami, Y., Nakayama, K., Nakajima, Y. and Abe, H. 2013. Protease-Deficient Saccharomyces cerevisiae Strains for the Synthesis of Human-Compatible Glycoproteins. *Bioscience, Biotechnology, and Biochemistry*, 77(12), pp.2461–2466.

Trifunovic, A., Hansson, A., Wredenberg, A., Rovio, A.T., Dufour, E., Khvorostov, I., Spelbrink, J.N., Wibom, R., Jacobs, H.T. and Larsson N.G. 2005. Somatic mtDNA mutations cause aging phenotypes without affecting reactive oxygen species production. *Proceedings of the National Academy of Sciences of the United States of America*, 102(50), pp.17993–17998.

Ulrey, C.L., Liu. L., Andrews, L.G. and Tollefsbol, T.O. 2005. The impact of metabolism on DNA methylation. *Human Molecular Genetics*, 14(SPEC. ISS. 1), pp.139–147.

Vit, A., Misson, L., Blankenfeldt, W. and Seebeck, F.P. 2014. Ergothioneine Biosynthetic Methyltransferase EgtD Reveals the Structural Basis of Aromatic Amino Acid Betaine Biosynthesis. *ChemBioChem*, 16(1), pp.119–125.

Vit, A., Mashabela, G.T., Mashabela, G.T., Blankenfeldt, W. and Seebeck F.P. 2015. Structure of the Ergothioneine-Biosynthesis Amidohydrolase EgtC. *ChemBiochem*, 16(10), pp.1490–1496.

Whiteman, M. and Halliwell, B. 1997. Thiols and disulphides can aggravate peroxynitrite-dependent inactivation of alpha1-antiproteinase. *FEBS Letters*, 414(3), pp.497–500.

Wu, G. Liu, J., Bi, L., Zhao, M.,Wang, C., Baudy-Floc'h, M., Ju, J. and Peng, S. 2007. Toward breast cancer resistance protein (BCRP) inhibitors: design, synthesis of a series of new simplified fumitremorgin C analogues. *Tetrahedron*, 63(25), pp.5510–5528.

Yamashita, Y., Yamashita, M. and Iida, H. 2013. Selenium content in seafood in Japan. *Nutrients*, 5(2), pp.388–395.

Yang, N.C., Lin, H.C., Wu, J.H., Ou, H.C., Chai, Y.C., Tseng, C.Y., Liao, J.W. and Song, T.Y. 2012. Ergothioneine protects against neuronal injury induced by beta-amyloid in mice. *Food and Chemical Toxicology*, 50(11), pp.3902–3911.

Zbidah, M., Lupescu A., Jilani K. and Lang, F. 2013. Stimulation of Suicidal Erythrocyte Death by Fumagillin. *Basic & Clinical Pharmacology & Toxicology*, 112(5), pp.346–351.

Zhang, T., Sun, L., Xin, Y., Ma, L., Zhang, Y., Wang, X., Xu, K., Ren, C., Zhang, C., Chen, Z., Yang, H. and Zhang, Z. 2012. A vaccine grade of yeast Saccharomyces cerevisiae expressing mammalian myostatin. *BMC biotechnology*, 12(1), p.97.

Zhang, Y., Yeh, J.R., Mara, A., Ju, R., Hines, J.F., Cirone, P., Griesbach, H.L., Schneider, I., Slusarski, D.C., Holley, S.A. and Crews, C.M. 2006. A chemical and genetic approach to the mode of action of fumagillin. *Chemistry and Biology*, 13(9), pp.1001–1009.

Zhao, Q., Wang, M,, Xu. D., Zhang, Q. and Liu, W. 2015. Metabolic coupling of two small-molecule thiols programs the biosynthesis of lincomycin A. *Nature*, 518(7537), pp.115–9.

Zhu, B.Z., Mao, L., Fan, R.M., Zhu, J.G., Zhang, Y.N., Wang, J., Kalyanaraman, B. and Frei, B. 2011. Ergothioneine prevents copper-induced oxidative damage to DNA and protein by forming a redox-inactive ergothioneine-copper complex. *Chemical Research in Toxicology*, 24(1), pp.30–34.

Zhu, H., Klemic, J.F., Chang, S., Bertone, P., Casamayor, A., Klemic, K.G., Smith, D., Gerstein, M., Reed, M.A. and Snyder, M. 2000. Analysis of yeast protein kinases using protein chips. *Nature Genetics*, 26(3), pp.283–9.

Ziemert, N., Podell, S., Penn, K., Badger, J.H., Allen, E. and Jensen, P.R. 2012. The natural product domain seeker NaPDoS: A phylogeny based bioinformatic tool to classify secondary metabolite gene diversity. *PLoS ONE*, 7(3), pp.1–9.

Chapter 6

Appendices

6.1 Appendices

>EGTA cDNA

<u>ATGTCCCCGTTGCCGTGTCC</u>TTCGAAAAAGGTCGAGATTGTCGATATACATCGA
AATGACGTGGAATTCTCGCTCGTGAATGAGATTCGCAAGGGCCTCAACCCTCCC
GAGGGTACTCCAAGATCATTGCCCACCATGCTGCTCTACGACGCTCAAGGGCTT

AAGCTCTTCGAGGAGATCACCTACGTGGATGAGTACTACCTGACCAACGCGGAA
ATCGAAGTGTTGCAGAACCACTCCAAGAAGATTGTGGAACGCGTCCCCGAGAA
CGCACAATTATTGGAGCTGGGTAGTGGGAACCTTCGTAAGATCAAGATCCTTCT
TCAAGAGTTCGAGCGGACAGGAAAGCACGTCGACTACTATGCGTTGGATCTATC
CCTGTCAGAGCTACAGCGGACCTTTGTCGAGGTATCATCTGACGAGTACTCTCA
CGTTGATCTCCACGGTCTTCACGGGACCTATGATGATGCCCTTGCCTGGCTGAGC
AATCCCCAGAACCTACAGCGTCCCACTGTGGTTATGTCTATGGGATCCTCAATT
GGGAATTTCAGTCGTGAAGGTGCAGCAGAGTTTCTTGCCCAATTTGCTCGGCTG
CTCAAGCCATCCGATCTGATGATCATTGGGCTAGATGCTTGTACAGACCCGGAC
AAGGTCTACAAGGCATACAACGATTCAAAGGGCATTACTCAGAGGTTCTACGA
GAATGGGCTATTACATGCGAATGCAGTCCTTGGATACGAGGCATTCCAACTTTC
GGAATGGGAGGTGGTGACAGACTACGACGTTGCCGGGGGCCGACATCGAGCAT
TCTACTCACCGAAGCAGAATGTTACAATCGATGGCGTGCTTCTGCAAAAAGGCG
AGAAATTGGTTTTTGAAGAGGCAACAAAGTATAGCCCTCAACAACGGGAGCAA
CTCTGGCGGGATGCAAACCTCGTCCTTTGTGAGGAGCTTGGAATTAGCTCTGAG
GAATACCATATCCATCTGCTGTCACCGCCAACCCTCAGCCTTCCCAGTCAACCG
TCCGAATATGCTGCCAATCCAGTTCCGAGCTTCAAAGAATTCCAGTCATTGTGG
ACCGCTTGGGACACTGTGACAAAGGCCATGGTGCCCCGCGAAGAACTCCTCGC
GAAACCTATCAAGCTTCGCAATGCATTGATCTTCTACTTTGGACACATCCCCACA
TTCACGGACATCCACTTGACACGGGCTCTTGGTGGCTCTCCAACAGAACCACGA
AACTATCGACAGATTTTCGAGCGTGGGATTGACCCCGACGTAGACAATCCCGAG
CACTGTCACTCCCATAGTGAGATTCCGGATGAATGGCCTCCCCTTGCTGAGATA
CTGGATTATCAGGATAGAGTCAGAAGTAGGGTTGATTCGGTTTTGCAGAGGGAT
GACATAACACAGAACCGCTGCCTGGGGGAAGCACTCTGGATTGGCTTCGAACA
CGAAGCGATGCACCTAGAGACCTTTCTCTATATGCTTTTGCAGAGTGACAAGAC
CCTCCCACCGCCCCTTGCAGACAGACCAGATTTTGAGAAGTTGTTCCATCAGGC
CAGAGCGAACGCGAAACCAAATGAATGGTTTGCTATACCAGAACAGACATTAT
CCATCGGTTTTGACGATACTGACGAACAATCTTTGCCTGATGTGTCTTTTGGATG
GGACAATGAGAAGCCTCAGCGAACGATCACAGTTCGTGCTTTCGAAGCACAGG
CTCATGCTATAACAAACGGCGAATATGCCAAATATCTGCAAGCGACTCGTCAGC
GCCGGCGGCCAGAGTCGTGGGTTCTAACTCATTCGGATGAGAATTATCCAATCT
CCAAGGGGGTGACTCTGGAGAGCAGCCAAGCCACAAAGGATTTCATGGACAAC
TTCGCTGTCCGCACCGTCTTTGGACCTGTTCCGCTTGAATTCGCGCAGGATTGGC
CTGTTATGGCTTCCTATGACGAACTGGCCCTATACGCCGAATGGGTGGGCTGCA
GACTTCCCACTTATGAGGAGGTCAAGAGTATCTACAACTACTCCGCTCAGCTGA
AGGAGACAAGACAACATGAGCCATCAGATCACGAGAGCAACGGTGTGAAGGGC
ATTAACCGTGATATGGTGACGAACGGGCACTCGAAGGTTCACCAGGATAAGCC
CCGGACCCCAGAACGTCAGCCAATCCAACCTCCTTCCCAAAGCACAATGCCAGT
ATTTGTTGACCTCCACGGTTGCAACGTTGGGTTCAAGCACTGGCACCCTACCCC
GGTCATCCAGAACGGCGATCGACTCGCCGGTCACGGTGAGCTGGGAGGAGTCT
GGGAATGGACCAGCACGCCACTGACGCCACATGATGGCTTCAAGGCCATGGAT
ATTTATCCAGGTTATCAGCGGACTTCTTTGATGGAAAGCACAACATTGTCCTG
GGTGGTTCATGGGCCACGCATCCTAGAATTGCGGGACGGACAACATTCGTCAAC
TGGTATCAGCACAACTATCCTTACACTTGGGCGGGAGCACGTCT<ins>CGTGCGCAGC</ins>
<ins>CAGTAG</ins>

> *Egt2a* cDNA

ATGTCCGCTCCCACACCCTTTGGTGCCTCTATGGCAAAATCTCACTTCATGTTCG
ACCCCGACTTCAAAAACCTCAATCATGGCTCGTTTGGCACATATCCCGTTGCAG
TGCAGACAGCTCTGCGACACTTCCAATCGCAAGTGGAGGCCCGTCCGGATCCGT
TCATCCGGCACATCCAGCCCCAATTGATAGACGAAGCCCGCCGCGCCGTGGCCT
CGCTGCTCAATGTGCCCACCAACGAGTGCGTGTTCGTCAAGAACGCCTCGACGG
GCGTCAACACCGTCCTGCGCAACCTTGTCTTCAAGCAGGGCGATGTGCTGGTGT
ATTTCGACACCGTGTACGGCGCTGTCGAGAAGACCCTTGTCTCGCTGACTGAGA
CCACGCCGCTGCAGCTGCGCAAGGTCCAGTACCAGTTCCCCATTAGCCATGACG
AGCTGGTGCGGAAGTTCCTGGAGGTCGTGGCGAGTGCTACGGCGGAGGGGTTG
ACGGTTCGTGTTGCGGTGTTTGATACGATTGTCAGTTTGCCTGGCGTGCGGTTC
CCGTTTGAGCGGTTGATCGAGGCGTGTCGCGCCGAGGGGATCTTGAGCGTTGTG
GACGGGGCACATGGGATCGGGCAGATTCCCCTGGATCTGGGTGCTTTGCAGCCG
GATTTCTTCACGACGAATTGTCACAAGTGGCTGTATACCCCCCGCGGCAGCGCC
ATCCTCTACGTCCCCCTTCGCAACCAGCATCTCATCCGGACCACTCTCCCCACTT
CCTGGGGCTTCATCCCATCCCCGGACTCCCCCACCACCGCGCCCTCGCTCATGC
GCAGCAGCGGCTCGGGCAAGTCCGCCTTCGAGGAGCTCTTCGAGTTCGTCGCGA
CCACCGACGACACGGCGTACCTGTGTGTTCCGGCAGCGCTGAAATTCCGCTCCC
AGGTCTGCGGCGGCGAGGACCGCATCTACGCTTACCTGGAGAAGCTGGCGATG
GAGGCCGGGGACATTGTTGCCGCGGCGCTGGGCACGGAGGTGATGCAGGAGCC
CGGCTTGAAGCCCGGAGAGGTCAGTCAGCTGCGCCGCTGTGCCATGGCGACCGT
GCGGCTGCCGTTTGCCGTGTCTGGTAGTGAGCAGGATCCGAAGACGGCCTCGGC
TCGATTGACGCTGCAGGCTGCGCAGGCCGCGGAGGTTGCTGGGGAGATCCAGA
AGGCGTTGGTGCGGGACTATGGGACCTTTGTGCCTGTGTTTGCGCACGGCGGGT
GGTTGTGGACCCGGCTGAGTGCGCAGGTTTACTTGGAGAAGAGCGATTTCGAGT
GGCTTGCAGGTGTGCTGAACGAGCTATGCAACAAGCTGGTGAAGAAGTTTGCCG
AGCCAAAGTTGTGA

> *Egt2b* cDNA

ATGTCTAGCGTTACGCCATCTGTCTTGAGACAGGCATCTCGTGCCTATGCTCGTC
GACTTTCGTCGACCCAGCATGGCTCCCTGGCGACCGCGTCCTTCCCCAGACGGG
CGCTCGCCACATCCAGTGGTGCAGCTTCGAGACGGACATATGTTACCGAAACCA
AAGCTGGAAACGCTCAGGTTTCGATCGACACAGCCATCAAACAGGAGCAGAAG
AACTTCATCAAGCAGACAGGTCTTGAGCCTGGAAAGGTTGAACTTCCTGCCTCT
GGCATCTCCGGAGATGCTTCAATGAGTCCCTCTGCGGGTATTTTGAAACAAGCA

ACTGTTATGGATCAGGGAACACGGCCTATTTATTTGGATATGCAGGCCACTACG
CCGGTTGATCCTCGTGTTCTCGATGCTATGCTTCCCTATCTCACCGGTATCTACG
GAAACCCGCATTCCAGGACTCACGCATATGGTTGGGAGTCGGAGAAGGCTGTC
GAACAAGCCAGAGAATATATTGCGAAATTGATTGGGGCGGATCCAAAGGAAAT
CATCTTTACGAGTGGCGCCACCGAAAGTAACAACATGAGCATCAAGGGTGTGG
CCAGATTCTTTGGTCGTTCCGGCAAGAAGAAGCACATTATCACATCGCAGACTG
AGCACAAGTGTGTCTTGGACAGCTGCCGGCATCTTCAAGATGAGGGATTCGAAG
TCACATATTTGCCCGTTCAAAATAACGGATTGATCCGGATGGAGGATCTCGAGG
CGGCCATTCGACCCGACACGGCTCTAGTCAGCATCATGGCTGTCAACAATGAGA
TTGGTGTTATTCAACCCTTGGAAGAGATCGGAAAGCTCTGCCGTGCGAAGAAGG
TTTTCTTCCACACTGATGCTGCTCAGGCAGTTGGCAAGATCCCCTTGGATGTCAA
CAAGCTGAACATCGATTTGATGTCTATCTCCAGCCACAAGATTTATGGGCCCAA
GGGTATTGGTGCTTGCTATGTTCGACGCAGACCCAGGGTTCGCCTTGAGCCCAT
CATCTCCGGTGGTGGACAGGAACGAGGATTGCGCAGTGGCACGCTCGCTCCTCA
CCTGGTTGTTGGTTTCGGTGAGGCTTGCCGCATCGCCAGTCAGGACATGGAGTA
TGATAGGAAGCACGTTGAGCGGCTGTCGAAGCGTCTGCTGGATGGACTTCTGGC
GATGGAACACACCACGCTCAATGGGGATGCTGAGCGCCATTACCCTGGATGCGT
CAACGTCTCGTTCGCTTATATTGAGGGCGAGTCTCTTCTGATGGCTCTGAAGGAC
ATTGCATTGTCGTCTGGTAGTGCCTGTACCTCTGCCTCGCTGGAACCCAGCTACG
TCCTTCGAGCATTGGGCAGCAGCGACGAGAGCGCTCACAGCAGCATTCGTTTTG
GCATTGGACGGTTCACAACAGATAGCGAGATTGACTACGTCCTCAAGGCTGTTC
AAGACCGTGTCCATTTCCTCCGAGAGCTGAGTCCTCTGTGGGAGCTGGTCCAGG
AGGGCATTGATCTAAACACC<u>ATCCAATGGAGTCAGCATTAG</u>

>EgtA Protein Sequence

MSPLPCPSKKVEIVDIHRNDVEFSLVNEIRKGLNPPEGTPRSLPTMLLYDAQGLKLFE
EITYVDEYYLTNAEIEVLQNHSKKIVERVPENAQLLELGSGNLRKIKILLQEFERTGK
HVDYYALDLSLSELQRTFVEVSSDEYSHVDLHGLHGTYDDALAWLSNPQNLQRPT
VVMSMGSSIGNFSREGAAEFLAQFARLLKPSDLMIIGLDACTDPDKVYKAYNDSKG
ITQRFYENGLLHANAVLGYEAFQLSEWEVVTDYDVAGGRHRAFYSPKQNVTIDGV
LLQKGEKLVFEEATKYSPQQREQLWRDANLVLCEELGISSEEYHIHLLSPPTLSLPSQ

PSEYAANPVPSFKEFQSLWTAWDTVTKAMVPREELLAKPIKLRNALIFYFGHIPTFT
DIHLTRALGGSPTEPRNYRQIFERGIDPDVDNPEHCHSHSEIPDEWPPLAEILDYQDR
VRSRVDSVLQRDDITQNRCLGEALWIGFEHEAMHLETFLYMLLQSDKTLPPPLADR
PDFEKLFHQARANAKPNEWFAIPEQTLSIGFDDTDEQSLPDVSFGWDNEKPQRTITV
RAFEAQAHAITNGEYAKYLQATRQRRRPESWVLTHSDENYPISKGVTLESSQATKD
FMDNFAVRTVFGPVPLEFAQDWPVMASYDELALYAEWVGCRLPTYEEVKSIYNYS
AQLKETRQHEPSDHESNGVKGINRDMVTNGHSKVHQDKPRTPERQPIQPPSQSTMP
VFVDLHGCNVGFKHWHPTPVIQNGDRLAGHGELGGVWEWTSTPLTPHDGFKAMD
IYPGYTADFFDGKHNIVLGGSWATHPRIAGRTTFVNWYQHNYPYTWAGARLVRSQ
*

>Egt2a Protein Sequence

MSAPTPFGASMAKSHFMFDPDFKNLNHGSFGTYPVAVQTALRHFQSQVEARPDPFI
RHIQPQLIDEARRAVASLLNVPTNECVFVKNASTGVNTVLRNLVFKQGDVLVYFDT
VYGAVEKTLVSLTETTPLQLRKVQYQFPISHDELVRKFLEVVASATAEGLTVRVAV
FDTIVSLPGVRFPFERLIEACRAEGILSVVDGAHGIGQIPLDLGALQPDFFTTNCHKW
LYTPRGSAILYVPLRNQHLIRTTLPTSWGFIPSPDSPTTAPSLMRSSGSGKSAFEELFE
FVATTDDTAYLCVPAALKFRSQVCGGEDRIYAYLEKLAMEAGDIVAAALGTEVMQ
EPGLKPGEVSQLRRCAMATVRLPFAVSGSEQDPKTASARLTLQAAQAAEVAGEIQK
ALVRDYGTFVPVFAHGGWLWTRLSAQVYLEKSDFEWLAGVLNELCNKLVKKFAE
PKL*

> Egt2b Protein Sequence

MSSVTPSVLRQASRAYARRLSSTQHGSLATASFPRRALATSSGAASRRTYVTETKA
GNAQVSIDTAIKQEQKNFIKQTGLEPGKVELPASGISGDASMSPSAGILKQATVMDQ
GTRPIYLDMQATTPVDPRVLDAMLPYLTGIYGNPHSRTHAYGWESEKAVEQAREYI
AKLIGADPKEIIFTSGATESNNMSIKGVARFFGRSGKKKHIITSQTEHKCVLDSCRHL
QDEGFEVTYLPVQNNGLIRMEDLEAAIRPDTALVSIMAVNNEIGVIQPLEEIGKLCR
AKKVFFHTDAAQAVGKIPLDVNKLNIDLMSISSHKIYGPKGIGACYVRRRPRVRLEP
IISGGGQERGLRSGTLAPHLVVGFGEACRIASQDMEYDRKHVERLSKRLLDGLLAM
EHTTLNGDAERHYPGCVNVSFAYIEGESLLMALKDIALSSGSACTSASLEPSYVLRA
LGSSDESAHSSIRFGIGRFTTDSEIDYVLKAVQDRVHFLRELSPLWELVQEGIDLNTI
QWSQH*